

**Experimental evaluation of electrode-based
technologies for in situ sediment remediation and
industrial brine treatment**

Submitted in partial fulfillment of the requirements for

the degree of

Doctor of Philosophy

in

Department of Civil and Environmental Engineering

Mei Sun

B.S., Environmental Science and Engineering, Tsinghua University

M.S., Civil and Environmental Engineering, Carnegie Mellon University

Carnegie Mellon University

Pittsburgh, PA

September, 2012

To them I dedicated

My farther Shenghui Sun

My mother Kun Yang

Acknowledgement

This is a long and challenging journey. I would like to take this opportunity to thank all the people who have inspired and helped me walk all the way through.

First of all, I thank my advisors, Greg and Kelvin, for giving me insightful advice all along this long journey. Their broad knowledge, sharp reasoning and comprehensive view on research have guided my work on the right track. And more importantly, they are always very constructive and energized. Once and once again, they cheered me up when I felt depressed by difficulties and failures in experiments. Their efforts are greatly appreciated.

I thank Dr Jeanne Vanbriesen and Dr. Danny Reible for serving as my PhD committee members, and give me thoughtful comments and suggestions throughout my research process.

The four years at 207C made it a family for me where there is always friendship and laughter. I sincerely thank all my labmates, current and previous, for their technical and emotional help, from academic to daily life. My PhD life would be much tougher without them. I especially appreciate the help from Ron Ripper, Zhiqiang Li, Juan Peng,

Yan Xv, Teresa Kirschling, and Brine Reinsch for their help in lab protocols, experimental setups and trouble shooting. I also appreciate the collaboration with Fei Yan in U Texas Austin.

And finally I would like to thank my family and other friends for their endless love and encouragement. My parents and grandparents, who have always been supporting me unconditionally all through my life, deserve credits for all my accomplishments. I also want to thank my boyfriend, Lun Yang, who always understands me and cares me. My time at CMU is amazing. The people I met here have led me into a new world full of great opportunities. Thank you all.

Abstract

This thesis evaluated the feasibility and performance of electrode-based technologies for managing environmental contaminants. Specifically, research presented here focuses on the use of electrodes for *in situ* sediment remediation, and for the selective removal of bromide from brines produced in hydraulic fracturing.

Sediment capping is an *in situ* remediation strategy to contain contaminants. Compared to traditional sand and sorbent-amended caps, reactive caps capable of transforming contaminants may improve the remediation efficiency. However, few materials that can provide long-term contaminant degradation are available for use in sediment caps. An electrode-based reactive cap using carbon electrodes as the reactive capping material is proposed in this study to stimulate abiotic and biotic contaminant degradation *in situ*. A thorough understanding of factors affecting cap performance is essential to apply such reactive caps in the field. The primary objectives of study presented here for reactive sediment capping are to demonstrate the ability of an electrode-based reactive cap to degrade sediment contaminants, to identify factors affecting contaminant degradation, and to investigate the impact of powered electrodes on contaminant biodegradation.

Preliminary results in this study demonstrated a laboratory scale simulated sand cap containing carbon electrodes connected to a DC power supply induced and maintained redox gradient in Anacostia River sediment for more than 100 days. Hydrogen and oxygen were produced by water electrolysis at the electrode surfaces and may serve as electron donor and acceptor for potential contaminant degradation. The hydrogen production rate was proportional to the applied voltage between 2.5 and 5 V, and not greatly affected by pH or the presence of metal cations. Increasing ionic strength and addition of natural organic matter promoted hydrogen production.

Complete nitrobenzene (NB) degradation was achieved in batch reactors with graphite electrodes. NB was stoichiometrically reduced to aniline (AN) at the cathode with nitrosobenzene (NSB) as an intermediate, followed by rapid oxidization of AN at the anode. The reduction rate of NB and NSB were enhanced by increasing the applied voltage between the electrodes from 2V to 3.5V, but diminishing returns were observed above 3.5 V. NB and NSB reduction rate constants were faster at lower initial NB concentrations. Humic acid and simulated Anacostia River sediment porewater both affected the degradation rate, but only to a limited extent (~factor of 3).

The effect of powered electrodes on contaminant biodegradation rates was investigated in sediment slurry using 2,4-dichlorophenol (DCP) as a probe compound. DCP was

reductively transformed to 4-chlorophenol in sediment slurry with powered or unpowered electrodes. Graphite felt electrodes did not change DCP removal rates in nutrient-amended sediment slurry and carbon paper electrodes decreased DCP removal rate in unamended sediment slurry. The observed negative effect of powered electrodes on DCP biodegradation rate may be caused by hydrogen production and increase of sediment pH near the cathode, since an increase of either hydrogen concentration or pH was found to depress the dechlorination rate in unamended sediment slurries without electrodes.

Another application of electrode-based contaminant removal technology evaluated in this study is selective bromide removal from mining brine produced in hydraulic fracturing of shale gas. Such brine (referred as “flowback” and “produced” water) has raised a number of environmental and human health issues. An important health concern associated with the brine is its high bromide concentration (~1g/L). If the brine is discharged to receiving waters that serve as drinking water sources, the bromide in it can lead to the formation of carcinogenic brominated disinfection byproducts (DBPs) during water treatment. However, the co-existence of other ions in the mining brine, especially chloride as high as 30-200 g/L, makes selective bromide removal technically challenging.

This study investigated the feasibility of using electrodes for selective bromide removal from mining brine. In this process, bromide is selectively oxidized to form bromine, without causing chloride and water oxidation. The bromine can then be outgassed from the solution and recovered. Results suggest that it is possible to selectively remove bromide from the brine at a relatively fast rate ($\sim 10 \text{ h}^{-1}\text{m}^{-2}$ for produced water and $\sim 60 \text{ h}^{-1}\text{m}^{-2}$ for flowback water), and with good current efficiency (60-90%) at reasonable energy costs (6 kJ/g Br). Although the presence of chloride and other brine components decreased the bromide removal rate compared to synthetic bromide solutions, the process parameters measured suggest that selective bromide removal from mining brines is feasible utilizing mature technologies used in the chlor-alkali process.

Table of Contents

Acknowledgement.....	III
Abstract.....	V
Table of Contents	IX
List of Tables	XI
List of Figures	XII
List of Figures	XII
Chapter 1. Introduction.....	1
1.1 Introduction to electrode-based reactive caps for contaminated sediment management	1
1.1.1 Sediment contamination	1
1.1.2 Important sediment contaminants	2
1.1.3 Electrode-based reactive capping for sediment remediation	4
1.1.4 Data gaps for electrode-based reactive sediment cap	7
1.1.5 Objective and tasks	8
1.2 Introduction to electrode-based bromide removal from mining brine.....	10
1.2.1 Mining brine production and properties.....	10
1.2.2 Significance of bromide removal in mining brine.....	13
1.2.3 Electrode-based selective bromide removal from mining brine	15
1.2.4 Data gaps for electrode-based bromide removal from mining brine.....	17
1.2.5 Objectives and tasks	19
1.3 Dissertation overview	19
Chapter 2. Background.....	22
2.1 Electrode-based aqueous contaminants removal and subsurface remediation	23
2.2 Sediment remediation technologies	31
2.2.1 Conventional sediment remediation technologies.....	31
2.2.2 Other emerging alternatives.....	35
2.3 Electrode-base chloride/bromide oxidation.....	38
2.4 Other bromide removal methods	45
Chapter 3. Redox control and hydrogen production in sediment caps using carbon cloth electrodes.....	47
Abstract.....	47
3.1 Introduction	49
3.2 Materials and methods.....	50
3.3 Results and discussions.....	56
3.4 Conclusions.....	69

Chapter 4. Nitrobenzene sequential reduction/oxidation by graphite electrodes and factors affecting degradation rate	71
Abstract.....	71
4.1 Introduction	73
4.2 Materials and methods.....	77
4.3 Results and discussions.....	80
4.4 Conclusions.....	99
Chapter 5. Effect of powered carbon electrodes on 2,4-dichlorophenol biodegradation in sediment slurry.....	100
Abstract.....	100
5.1 Introduction	102
5.2 Materials and methods.....	106
5.3 Results and discussions.....	112
5.4 Conclusions and Implications for Sediment Capping.....	128
Chapter 6. Electrode-based selective oxidation of bromide in mining brines from hydraulic fracturing sites	131
Abstract.....	131
6.1 Introduction	133
6.2 Materials and methods.....	138
6.3 Results and discussion	143
6.4 Conclusions.....	160
Chapter 7. Conclusions, implications, contributions, and suggestions for future research	161
7.1 Electrode-based reactive sediment cap.....	161
7.1.1 Summary and conclusions.....	161
7.1.2 Engineering implications	163
7.1.3 Contributions and benefits	164
7.1.4 Suggestions for future research	166
7.2 Electrode-based selective bromide removal in mining brines	168
7.2.1 Summary and conclusions.....	168
7.2.2 Engineering implications	169
7.2.3 Contributions and benefits	170
7.2.4 Suggestions for future research	172
Reference	174
Appendix A. Supplementary materials for Chapter 3.....	184
Appendix B. Supplementary materials for Chapter 4.....	186
Appendix C. Supplementary materials for Chapter 5.....	189
Appendix D. Supplementary materials for Chapter 6.....	192

List of Tables

Table 1-1. Frequency of contaminant sub-group in sediment sites	3
Table 1-2. Concentrations for selected common constituents of flowback water from natural gas development in the Marcellus Shale	12
Table 2-1. Typical data for commercial chlor-alkali cells	41
Table 6-1. Theoretical minimum energy consumption for different technologies.....	135
Table 6-2. Properties of brine samples	151
Table 6-3. Species with lower standard equilibrium potential (E^0) than bromide that may exist in mining brine	154
Table B-1 pH, working electrode potential and current information for each experiment (average from triplicates \pm standard deviation)	188
Table C-1 Anacostia River sediment porewater characteristics	189
Table C-2 Anacostia River sediment solid characteristics	189
Table C-3 Composition of mineral mix.....	190
Table C-4 Composition of vitamin mix.....	190

List of Figures

Figure 1-1. Conceptual model for the electrode-based reactive sediment cap with contaminants reduction near cathode and oxidation near anode	4
Figure 1-2. Conceptual model for the electrode-based bromide removal from mining brine with bromide oxidation at anode and hydrogen production at cathode	17
Figure 2-1. Conceptual model for the electrokinetic process	25
Figure 2-2. Conceptual model for the (a) horizontal and (b) vertical Lasagna process...	27
Figure 2-3. Conceptual model for the e-barrier	30
Figure 2-4. Scheme of cell configurations used in chlor-alkali process.....	41
Figure 2-5. Flow chart of commercial bromine production process.....	43
Figure 3-1. Scheme (side view) of (a) the T-cell reactors for studying sediment cap redox control and (b) the H-cell reactors for studying the geochemical effects on hydrogen production rate.....	54
Figure 3-2. (a, b, c)Vertical ORP and (d, e, f) pH profiles developed in sediment and cap containing carbon cloth electrodes (T-cell 1 and T-cell 2) imposed to a 4V external voltage (a~d) or in control sediment (e, f)	61
Figure 3-3. Hydrogen production at 4V applied voltage and initial pH 7 in 20 mM NaHCO ₃ and 20 mM NaCl solution: (a) hydrogen concentration (b) and cumulative amount.....	63
Figure 3-4. Influence of applied voltage on (a) hydrogen production rate and (b) cathode solution pH.	65
Figure 3-5. Influence of initial pH on hydrogen production rate.	66
Figure 3-6. Influence of aqueous chemical species on (a) hydrogen production rate and (b) current efficiency.....	69
Figure 4-1. Sequential reduction/oxidation of nitrobenzene at 3V applied voltage	82
Figure 4-2. First order kinetic model fit for nitrobenzene (NB) reduction to aniline (AN) via nitrosobenzene (NSB) at 3V	85
Figure 4-3. Effect of applied voltage on (a) nitrobenzene (k_{NB}), nitrosobenzene (k_{NSB}) reduction rate constants, and hydrogen production rate constant (inset), and (b) electrode potential peaks after NB addition in the working chamber.....	87
Figure 4-4. Effect of initial nitrobenzene concentration on nitrobenzene (k_{NB}) and nitrosobenzene (k_{NSB}) reduction rate constants, and on electrode potential peaks after NB addition in the working chamber.	89
Figure 4-5. Impact of (a) NOM presence and (b) humic acid concentration on nitrobenzene (k_{NB}) and nitrosobenzene (k_{NSB}) reduction rate constants.	91
Figure 4-6. Effect of flow conditions (Peclet Number, Pe) on transformation in the sediment cap for a range of reactivity (Damkohler numbers, Da).	97

Figure 5-1. (a) removal of 2,4-dichlorophenol (DCP), production of (b) 4-chlorophenol (CP) (c) hydrogen, and (d) methane in nutrient-amended unpowered sediment slurry, sediment slurry powered with graphite felt electrodes at 2V applied voltage, and a powered but sterilized sediment slurry	114
Figure 5-2. Effect of applied voltage on 2,4-dichlorophenol (DCP) degradation in nutrient-amended sediment slurry with graphite felt electrodes.....	116
Figure 5-3. Effect of applied voltage on 2,4-dichlorophenol (DCP) degradation in unamended sediment slurry with carbon paper electrodes.....	119
Figure 5-4. Effect of headspace hydrogen concentration on (a) 2,4-dichlorophenol (DCP) degradation and (b) methane production in unamended sediment slurry without electrode	122
Figure 5-5. Effect of pH on (a) 2,4-dichlorophenol (DCP) degradation and (b) methane production in unamended sediment slurry, and (c) DCP degradation in nutrient-amended sediment slurry without electrode.....	128
Figure 6-1. Linear voltammetry of Br ⁻ and Cl ⁻ solutions with graphite rod electrodes .	145
Figure 6-2. Current and cell voltage profile in H-cell reactor with 76 g/L chloride solution before and after adding 1.2 g/L bromide	147
Figure 6-3. Bromide removal in 1.2 g/L Br ⁻ + 76 g/L Cl ⁻ solution by graphite rod anode poised at 1V vs. Ag/AgCl electrode	148
Figure 6-4. Effect of chloride concentration on bromide removal rate, current efficiency and energy consumption in synthesized brine by graphite rod anode poised at 1V vs. Ag/AgCl electrode	150
Figure 6-5. Bromide removal rate (a), current efficiency and energy consumption (b) in synthetic brine, flowback water and produced water by graphite rod anode poised at 1V vs. Ag/AgCl electrode.....	153
Figure A-1 Vertical ORP (left) and pH (right) profiles over time developed in sediment and cap containing carbon cloth electrodes	185
Figure B-1 Modeled first-order NSB reduction rate (k_{NSB}) from NB reduction (similar experiments as Figure 1) and NSB reduction (separate experiments with NSB directly added into reactors).....	186
Figure B-2 Electrode potential in the working chamber vs. time during NB reduction at (a) different applied voltage (initial NB 100 μ M) and (b) different initial NB concentration (at 3 V)	187
Figure C-1 effect of sediment slurry pH on extraction efficiency of DCP and 4-CP.....	191

Chapter 1. Introduction

This thesis investigates applications of electrode-based technologies for managing environmental contaminants. Specifically, research presented here focuses on the use of electrodes for *in situ* sediment remediation, and for selective removal of bromide from brines produced in hydraulic fracturing. These applications are closely related and rely on the same underlying electrochemistry principles, but are employed in distinct environment matrices and thus have significantly different design and operational considerations. Therefore, these two applications are introduced in this chapter separately.

1.1 Introduction to electrode-based reactive caps for contaminated sediment management

1.1.1 Sediment contamination

Aquatic sediment contamination is a ubiquitous problem and requires innovative solutions to manage and contain the contaminated sediments to mitigate adverse effects. Sediment consists of a variety of materials that by gravity settle out of the water columns of rivers, lakes, estuaries and oceans, and accumulate. Sedimented materials include sand, silt, clay, organic matter, or other minerals. The close contact with the water column makes sediment both a dynamic source and sink for contaminants, which

may adversely affect human health or the environment. Sediment is the habitat of many aquatic species at the base of the aquatic food web, and thus has significant impacts on the health of aquatic food chain. As estimated by the U.S. Environmental Protection Agency in 1998, of the 12 billion cubic yards of total surface sediment (upper five centimeters) in the US, approximately 10 percent (1.2 billion cubic yards) is sufficiently contaminated with toxic pollutants to pose significant health risks [1].

1.1.2 Important sediment contaminants

Sediment contamination comes from multiple sources that discharge to receiving waters including: industrial waste and municipal sewage; storm water runoff from city streets, farms, mining operations, waste dumps, industrial manufacturing and storage sites; dry and wet atmospheric deposition; contaminated ground water discharge, and contaminants from surface water [1]. Heavy metals and metalloids, polycyclic aromatic hydrocarbons (PAHs), pesticides, polychlorinated biphenyls (PCBs), and other organics are the most frequently reported contaminants in sediments (Table 1-1). Hydrophobic organic contaminants that have accumulated in sediment are released slowly into the water column as can act as a long-term low level source of contamination into the food web. Although some contaminants do attenuate, the degradation rates are generally slow, and these chemicals tend to persist in sediment for long time. The use of many

contaminants such as DDT, PCBs and mercury were banned or restricted decades ago. However, they remain in the sediment and cause adverse effects to aquatic organisms and to human health.

Table 1-1. Frequency of contaminant sub-group in sediment sites

(Table reproduced from USEPA report [2])

Contaminant Sub Group	Number of sites	Percentage (%)
Metals	913	81.01
Miscellaneous Inorganic and Organic Compounds	449	39.84
Polynuclear Aromatic Hydrocarbons (PAHs)	445	39.49
Pesticides	369	32.74
Non-halogenated Volatile Organic Compounds (VOCs)	263	23.34
Non-halogenated Semivolatile Organic Compound (SVOCs)	242	21.47
Halogenated VOCs	211	18.72
Polychlorinated biphenyls (PCBs)	165	14.64
Benzene, Toluene, Ethylbenzene, Xylenes (BTEX)	151	13.4
Phenols	84	7.45
Halogenated SVOCs	58	5.15
Explosives and Propellants	38	3.37
Other Organic (Coal Tar, Creosote)	4	0.35
Radioactive Materials	3	0.27
Other	2	0.18
No Group Determined	1	0.09

Notes: Data were available for 1,127 sites

Source: DOD, Office of the Under Secretary

1.1.3 Electrode-based reactive capping for sediment remediation

To address sediment contamination, various remediation technologies have been developed and applied. A more complete review of available remediation strategies, with their advantages and limitations, is available in Chapter 2.

Several electrode-based techniques have been studied and applied for contaminated site remediation (typically for *in situ* groundwater treatment), as summarized in Chapter 2. In this work, an electrode-based reactive cap is proposed for degrading contaminants moving into the cap, and containing contaminants in the underlying sediment. In brief, the electrodes are placed in the sand cap above the sediment, perpendicular to the direction of seepage flow and contaminant transport (Figure 1-1).

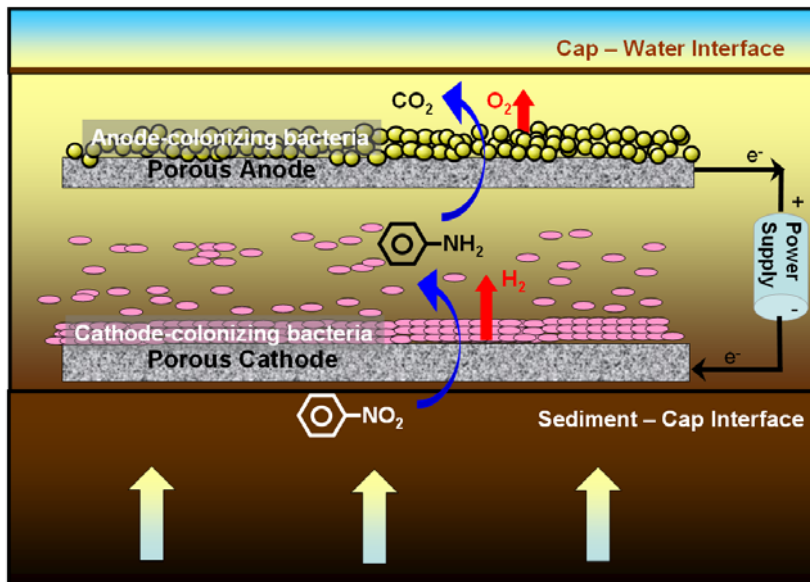


Figure 1-1. Conceptual model for the electrode-based reactive sediment cap with contaminants reduction near cathode and oxidation near anode

As contaminants migrate into the cap, they will be exposed to a reducing environment in the vicinity of the cathode, followed by an oxidizing environment in the vicinity of the anode (the opposite order can also be created by reversing the polarity of the electrodes). Both magnitude and thickness of the reducing and oxidizing zones created by the electrodes will, in principle, be controllable in real time by manipulating the applied voltage. Thus, for a constant seepage velocity the residence times of contaminants within these zones are scalable. In this manner, the electrode-based sediment cap may be specifically engineered and adjusted for targeted degradation of contaminants or their mixtures on a site-by-site basis. The electrodes polarized at low voltage will accelerate both organic and inorganic contaminants degradation by, 1) rapidly establishing and maintaining a controllable redox gradient within the cap; 2) reducing or oxidizing contaminants electrochemically on the electrode surface; and 3) providing electron acceptor and donor to stimulate contaminant biodegradation. The three proposed functions of the electrode-based reactive cap have the potential to specifically address several typical challenges encountered in sediment remediation.

First, depending on the nature of contaminants, the degradation processes are commonly limited by the availability of either electron donor (e.g., for heavy metal or chlorinated solvent stabilization) or electron acceptor (e.g., for hydrocarbon oxidation). Instead of delivering the donors/acceptors by pumping or mixing chemicals into the

sediment as other biological/chemical treatments do, the electrodes within the cap can continually provide low concentrations of donor/acceptor at the sediment-water interface. Hydrogen and oxygen from water electrolysis can be utilized as electron donor and acceptor, respectively, by broad groups of bacteria. The electrodes themselves may serve as an electron donor or acceptor. Bacteria have been shown to respire on various electrodes in the presence of contaminants [3-5].

Second, for some contaminants complete contaminant degradation and mineralization may only be feasible through sequential reduction and oxidation. For example, in a reducing environment tetrachloroethene (PCE) may be sequentially dechlorinated to trichloroethylene (TCE), dichloroethene (DCE), and vinyl chloride (VC). However, VC may accumulate under reducing conditions but mineralize in an oxidized environment [6]. Similarly, polychlorinated biphenyl (PCBs) may undergo partial, reductive dechlorination [7], and the resultant lightly chlorinated PCBs become susceptible to aerobic biodegradation [8]. Typically sediments are dominated by reducing conditions, with a few centimeters (at most) of an oxidized layer at the sediment-water interface. This thin oxidized layer is too thin to provide sufficient residence time for degradation of many contaminants [9]. The electrodes can create, and microorganisms can help to maintain, a redox gradient in the cap, which may not develop spatially or temporally

under natural conditions, providing the necessary residence times through the reductive and oxidative zones for specific contaminant transformation to be engineered.

Third, the observance of contamination in mixtures confounds single-approach remedial or sequestration designs. For example, polyaromatic hydrocarbons (PAHs) contamination is often accompanied by heavy metals. While an aerobic environment is optimal for oxidizing PAHs to CO₂, an anaerobic environment is needed for heavy metals reductive immobilization. This challenge may be met through the electrode-based reactive sediment cap which provides precise control of disparate redox conditions and may be tuned for simultaneous delivery of electron donor and acceptor for stimulating contaminant degradation.

1.1.4 Data gaps for electrode-based reactive sediment cap

There are many questions that need to be answered before the electrode-based reactive sediment caps can be applied at field scale, including:

- (1) Can electrodes emplaced at the sediment-water interface provide electron donor and acceptor and control redox conditions to promote contaminant degradation?
- (2) Can electrodes provide abiotic oxidation/reduction of contaminants?

- (3) Can electrodes stimulate appropriate microbial communities to enhance biodegradation?
- (4) Can the contaminant degradation rate in the cap be manipulated by adjusting the applied voltage?
- (5) How do sediment geochemical conditions affect short- and long-term reactivity of the cap?
- (6) Which electrode materials will be suitable for such a cap?
- (7) How does construction and operation cost for such an electrode cap compare to other remediation technologies?

Work in this thesis addressed questions (1)-(4) to determine the feasibility of the approach, and question (5) to understand the performance of the cap under different site conditions. Question (6) and (7) are important for cap design, but were not investigated in detail in this thesis.

1.1.5 Objective and tasks

The main objective of this thesis work is to assess the feasibility of using carbon electrodes as reactive sediment caps. Specifically, the ability of a carbon electrode-based sediment cap to control the redox gradient near the sediment-water interface, to deliver

electron donor/acceptor, and to stimulate both abiotic and biotic degradation of contaminants in the presence of common sediment porewater constituents were determined.

Three tasks associated with the research objectives are summarized here.

Task 1: Demonstrate the ability to control redox conditions and produce hydrogen as electron donor in an electrode-based sediment cap, and determine geochemical factors affecting the hydrogen production rate.

Task 2: Evaluate the ability of abiotic degradation by sequential reduction/oxidation of nitrobenzene on electrodes, and determine the electrode operating parameters and geochemical conditions affecting the degradation rate.

Task 3: Determine the effect of powered electrodes on dechlorination of 2,4-dichlorophenol in a sediment slurry.

Polarized carbon electrodes were evaluated to determine their suitability for use in an electrode-based reactive sediment cap. Although noble metal electrodes usually have higher catalytic reactivity for contaminant degradation, inexpensive carbon is more

likely to be employed for sediment applications. Also, carbon electrodes are less sensitive to catalyst poisoning. Thus, several different carbon materials were examined as electrode material.

1.2 Introduction to electrode-based bromide removal from mining brine

1.2.1 Mining brine production and properties

Large volume of mining brine is produced by shale gas hydraulic fracturing. In order to liberate natural gas trapped in low-permeable shale, aqueous fracturing fluid is pumped underground to fracture the rock. When cracks form to enable natural gas release, the injected liquid returns to the surface as concentrated brine, which is referred to as “flowback water” and “produced water”. “Flowback water” is the brine recovered from the well at the early stage of well installation, while produced water is the brine recovered from the well during well gas production [10]. Rapid development of the onshore natural gas exploration in deep shales (e.g., Barnett Shale in Texas, Marcellus Shale in northeast US) poses challenges for managing those brines to protect groundwater and surface water, and to ensure sustainable gas production without negative environmental effects.

The amount of fracturing fluid injected in a typical hydraulic fracturing procedure for shale gas mining is 18 to 55 million barrels per year, or 19-40 barrels per million cubic feet gas (1 barrel = 42 gallon). Of the injected fracturing fluids, ~25% returns to the surface in the Marcellus shale during the initial phase (generally regarded as the first 30 days) of flowback [11]. The produced mining brine contains high concentration of total dissolved solids (TDS) as high as 5 times of concentration in sea water, as well as organic matter such as heavy and light petroleum hydrocarbons. The example of constituents in flowback water from Marcellus Shale gas production is summarized in Table 1-2.

The management of mining brine has become an emerging public health and environmental concern, because the high concentration of salinity, hardness, heavy metals, and the existence of other components (including radionuclides, oil, bacteria, and potentially problematic ions such as bromide and iodide). These components may significantly change the properties of the water bodies receiving the mining brine discharge. Currently, dilution and surface discharge after primary treatment, deep well injection, reuse for on-site hydraulic fracturing, and road spreading for dust or ice control are favored disposal methods for the mining brine. However, deep well injection is limited by the availability and capacity of suitable injecting sites, reuse for on-site hydraulic fracturing is limited by the distance between wells producing water

and requiring water, and surface discharge and road spreading may cause potential human health and environmental risks, mainly due to the presence of bromide, radioactive materials and heavy metals. Thus, new cost-effective methods must be developed to manage the concentrated shale gas mining brine.

Table 1-2. Concentrations for selected common constituents of flowback water from natural gas development in the Marcellus Shale

(Table reproduced from [10], the data were obtained from flowback water from several production sites in western Pennsylvania)

Constituents	Low¹ (mg/L)	Medium² (mg/L)	High³ (mg/L)
Total dissolved solids	66,000	150,000	261,000
Total suspended solids	27	380	3200
Hardness (as CaCO ₃)	9100	29,000	55,000
Alkalinity (as CaCO ₃)	200	200	1100
Chloride	32,000	76,000	148,000
Sulfate	ND ⁵	7	500
Sodium	18,000	33,000	44,000
Calcium, total ⁴	3000	9800	31,000
Strontium, total	1400	2100	6800
Barium, total	2300	3300	4700
Bromide	720	1200	1600
Iron, total	25	48	55
Manganese, total	3	7	7
Oil and grease	10	18	260

Notes:

1. "Low" concentrations are from early flowback at one well.
2. "Medium" concentrations are from late flowback at the same well for which the "low" concentrations are reported.
3. "High" concentrations are the highest concentrations observed in late flowback from several wells with similar reported TDS concentrations.
4. Total concentration = dissolved phase + suspended solid phase concentrations.
5. Not detected

1.2.2 Significance of bromide removal in mining brine

Among the mineral components in mining brine, bromide has drawn particular attention. A water body receiving the high concentration of bromide (either by direct discharge or road runoff loaded with brine spreading) may be considerably degraded in quality as a drinking water source because the presence of bromide leads to formation of carcinogenic brominated disinfection byproducts (DBPs).

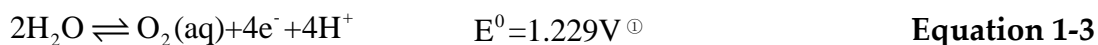
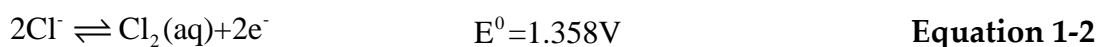
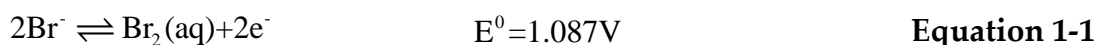
DBPs are formed during drinking water disinfection when disinfectants (such as chlorine) react with bromide and/or natural organic matter present in the source water. Bromide can serve as the precursor of many DBPs which are suspected carcinogens, such as bromate, brominated trihalomethanes (THMs) and brominated haloacetic acids (HAAs). These brominated DBPs form through two steps: aqueous chlorine first converts bromide in the water to hypobromous acid, and the hypobromous acid can then react with the organic matter in the same way as hypochlorite acid to form various bromochlorinated DBPs. Generally, bromine is more effective than chlorine in participating in substitution reactions with organic molecules, and high concentration of bromide will favor the formation of brominated DBPs over the chlorinated species. Since the brominated DBPs are considered more carcinogenic than their chlorinated analogues [12], it is important to remove the high level of bromide in mining brine before surface discharge.

In southwestern Pennsylvania, associated occurrence of increase in brominated DBPs, TDS and bromide concentration has already been observed in drinking water utilities using the Monongahela River [13] and Allegheny River [14] as source water, which received mining brine discharge from Marcellus Shale. This event lead to a request issued by Pennsylvania Department of Environmental Protection forbidding mining brine discharging from the Marcellus Shale gas mining to Chapter 95 exempt facilities without bromide removal capability. It also leads to a request by the Water Users Advisory Committee of the Ohio River Valley Water Sanitation Commission to develop bromide control and concentration standards [15]. To help ensure drinking water safety in the region, it will likely be necessary to have bromide levels regulated in regions with shale gas mining and to restrict concentrated mining brine direct discharges to surface and ground water. To achieve this, economical methods to remove bromide for the mining brines prior to disposal are needed.

Currently available water treatment technologies for bromide removal are reviewed in Chapter 2. The unique quality and quantity of the mining brines creates special challenges for these methods [10], and new methods are needed.

1.2.3 Electrode-based selective bromide removal from mining brine

In this study, electrolytic bromide oxidation to bromine is proposed for selective bromide removal from mining brine. The anode potential is precisely controlled to ensure bromine generation without chlorine and oxygen generation, based on the fact that the oxidation of bromide is thermodynamically favorable at potentials that are lower than required for the oxidation of chloride and water (Equation 1-1 to Equation 1-3) [16].



The bromide-containing brine is processed in an electrolyzer, with the anode and cathode chambers separated by a cation-permeable membrane. Bromide is oxidized to bromine at the anode (Equation 1-1). The produced bromine can be bubbled out of the electrolyte and recovered in separate containers, which can be commercialized for many applications, such as the production brominated flame retardants, gasoline additives, pesticides, and applied in medical and veterinary use. The bromide-depleted effluent from the anode then enters the cathode where the protons are reduced to form

^① The listed values are standard equilibrium potentials. However, due to the over potential required for many common electrode materials, oxygen generation usually take place at potential near 2V.

hydrogen gas (Equation 1-4). The brine first enters the anode because the cathode effluent has a high pH due to consumption of protons, whereas the bromine separation requires acidic conditions. The complete process is illustrated in Figure 1-2.



Compared to the industrial bromide production process which runs at high potential to oxidize chloride to chlorine first, and use chlorine to oxidize bromide to bromine, the direct bromide oxidation process utilized in this study has the advantage of requiring less energy input, not only because the less electric potential needed for bromide oxidation than chloride oxidation, but also no excess reagent (chlorine) has to be produced or added to drive complete bromide removal. The elimination of chlorine involvement also makes this technology cleaner and safer, and easier to purify the produced bromine as a commodity. The high TDS in mining brine also offers a natural supporting electrolyte so ohmic loss is minimized. The produced bromine and hydrogen can be collected as valuable byproducts for commercial use to recover some of the cost of brine treatment.

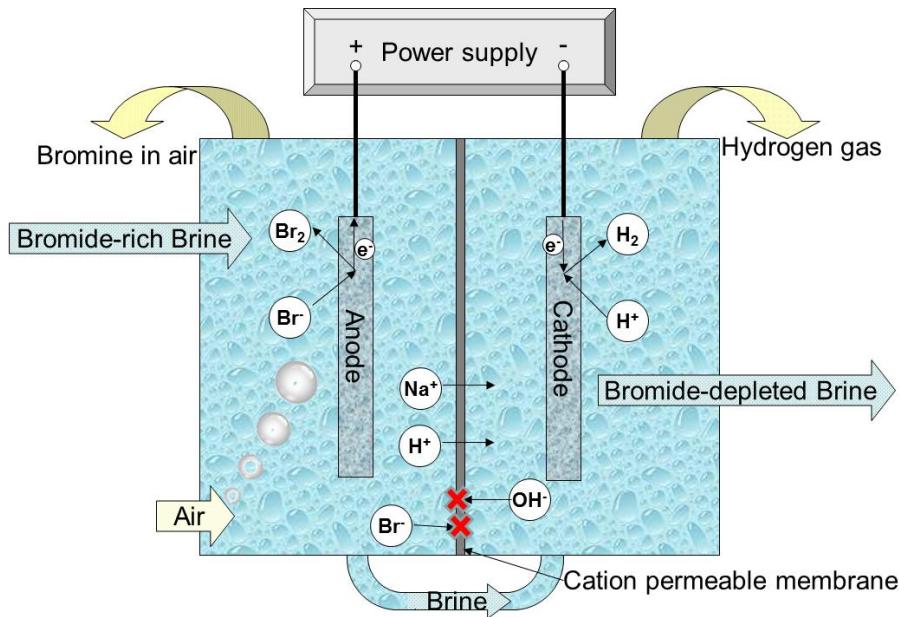


Figure 1-2. Conceptual model for the electrode-based bromide removal from mining brine with bromide oxidation at anode and hydrogen production at cathode

1.2.4 Data gaps for electrode-based bromide removal from mining brine

Although bromide oxidation has been developed for the bromine industry and for drinking water treatment, these approaches cannot be readily applied in mining brine management. Industrial bromine oxidation (both by chlorine and by electrodes) focuses on bromine production and is not aimed at removing bromide to very low levels as is needed for treatment of the processed brine. The studies for drinking water treatment only worked in water with simple components (low salt, low hardness, and low organic matter), which may not be applicable for the complicated water chemistry of the mining

brine. In order to apply the electrode-based bromide removal technique in brine management, several questions need to be answered.

- (1) Can electrodes selectively oxidize bromide only, without causing chlorine and oxygen production?
- (2) What current efficiency and percentage removal can be achieved?
- (3) How will the components in mining brine (e.g., hardness, organic matters) affect bromide removal?
- (4) What are the most cost-effect design and operation parameters (e.g., electrode potential, hydraulic retention time, electrode surface area per reactor volume, etc.) for selective bromide oxidation?

Questions (1)-(3) are investigated in bench scale batch reactors. Question (4) is briefly discussed at the end of this study. Further understanding of an electrolysis system may perform under flow conditions at large scale would also be needed for a comprehensive evaluation of the effectiveness in bromide removal. Questions about bromine recovery and utilization are not listed above, because this process is probably independent of the mining brine nature, and have been well developed by the bromine industry.

1.2.5 Objectives and tasks

The main objective of this thesis work is to determine the feasibility of selective bromide electrolysis in mining brine with high salinity and other unknown content, and to make preliminary energy estimates for a scaled up process for treating mining brine.

One tasks associated with this research objective is:

Task 4: Evaluate the feasibility of using electrodes to selectively remove bromide in mining brine, including verify selective bromide oxidation in presence of high concentration of chloride, investigate the effect of chloride concentration on bromide removal results, compare bromide removal effect in actual mining brine and pure bromide/chloride solution, and do a general estimation of required electrolyzer configuration, operation condition and energy cost.

Carbon materials were selected as electrodes because of their relatively low cost and stability.

1.3 Dissertation overview

This dissertation is presented in seven chapters and four appendices. The core of the dissertation consists of Chapter 3, 4, 5 and 6, which comprise materials either published

or prepared for publication in peer-reviewed journals. Chapter 1 provides an introduction to the work, brief background information and research objectives as well as the research tasks that were performed. Chapter 2 summarizes available technologies in contaminated sediment remediation, bromide removal and other related electrode-based technologies used for remediation. Chapter 7 contains conclusions, novel contributions, environmental implications of this work, and suggestions for future work. A summary of chapters 3 to 6 and the appendices are listed below.

Chapter 3 presents the study on redox control and hydrogen production in the electrode-based sediment cap. This material, written by Mei Sun and co-authored by Fei Yan, Ruiling Zhang, Danny D. Reible, Gregory V. Lowry, and Kelvin B. Gregory, was published in *Environmental Science & Technology* in 2010 under the title “Redox control and hydrogen production in sediment caps using carbon cloth electrodes” [17].

Chapter 4 investigates the ability of electrodes to abiotically reduce and oxidize the model compound (nitrobenzene) under various conditions relevant to sediment environments. This material, written by Mei Sun and co-authored by Danny D. Reible, Gregory V. Lowry, and Kelvin B. Gregory, was published in *Environmental Science & Technology* in 2011 under the title “Effect of applied voltage, initial concentration and

natural organic matter on sequential reduction/oxidation of nitrobenzene by graphite electrodes”[18].

Chapter 5 evaluates the effect of electrodes in biodegradation of another model compound (2,4-dichlorophenol) in sediment remediation. This material, written by Mei Sun and co-authored by Gregory V. Lowry, and Kelvin B. Gregory, is under preparation for possible publication.

Chapter 6 assesses the feasibility of using selective oxidation by electrodes to remove bromide from mining brine. This material, written by Mei Sun and co-authored by Gregory V. Lowry, and Kelvin B. Gregory, is under preparation for publication.

Chapter 2. Background

For both the case of contaminated sediment (and other porous environmental matrices) remediation and aqueous bromide extraction, there are several currently available technologies. Some of them are electrode-based and the rest rely on other physical/chemical/biological techniques. This chapter summarizes the traditional and novel strategies used for sediment remediation and halogens extraction, as well as the development of electrode-based contaminants removal applications, which set up a comprehensive background for the research presented in this thesis.

The subjects reviewed in detail below, include:

- 2.1 Electrode-based aqueous contaminants removal and subsurface remediation
- 2.2 Sediment remediation technologies
- 2.3 Electrode-base chloride/bromide oxidation
- 2.4 Other bromide removal methods

In many of the topics reviewed below, there are numerous papers, reports and patents. Limited by the length of this dissertation, only a few representative ones are cited for each topic to briefly summarize the general principles, configurations and applicable situations of each technology.

2.1 Electrode-based aqueous contaminants removal and subsurface remediation

Electrochemical technologies have significant contribution to improve our environment quality, including remediation/decontamination, electrochemical sensors for monitoring toxic substance, clean energy generation, and environmental benign chemistry. Some electrode-based technologies in contaminants removal sharing similar principles and/or configurations as the proposed electrode-based systems in this work are summarized here. These electrochemical treatment have been developed for removing contaminants from environment matrices, including *in situ* application by inserting electrodes into the contaminated subsurface (soil or sediment), and *ex situ* treatment of contaminated water or liquid extractant from the contaminated subsurface.

Electrokinetic process

Electrokinetic processes were explored for the remediation of metals [19, 20], radionuclides [21] and organic contaminants [22] in soil, as well as in wastewater treatment sludge [23] and sediment [24]. In brief, an electric field is applied across electrode pairs that are vertically implanted into the ground on each side of the contaminated soil (Figure 2-1). Dissolved species desorb from soil particles and transport towards the electrodes via electroosmosis, electromigration, and electrophoresis. After accumulating the contaminants near or on the electrodes,

secondary processes can be utilized to stabilize or recover the contaminant. For example, electroplating or precipitation may be used to immobilize metals, pumping can be used to treat dissolved compounds, and complexing with ion exchange resins may be utilized for removing charged species from the subsurface [25]. Electrokinetic process may be improved by adding surfactants and/or complexing agents to promote contaminant solubility and transport and recover properties [26]. Recent evolutions combine the electrokinetic process with permeable reactive barriers [27], bioremediation [28], chemical reduction/oxidation [29] or phytoremediation [30]. The application of electrokinetic process is limited by the availability of drilling or implementation technology to install the electrodes. This is especially problematic in sediment environments where contaminants are broadly dispersed. Extraction of enriched contaminants around the electrodes from underwater sediment is also more challenging than in soils. Besides, sediment also has a high organic carbon content which may tightly trap organics and metals, and make contaminants moving toward electrodes slow. All these factors limit the application of electrokinetic process in sediment remediation.

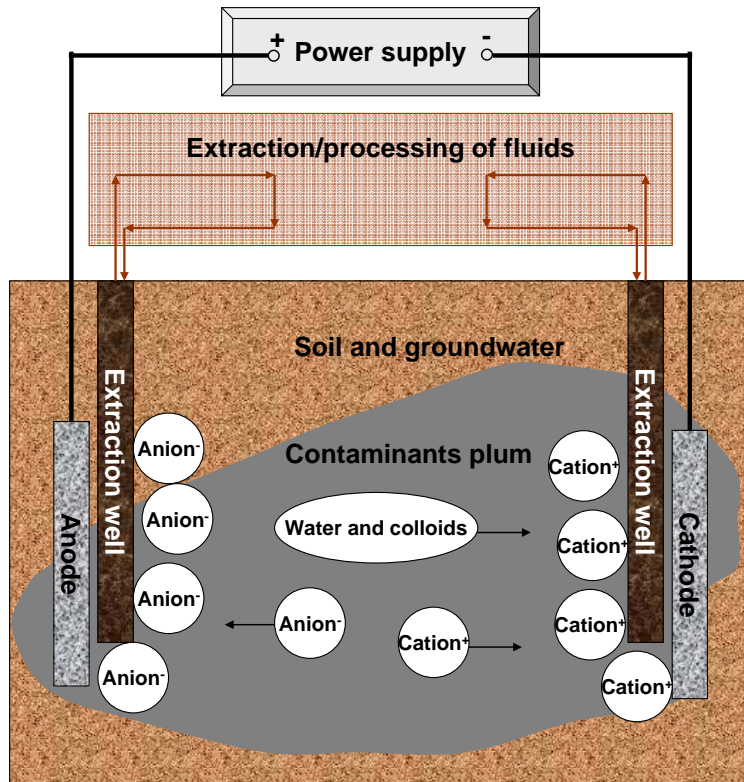


Figure 2-1. Conceptual model for the electrokinetic process

(Figure adapted from [31])

Although sharing similar configuration, the electrokinetic process functions differently than the proposed electrode-based sediment caps in this work. The electrokinetic process relies on altering the contaminants flux to enrich and extract the contaminants around the electrodes, while the reactive cap is designed to sequester and degrade the contaminants passing through without significantly altering the contaminant transport properties. Thus, electrodes for electrokinetic migration are emplaced at much greater distances from each other (across the entire contaminated area) than the electrodes for a

reactive cap which are only a few centimeters apart. This difference in configuration leads to a difference in energy requirements: with the voltage gradient in range of several V/cm [32], the electrokinetic process needs much higher voltage (40-200 V) than the reactive cap (a few volts).

Lasagna process

The Lasagna process is a variation of the traditional electrokinetic approach. It is so called because of its layered arrangement of electrodes and multiple treatment zones (Figure 2-2). Contaminants move in soil pore water due to a potential gradient imposed by the electrodes in the same way as in electrokinetic treatment. However, rather than cumulating the contaminants around the electrodes, in Lasagna process, permeable treatment zones are constructed between contaminated zone and electrodes, where the contaminants can be removed by adsorption, immobilization, or degradation. The process is especially effective for remediating low-permeability soils, or heterogeneous soil. Both vertical and horizontal configurations have been conceptualized, but fieldwork to date is more advanced for the vertical configurations [33].

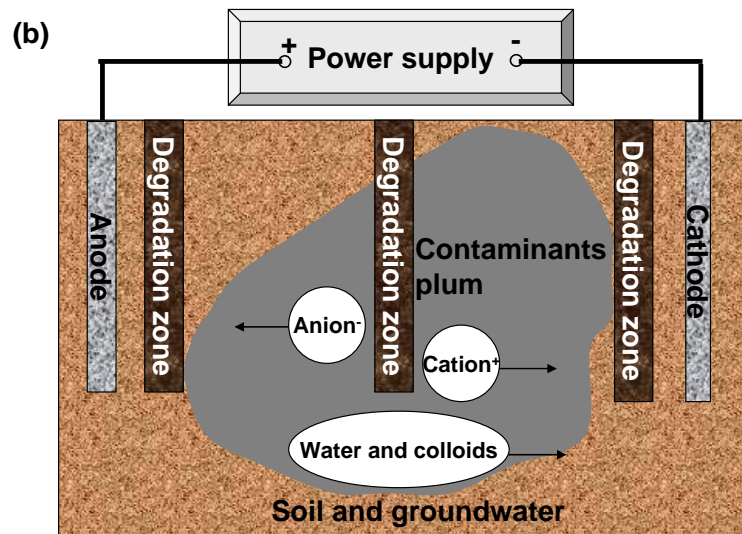
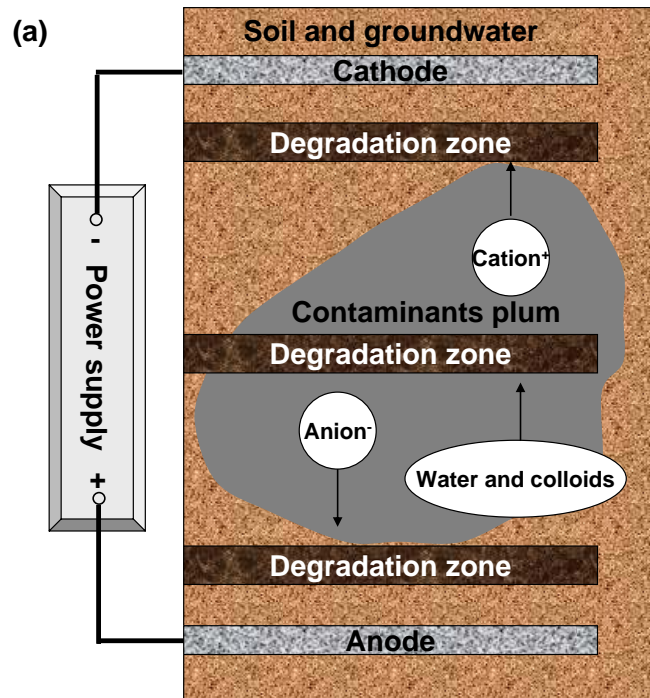


Figure 2-2. Conceptual model for the (a) horizontal and (b) vertical Lasagna process

(Figures adapted from [33])

Like the general electrokinetic process, the Lasagna process also heavily disrupts the local pore water flow, and the contaminants treatment occurs in a specifically defined treatment zone, which is different from the electrode sediment cap where the decontamination takes place on and in the vicinity of the electrodes surface.

Electrolytic treatment of contaminated water/wastewater and porous media

Electrolytic treatment focuses on the oxidation or reduction of contaminants to transform the contaminants. Electrolytic reactions have been extensively studied for the removal of a variety of compounds from wastewater [3, 34-36] as well as in porous media [37-39]. Electrochemical degradation of contaminants taking place in porous media undergoes the same chemical oxidation/reduction reactions as in water, but surface phenomena (such as adsorption/desorption and mass transfer resistance in soil or sediment pores) make the overall process in porous media more complicated. Lab- and pilot- scale studies have been established on the metals immobilization [4], chlorinated solvents dechlorination [40, 41], aromatics oxidation [5], etc.. In some of the electrolytic process, indigenous or cultured microbes were added to the treated soil or sediment to enhance the treatment performance [4, 5, 38]. In these studies, contaminated water or soil was introduced in batch or column reactors, where a pair (sometimes a couple of pairs) of electrodes was inserted. The contaminants approach the electrodes not by electroosmosis, electromigration, or electrophoresis, but by flow

convection. Electrode-stimulated reduction and/or oxidation transforms the contaminants to less toxic form, therefore reduces the risk concern.

The electrolytic reactive barrier (e-barrier) is one of the very few example of electrolytic treatment applied in field. The e-barrier couples electrolytic reactions to the application of permeable reactive barrier. Rather than placing electrodes across the whole contaminated area as the electrokinetic process does, the e-barrier is consisted by a pair of closely spaced electrodes perpendicular to the groundwater flow direction, and destruct the contaminants through reduction/oxidation reactions (Figure 2-3). Contaminants can be removed by the e-barrier through: (1) direct contaminants electrolysis on electrode surface (heterogeneous reaction), (2) reaction between contaminants and the produced hydrogen or oxygen (homogeneous reaction), and (3) reaction between contaminants and the produced free radicals (e.g., $\cdot\text{OH}$ generated by dissolved oxygen reduction at cathode or water oxidation at the anode) [42]. The e-barrier is an emerging technology that has yet to be commercialized, but the removal of contaminants such as energetic compounds and chlorinated solvents have been tested in lab and field studies [42, 43].

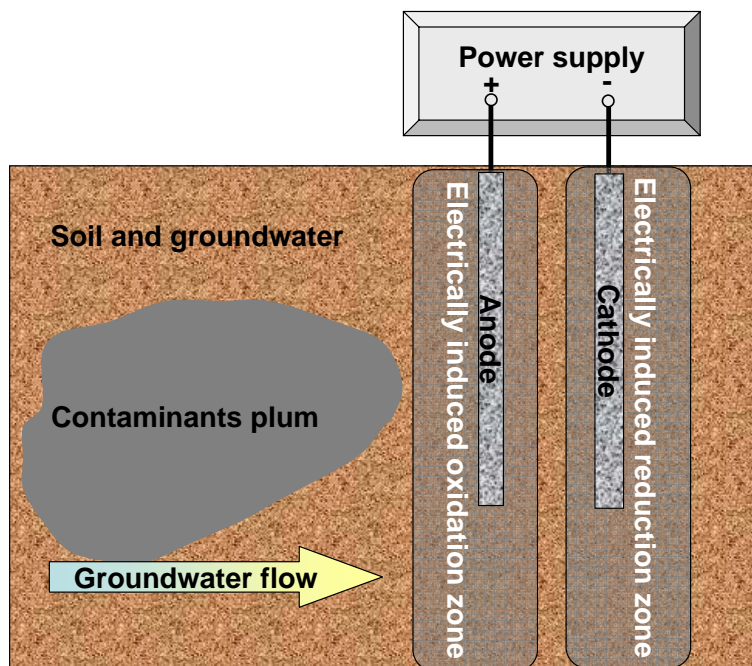


Figure 2-3. Conceptual model for the e-barrier

(Figure adapted from [44])

The concept of the e-barrier is very close to the reactive sediment cap. They are both minimally disruptive to the local hydrologic conditions, and both remove contaminants through electrode-stimulated reactions. However, the reactive cap extends the function of the e-barrier by including both abiotic and biotic reactions. The reactive cap may stimulate intrinsic microbial activity to transform the contaminants either via the electrolytically generated hydrogen (at the cathode) and oxygen (at the anode), or through the direct respiration to the electrodes themselves (see Chapter 5 for further discussion). Such process has been preliminarily demonstrated by the fact that carbon electrodes can enhance PAHs biodegradation and increase numbers of PAHs degrading

genes in sediment slurries and in sand cap above contaminated sediment [45]. Similarly, PCBs removal can also be enhanced by titanium electrodes in sediment-water microcosms [46].

2.2 Sediment remediation technologies

Contaminated sediments are challenging to remediate. The contamination is often spread over large areas and the site characteristics are dynamic and heterogeneous. Sediments are subject to modification and mixing by flooding, winter ice, and boat traffic. Moreover, engineering construction in an aquatic environment usually is more challenging and costly than in other media, thus remediation technologies for sediment are not as established as for soil and groundwater. The proper remedial approach is selected on case-by-case basis.

2.2.1 Conventional sediment remediation technologies

The most commonly utilized strategies are monitored natural attenuation, dredging, and *in situ* capping [47].

Monitored natural attenuation

Monitored natural attenuation (MNA) is a technique used to monitor the progress of natural attenuation processes to manage contaminated sediment. It relies on natural

occurring processes, including dispersion, dilution, sorption, volatilization, chemical or biologic transformation of contaminants, as well as the natural burial of clean sediments, to contain, destroy, or reduce the concentration, bioavailability or toxicity of contaminants in sediment [1, 47].

Generally, MNA is not suitable for the sites with severe contamination and substantial risks to aquatic life, wildlife, and human health. Also, MNA does not work for the cases when the transformation products are more persistent and toxic than the original contaminants. Rather, it is likely to be effective after the contamination sources are controlled and the source zone has been cleaned up by active remediation strategies. It is also applied to the conditions when active methods are not practical or can not significantly shorten remediation time frame [1]. MNA has the advantages of low cost and less disruption to local environment and communities. However, it also has significant limitations of long remediation time frame, low public acceptance and potential risk of exposure by leaving untreated contaminants in place.

Dredging

Dredging effectively remove the contaminants by excavating the contaminated sediment from a water body. Once removed, the contaminated is usually transported for *ex situ* treatment and/or disposal. This method has been the most extensively used

for cleaning the Superfund sites with contaminated sediment. Over 100 sites have been dredged as at least an initial removal action [47].

Dredging is suitable for discrete areas with high concentration of contaminants. In some situations, combinations of dredging and MNA may be the best option. For example, the source zone of contamination can be removed by dredging, followed by MNA in the rest of the site [1].

Since the contaminated sediment been physically removed, dredging has the advantages of quickly achieving remedial goals and reduced future exposure risks. However, these advantages come with the price of extensive and costly infrastructure, the potential for contaminant re-suspension during dredging, destruction to the aquatic community and their habitat, and potential secondary contamination during dredged sediment transport and disposal [47]. Given the high cost and inefficiency of dredging, alternate technologies have been developed that provide *in situ* contaminant control and degradation, such as capping.

In situ capping

In situ capping is utilized for contaminant control at many sites. It isolates contaminants by placing clean material at the sediment-water interface, limiting the interactions of

contaminated sediment with the biologically active zone. Early capping remediation, also known as “passive capping”, uses materials such as clean sediment, sand, or gravel [48, 49] to cover the contaminated material. Recently developed “active capping” incorporates amendments to the capping material that better retain or degrade the contaminants. In this strategy, permeable or impermeable geotextiles, liners, and adsorbents in multiple layers [50-54] may be utilized. Compared to traditional caps, these amended caps can better constrain and sequester contaminants, thereby attenuating the flux of contaminants, while also reducing the thickness of the cap layer required over passive caps. In both cases, the caps are functionalized through physical and chemical isolation and stabilization [47].

As of 2004, *in situ* capping has been applied for the remediation of about fifteen Superfund contaminated sediment sites, serving as the primary approach for some sites, and been combined with dredging and/or MNA at other sites. Site conditions are especially conducive to *in situ* capping when there are (1) sufficient water depth, (2) limited or less important habitat disruption, and (3) high engineering feasibility (readily-available material, a compatible infrastructure, easily controlled disruption during construction, favorable hydrodynamic and geochemical conditions, and adequate mechanical support of sediment exists) [47].

The advantages of *in situ* capping include; immediate exposure reduction and less infrastructure requirements and waste disposal compared to dredging. However, like MNA, capping has the intrinsic limitation of retaining the contaminated sediment in the aquatic environment, leading to a long-term risk associated with contaminant re-exposure if the cap loses its integrity or sequestration capacity [47]. Further, the record of decision for remediation of many contaminated sediments most often stipulates some degree of contaminant mass removal which requires either dredging of sediments or degradation of the contaminants *in situ*. While *in situ* capping technologies have been effective for short-term reduction of risk, the contaminant mass remains in place. Thus, new technologies are needed which can provide *in situ* contaminant degradation.

2.2.2 Other emerging alternatives

Due to the inherent limitations of MNA, dredging and capping strategies, there has been remarkable increase in recent development of sediment contaminants degradation. These strategies rely on the amendment of chemicals to induce biological and/or chemical contaminant degradation to the sediment or cap. The goal is to reduce contaminant mass while limiting disturbance of the contaminated sediment.

In situ biological and chemical treatment

In situ sediments treatment involves the stimulation of biological and/or chemical contaminant degradation. This strategy is primarily under development at the bench-scale and pilot-scale level. Biological contaminant degradation can be stimulated by adding electron acceptors (e.g., oxygen, nitrate or sulfate), electron donors (e.g., hydrogen or fermentable organic substrates), nutrients, and/or microorganisms into the sediment. Chemical treatment aims to enhance contaminants transformation by oxidation (e.g., for PAHs), reduction (e.g., for PCBs) or stabilization (e.g., for metals) by providing chemical reagents, such as hydrogen peroxide, zero-valent iron, or lime stone into the sediment. Although these approaches are promising, most of them are in the early stages of development, and few methods are currently commercially available, mainly due to the technical limitations such as the ability to effectively deliver and mix reagents *in situ* [47].

Reactive materials amended capping

Another innovative *in situ* sediment remediation strategy under development is “reactive capping”. It combines the advantages of both traditional capping and biological/chemical treatment. Not only does the cap function as a physical barrier to isolate the contaminated sediments, but it also makes use of reactive materials that can degrade the contaminants as the key components of the cap. Thus the reactive cap can potentially offer a long-term solution to sediment contamination by reducing the

exposure risk. Given the caps that can degrade contaminants rapidly enough to eliminate contaminant flux to the overlying water body, it significantly reducing the cap thickness required for contaminants sequestration. These advantages make the development of technically feasible and cost-effective reactive caps advantageous for contaminated sediment control.

Several lab studies have shown the promising future for amendment of reactive materials into sediment caps. A recent example of an abiotic reactive cap strategy was designed for 2-chlorobiphenyl simultaneous adsorption and dechlorination by granular activated carbon impregnated with reactive iron/palladium bimetallic nanoparticles by Choi *et al* [55]. The non-chlorinated product, biphenyl, is less toxic and more readily oxidized by bacteria in the sediment. There has also been recent development of biologically reactive caps. Hyun *et al* [56] reported that a microbial active sand cap on a coal tar-contaminated river sediment amended with oxygen and nutrients stimulated microbial contaminant degradation and reduced contaminant flux to the water column. It was also suggested that natural attenuation of chlorinated solvents can occur under capping conditions, but complete dechlorination can be only achieved when microorganisms present in the sediment were provided with electron donor [57]. Reactive caps utilizing both abiotic and biotic contaminants degradation have also been explored. Sun *et al* [58] demonstrated nitrobenzene reduction in a cap integrated with

cinder (extrusive igneous volcanic rock) and Fe(0) and pre-incubated nitrobenzene degrading bacteria.

Despite these promising findings, materials and methods to enhance contaminant degradation in sediment caps are limited. Very few, if any, cost-effective materials have been identified which stimulate contaminant degradation over the long timescales (perhaps decades to centuries) required for *in situ* sediment remediation. Also, currently available reactive cap strategies still have the delivery and mixing problems as encountered by other *in situ* biological and chemical treatment. Therefore, the work described in chapter 3 to 5 investigated the feasibility and performance of an electrode-based sediment cap to facilitate transformations and detoxification of contaminants, and reduce risk to the ecological and human health.

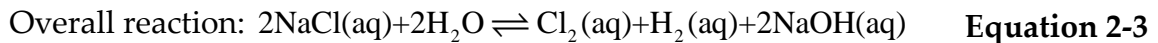
2.3 Electrode-base chloride/bromide oxidation

As valuable commercial products, chlorine gas and bromine liquid are produced in industry by oxidizing their corresponding ions (Cl⁻, Br⁻). Brine and seawater are common sources for the halogen ions. Electrolytic chloride oxidation process in chlor-alkali industry, as well as indirect bromide oxidation process in bromide industry is extensively studied and successfully commercialized for decades. Direct electrolytic

bromide oxidation in brine and fresh water were also reported recently. These studies provide a potential method for bromide removal from brine produced by hydraulic fracturing gas mining.

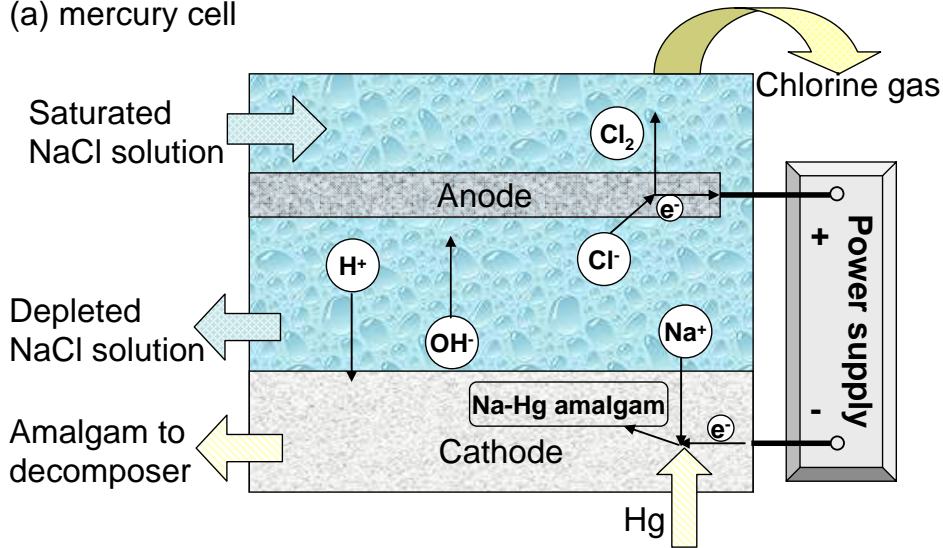
Industrial chlorine production: Chlor-alkali process

In chlor-alkali industry, chlorine is produced by electrolysis of aqueous sodium chloride (normally natural brine), with sodium hydroxide and hydrogen as the secondary products. The half-cell reactions and the overall reaction are as Equation 2-1 through Equation 2-3. However, in some cases an oxygen cathode is used in alternative, as shown in Equation 2-4.

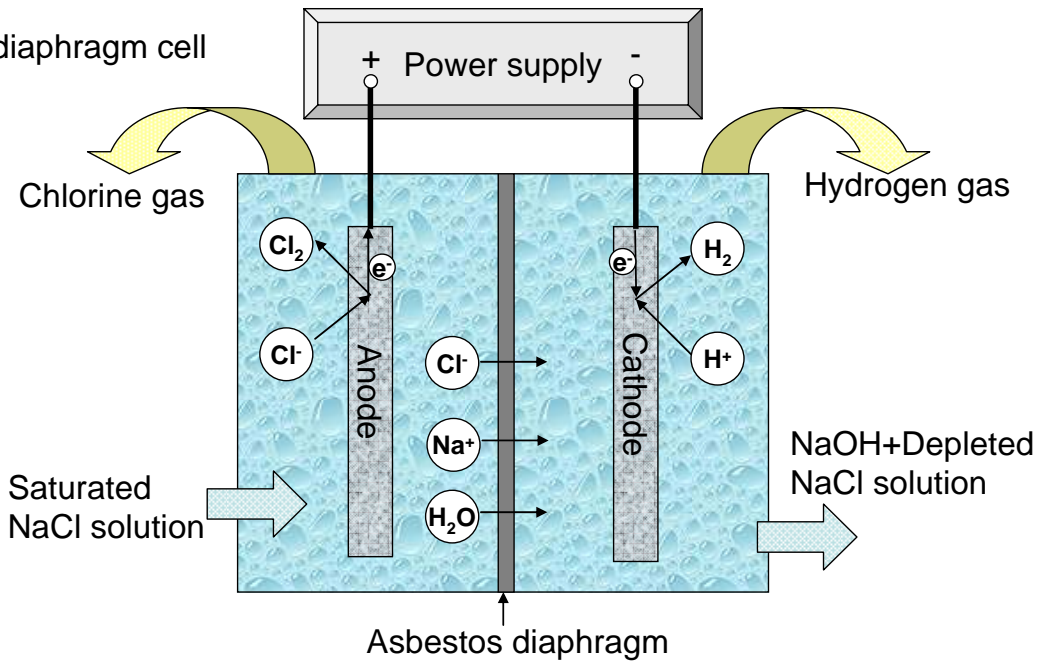


Three main categories of cell configurations dominate the chlor-alkali process: diaphragm cell and membrane cells. Their working principles are illustrated in Figure 2-4. Some typical operation data are summarized in Table 2-1.

(a) mercury cell



(b) diaphragm cell



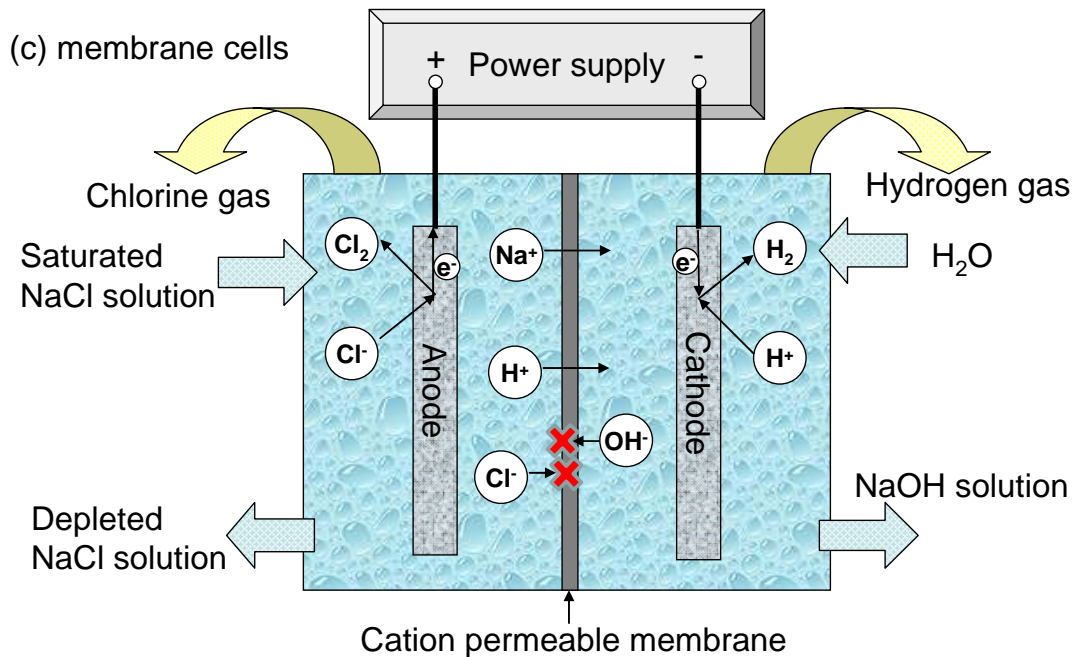


Figure 2-4. Scheme of cell configurations used in chlor-alkali process

(Figure adapted from [59])

Table 2-1. Typical data for commercial chlor-alkali cells

(Table reproduced from [60])

	Mercury cell	Diaphragm cell	Membrane cell
Cell voltage (V)	4.4	3.45	3.5
Current density (A/cm ²)	1.0	0.2	0.45
Current efficiency for Cl ₂ (%)	97	96	93
Energy consumption for electrolysis (kWh/ton NaOH)	3150	2550	2700
Production rate/single cell (tons NaOH/year)	5000	1000	100

Graphite or other forms of carbon are typical anode materials throughout the history of chlor-alkali process, with the corrosion rate of 5-7 lb per ton of chlorine produced [60].

Titanium based electrodes coated with transition metal oxides (e.g., ruthenium dioxide, cobaltic oxide), namely dimensionally stable anodes (DSA) were also developed and began to replace graphite anodes since early 1960s. Mercury and steel (or nickel alloys coated steel) are used as cathodes.

Industrial bromine production

Industrial bromine production does not use similar direct electrolysis as in chlor-alkali process. Rather, bromide is oxidized to bromine by chlorine gas as described in Equation 2-5 in an acidified solution. Bromine is produced in dissolved form in brine, stripped out using air or steam, and sequentially recovered in a commercially desirable form (such as converting bromine in air into ferric bromide through reaction with iron turnings). The whole process can be illustrated in Figure 2-5.



Industrial bromine production also uses natural brines or seawater as raw material for obtaining elemental bromine. Chlorine can be introduced to the brine in variety of means: blowing gaseous chlorine, adding equivalent reagents (e.g., bleach), or on-site electrolysis of the brine (the same procedure as in the chlor-alkali process, as described in previous section) [61].

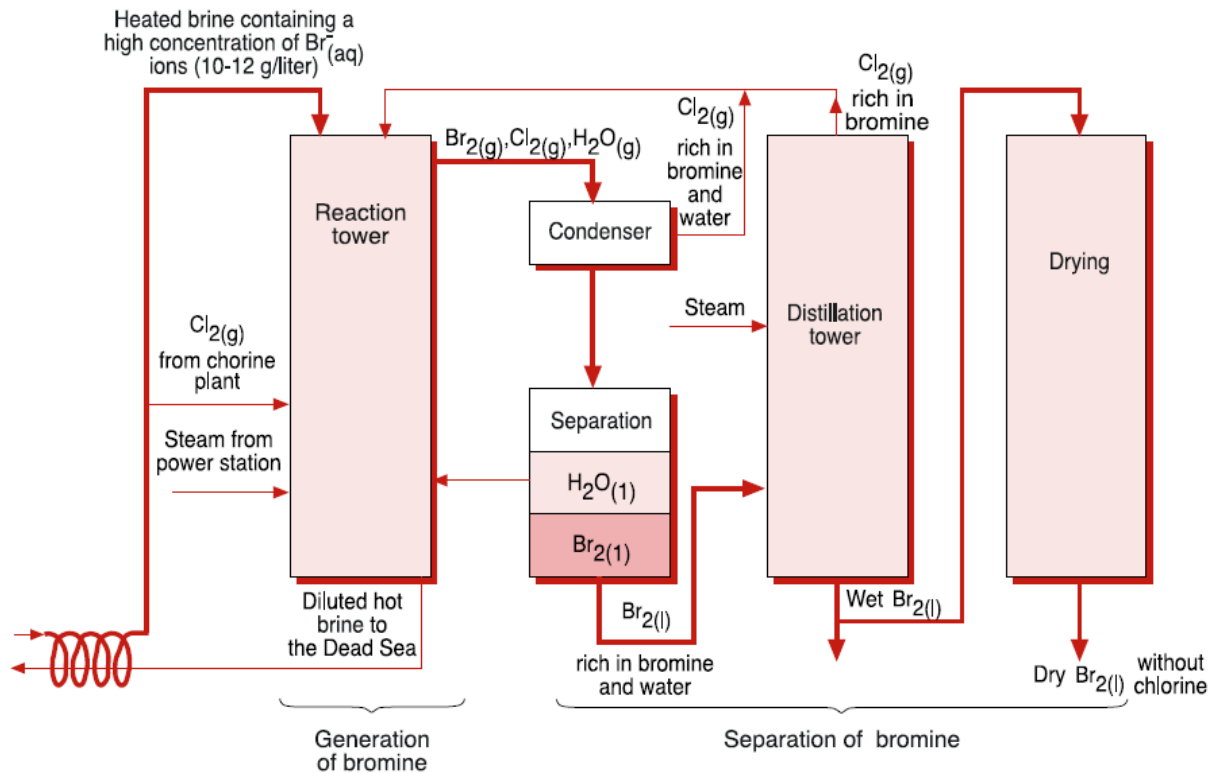


Figure 2-5. Flow chart of commercial bromine production process

(Figure reproduced from [62])

Direct electrolytic bromide oxidation in brine

Recent studies have been developed to directly oxidize bromide to bromine (Equation 2-6) by electrodes instead of chlorine. Yalcin *et al* [63] examined the electrolysis of seawater bittern from a thermodynamic point of view, reporting the possibility of oxidizing bromide to bromine with graphite and platinum as the anode and cathode, respectively. During electrolysis, the anode potential was controlled to achieve about half of the bromide removal without chlorine evolution. However this study was

preliminary and theoretical and no further details were given. Qi and Savinell [64, 65] developed a continuous flow-through system using porous graphite felt electrodes to directly oxidize bromide for bromine production from synthesized brine with high concentration of chloride (3 M NaCl/0.05 M NaBr/0.001 M HCl). Their work focused on electrochemical modeling; bromide removal and bromine recovery was not described.



Direct electrolytic bromide oxidation in fresh water

Industrial bromide oxidation focuses on bromine production, while not necessarily caring about the residual bromide concentration of the processed brine. However, there are environmental concerns about bromide discharges into drinking water sources, which can lead to the formation of carcinogenic brominated disinfection byproducts (DBPs) during water treatment, as discussed in Chapter 1. Also, the bromide in surface or ground water may be at very low but still risky concentration, and the removal becomes prohibitively expensive. Therefore, although the techniques for industrial bromide oxidation are mature, its implementation for water treatment processes is also interesting. Direct bromide removal by electrolysis (Equation 2-6) has been examined for treatment of surface water as a drinking water source [66, 67], and removal of low level of bromide (~200 ppb) was achieved with bromide residual at ~10 ppb. A similar process was patented using dimensionally stable anodes (DSA) for bromide removal

from drinking water [68]. However, the voltage used in these studies was high enough to cause chlorine and oxygen production, which is energetically expensive. Also, it is not clear the bromine produced in such condition was formed by direct electrolysis or oxidized by *in situ* electro-generated chlorine.

Electrochemical disinfection

Recent studies have been reported on site generation of chlorine or bromine using electrodes as an alternative to the traditional chlorination, referred as “electrochemical disinfection”. Among these processes, electro-generation of chlorine utilizes the same reaction as for the chlor-alkali process (Equation 2-1) and electro-generation of bromine utilizes analogs of the bromide oxidation reaction (Equation 2-6). Various electrode materials and electrochemical cell configurations have been explored against a wide variety of microorganisms [69].

2.4 Other bromide removal methods

Silver-doped activated carbon aerogels adsorption [70] and aluminum coagulation [71] have been proposed to remove low concentrations of bromide, but high chloride concentrations render this approach ineffectual. Other currently available water treatment technologies can not specifically extract bromide from water, but rather

remove it together with other dissolved solids. Removal of TDS, as referred to desalination, has been widely studied using seawater to produce portable water in arid climates and near marine water sources. Available desalination techniques include thermal distillation, ion exchange, reverse osmosis, forward osmosis, nanofiltration, ultrafiltration, electrodialysis, reverse electrodialysis, electrodeionization, and capacitive deionization. However, all of them require enormous energy input, and become economically infeasible considering the quantity and quality of the mining brine [10].

Chapter 3. Redox control and hydrogen production in sediment caps using carbon cloth electrodes^①

Abstract

Sediment caps that degrade contaminants can improve their ability to contain contaminants relative to sand and sorbent-amended caps, but few methods to enhance contaminant degradation in sediment caps are available. The objective of this study was to determine if powered carbon electrodes emplaced within a sediment cap could create a redox gradient and provide electron donor for the potential degradation of contaminants. In a simulated sand cap overlying the sediment from the Anacostia River (Washington, DC), electrochemically induced redox gradients were developed within 3 days and maintained over the period of the test (~100 days). Hydrogen and oxygen were produced by water electrolysis at the electrode surfaces and may serve as electron donor and acceptor for contaminant degradation. Electrochemical and geochemical factors that may influence hydrogen production were studied. Hydrogen production displayed zero order kinetics with ~75% current efficiency. The production rate was proportional to the applied voltage between 2.5V to 5V, and not greatly affected by pH or presence of divalent metal ions. Hydrogen production was promoted by increasing

^① This chapter was published in *Environmental Science & Technology* in 2010 under the title “Redox control and hydrogen production in sediment caps using carbon cloth electrodes”.

ionic strength and in the presence of natural organic matter. These findings suggest that electrochemical reactive capping can potentially be used to create “reactive” sediments caps capable of promoting chemical or biological transformations of contaminants within the cap.

3.1 Introduction

Contaminated sediments often contain complex mixtures of toxic anthropogenic organic and inorganic contaminants, and are ubiquitous and costly to remediate [72]. The high cost and limited effectiveness of dredging [73-75], and slow rates of monitored natural recovery [76], lead to the use of *in situ* sediment caps for abatement of risk from contaminated sediments. However, capping does not necessarily provide removal or detoxification, and the risk to human and environmental health may return once the capping material becomes saturated. Reactive caps which include a reactive component for biotic or abiotic contaminant degradation have been proposed and have great potential advantages in contaminant degradation for sediment remediation.

The redox gradient in the cap is crucial for sediment remediation, because it plays an important role in the availability of electron donors/acceptors for contaminant transformation. Redox stratification develops naturally below the sediment water interface as the result of the indigenous microbial activity. Depth-dependent microbial populations varying with the stratified geochemical redox zones within a sand sediment cap have been observed [77]. The chemical species in each stratified zone indicated a corresponding biogeochemical process and led to the suggestion that microbial contaminant degradation may be engineered within a reactive sediment cap

[9]. By placing electrodes in the sediment cap and applying an external voltage, a desired redox gradient can be established and reinforced in the cap to affect contaminant degradation. This engineered redox gradient will drive the evolution of microbial populations, facilitate their localization and function with respect to contaminant degradation.

The electrode-based reactive cap may also support contaminants degradation by providing electron acceptor (oxygen) and donor (hydrogen) from water electrolysis at the anode and cathode, respectively. The ability to stimulate desirable microbial populations for biodegradation will also depend on the *in situ* concentrations of oxygen and hydrogen, and therefore on their rates of evolution from the electrodes.

The specific objectives of this study are to 1) engineer redox gradients in a simulated sediment cap with carbon electrodes; 2) study the impact of various geochemical porewater parameters and electrochemical conditions on hydrogen production rate from the cathode.

3.2 Materials and methods

Chemicals

All the chemicals used are reagent grade unless otherwise noted. Sodium bicarbonate (NaHCO_3), sodium chloride (NaCl), calcium chloride ($\text{CaCl}_2 \cdot 2\text{H}_2\text{O}$), sodium hydroxide (NaOH) and chloride acid (HCl) were supplied by Fisher Scientific (Pittsburgh, PA). Magnesium chloride ($\text{MgCl}_2 \cdot 6\text{H}_2\text{O}$) was purchased from ICN Biomedicals Inc (Costa Mesa, CA). Humic acid sodium salt (50-60% as humic acid) was purchased from Acros Organics (Geel, Belgium). Hydrogen standard (1%) and nitrogen were purchased from Butler Gas Products (Pittsburgh, PA).

Electrode materials

Carbon materials were chosen because of their low price, resistance to poisoning, and flexible and porous texture for easier application with existing cap technology. Woven carbon cloth (BASF Fuel Cell, Inc., Somerset, NJ) was used as both cathode and anode in all experiments.

Engineered Redox Gradient in sediment

Three T-cell reactors were used to evaluate the ability of carbon electrodes to control the redox gradient in a sand cap overlying Anacostia River (Washington, DC) sediment (Figure 3-1a). The reactor, as described elsewhere [49], was filled with sieved (2mm) sediment from the Anacostia River at room temperature ($23 \pm 2^\circ\text{C}$). A 14cm \times 7cm carbon cloth was placed on top of the sediment as the cathode. A 2.5-cm layer of sieved

(0.425mm) sand (Riccelli Enterprises, Rush NY) was placed over the cathode and a second, identical, carbon cloth on the sand layer as the anode, followed by a 0.5cm sand layer. The sediment and sand layers were saturated with tap water. The electrodes of T-cell 1 and T-cell 2 were connected by copper wire to 4V Extech 382202 DC power supply (Extech Instruments Corp., Waltham, MA). Power to T-cell 1 was continuously applied for ~100 days whereas power to T-cell 2 was removed after 30 days of continuous operation in order to examine the recovery of the sediment cap following stimulation. A third T-cell served as an unpowered control reactor. The potential was continuously applied except during microelectrode pH and Oxidation-Reduction Potential (ORP) measurement. pH was measured by MI-405 pH microelectrode (Microelectrodes Inc, Bedford, New Hampshire) and ORP was measured by Pt microelectrode against Ag/AgCl reference (fabricated as described elsewhere [78]). pH and ORP measurement required 2 and 5 minutes, respectively, to reach equilibrium. Vertical profiles of pH and ORP from the water-sand interface to a depth of 44 mm with 2 mm intervals were acquired and ORP data were converted and reported as versus standard hydrogen electrode (SHE).

Geochemical Impacts on Electron Donor Supply Rate

Experiments to evaluate the impact of environmentally relevant geochemical porewater parameters on H₂ production were carried out in triplicate H-cell reactors (Figure 3-1b)

described elsewhere [3]. The two chambers were separated by a cation-exchange membrane (Nafion 117; Electrosynthesis Inc., Lancaster, NY). Electrodes were 12.6cm × 6.25cm carbon cloth. The electrodes were connected to an E3620A DC power supply (Agilent Technologies, Santa Clara CA) via 0.64-cm diameter × 15.2-cm graphite rods (GraphiteStore.com, Inc., Buffalo Grove, IL) by graphite epoxy (377H; Epoxy Technology, Inc., Billerica, MA). The reactors were completely mixed by magnetic stir bars at room temperature. Both cathode and anode chambers contained 250ml buffer solution and 60ml headspace. Unless specified, the buffer solution contained 20mM NaHCO₃ and 20mM NaCl (as supporting electrolyte, conductivity ~4mS/cm). Buffer solution was prepared anaerobically and pH adjusted by HCl or NaOH. Identical control experiments using the same tap water as used in the T-cell experiments were also performed to verify comparison and showed same results as in DI water (results not presented).

The electrolyte pH in the H-cell was measured using a gel-filled 8mm pH electrode (Fisher Scientific, Pittsburgh, PA). Current was recorded by a Model 2700 digital multimeter (Keithley Instruments, Inc., Cleveland, Ohio). Headspace H₂ concentration was determined using GC/TCD as described elsewhere [79].

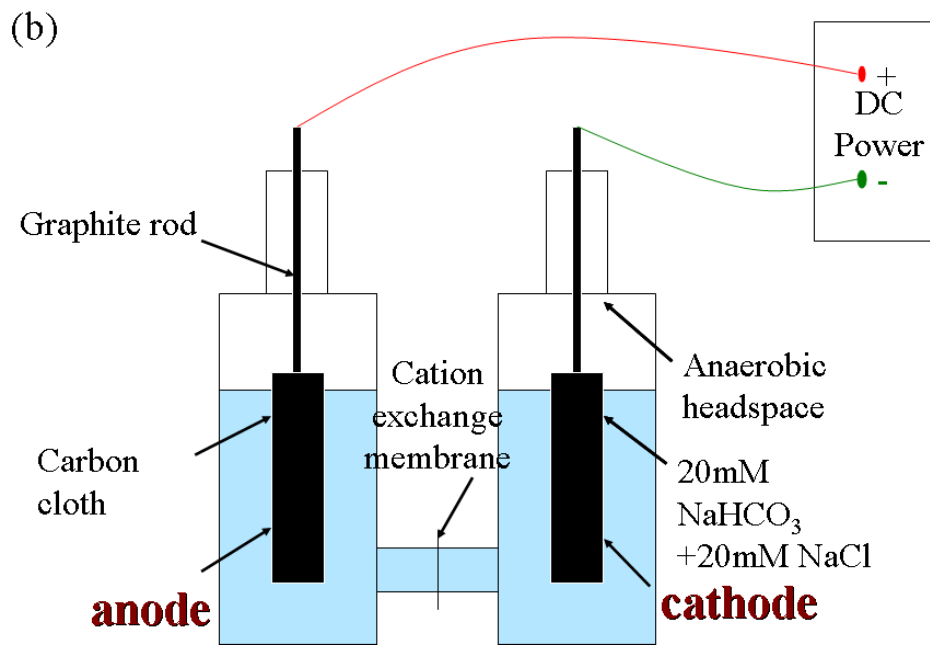
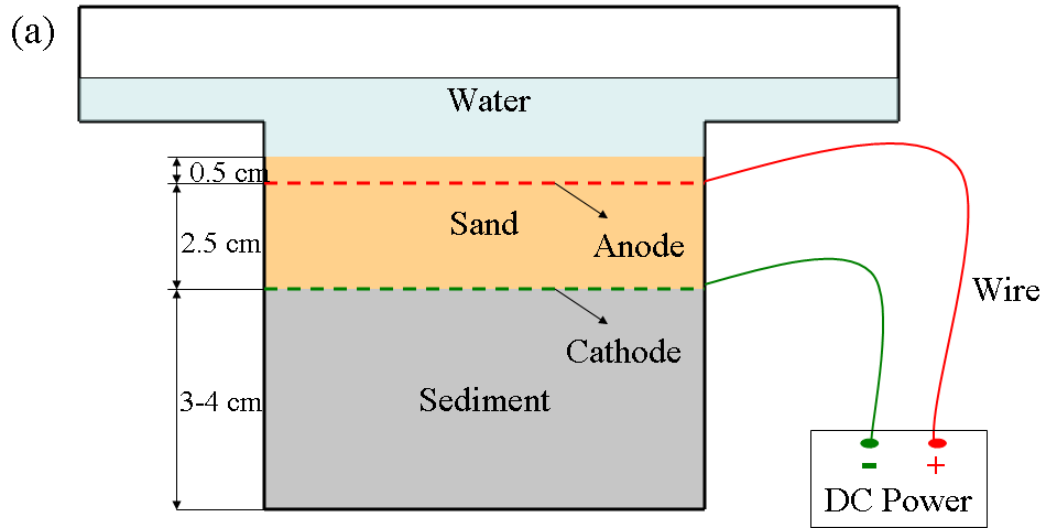


Figure 3-1. Scheme (side view) of (a) the T-cell reactors for studying sediment cap redox control and (b) the H-cell reactors for studying the geochemical effects on hydrogen production rate.

Calculation of hydrogen production rate and current efficiency

The hydrogen concentrations in headspace of the H-cell reactors were monitored over 24 hours, and cumulative hydrogen production (n_{H_2}) was calculated according to Henry's Law, assuming equilibrium between headspace and aqueous phases (Equation 3-1):

$$n_{H_2} = C_{H_2,a}V_a + C_{H_2,w}V_w = C_{H_2,a}V_a + \frac{C_{H_2,a}}{K_H}V_w \quad (\text{mol}) \quad \text{Equation 3-1}$$

Where $C_{H_2,a}$ and $C_{H_2,w}$ are the air and water phase hydrogen concentration, respectively (mol/L); V_a and V_w are the volume of air and water in H-cells, respectively (L); K_H is the Henry's constant for hydrogen (1260 bar/mol/L) at 25°C.

The hydrogen production reaction was fitted using a zero-order kinetic reaction and the rate constants were normalized to electrode surface area to compare with rates observed in other reports.

Current efficiency (η), an estimation of the fraction of the current captured as hydrogen, was calculated as the ratio of measured cumulative hydrogen production (n_{H_2}) to the theoretical hydrogen production ($n_{H_2,t}$) (Equation 3-2):

$$\eta = \frac{n_{H_2}}{n_{H_2,t}} \times 100\% \quad (\text{dimensionless}) \quad \text{Equation 3-2}$$

Where theoretical hydrogen production ($n_{H_2,t}$) was calculated by integrating current equivalent with time (Equation 3-3):

$$n_{H_2,t} = \frac{\int_0^{t_{\text{total}}} I dt}{nF} \quad (\text{mol}) \quad \text{Equation 3-3}$$

I is the current (A), n (=2) is the number of electrons to form one hydrogen molecule; t_{total} is the total reaction time (s); F the Faradic constant (96485 C/mol).

3.3 Results and discussions

Redox control and pH change in sediment

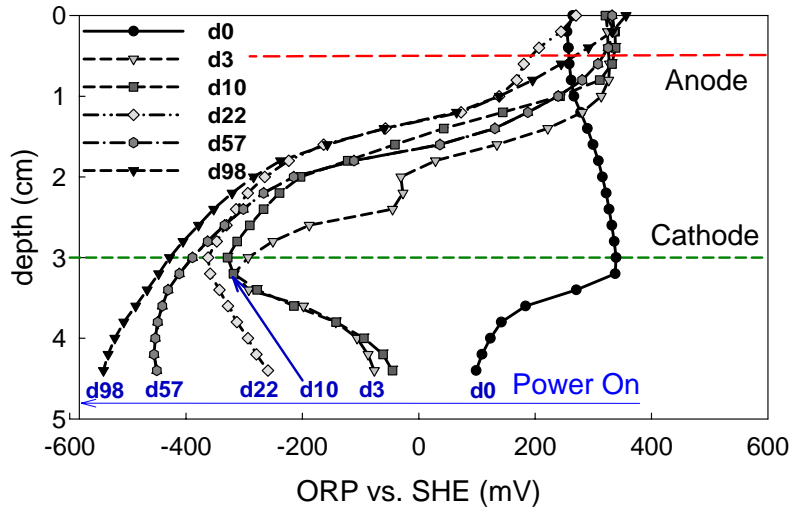
Poised electrodes emplaced in a sediment cap rapidly established a depth-dependent stratification of redox potential over Anacostia river sediment (Figure 3-2 shows data in selected days, all the data are shown in Appendix Figure A-1). A 4V applied voltage was chosen to ensure adequate hydrogen evolution as detailed later. Prior to the application of voltage, the ORP at the anode was +270mV and increased with depth through the sand cap to around +350mV at the cathode. The sediment below the cathode became more reduced with depth, a likely result of natural microbial processes [9]. After 3 days with applied voltage between the electrodes, the ORP in the vicinity of the anode had slightly increased to near +350mV and the ORP in the vicinity of the cathode had decreased sharply to approximately -300mV. The ORP measured in both

powered T-cell reactors changed similarly under applied voltage, indicating reproducibility; the redox conditions stratified through the sediment cap and developed a relative steady state after approximately one month. T-cell 2 was disconnected from the power supply on day 30 to monitor the ORP during recovery. The depth-dependent stratification of ORP through the sand cap in T-cell 1 continued until day 98. In contrast, ORP stratification in T-cell 2 gradually diminished after the power off (Figure 3-2b): on day 98, the ORP in the vicinity of the anode was +240mV and near the cathode, +210mV. Over the course of the experiment, the control T-cell 3 (with imbedded, but unpowered electrodes), remained oxidizing in the vicinity of and between both anode and electrodes (Figure 3-2c).

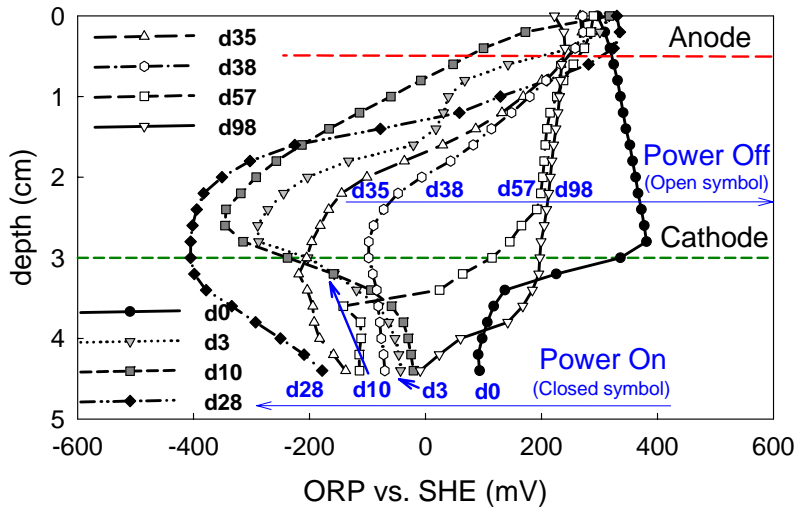
A depth dependent stratification of redox conditions in the control reactors was only observed within the sediment but not in the cap. Such gradients develop naturally under the sediment-water interface and are indicative of the microbial oxidation of sediment organic matter coupled to the reduction of terminal electron acceptors in an order which reflects the maximum energy yield for the microbial community [80]. By applying a voltage through the electrodes, however, the location and size of the respective oxidation and reduction zones can be controlled.

The pH profile in the sand cap demonstrated a similar, depth-dependent gradient (Figure 3-2d and e). On day 0, the pH between the anode and cathode in all T-cells varied from around 8 at the anode to 6.5 at the cathode. Soon after external power application, the pH gradient through the cap increased sharply: pH in the vicinity of the anode dropped while near the cathode, the pH changed from circumneutral to near pH 11 on approximately day 9. The pH in the control reactor remained relatively steady with time and depth (Figure 3-2f). The rapid increase of pH near the cathode is the result of the reduction of water-derived protons for H₂ formation. Following removal of power from T-cell 2 on day 30, the pH began to return to circum neutral, but did not completely recover over the course of the experiment (Figure 3-2e). The pH change was expected in this system since no buffer was added to balance the buildup of H⁺ and OH⁻ at the electrodes. Under field conditions, such large pH increases would not be expected; since under field conditions, sediment porewater may be buffered by solid and dissolved organic and inorganic acid/base in the cap, and porewater seep may flush excessive H⁺ to the anode to neutralize excessive OH⁻ [40]. The addition of modest amounts of a buffering solids in the cap design, e.g. iron carbonate (siderite), could maintain pH if needed.

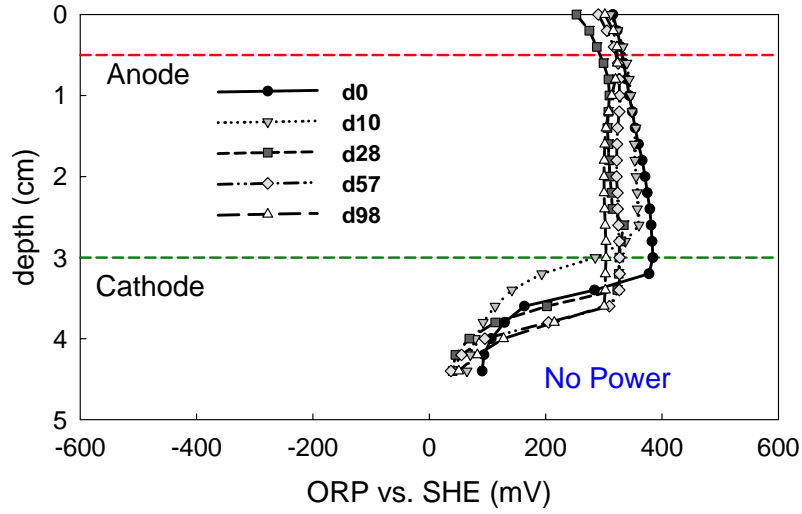
(a) ORP in T-cell 1



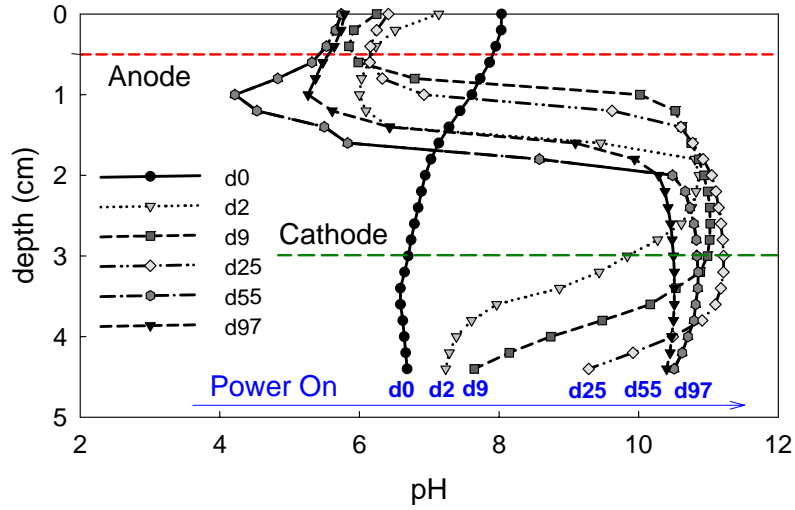
(b) ORP in T-cell 2



(c) ORP in T-cell 3



(d) pH in T-cell 1



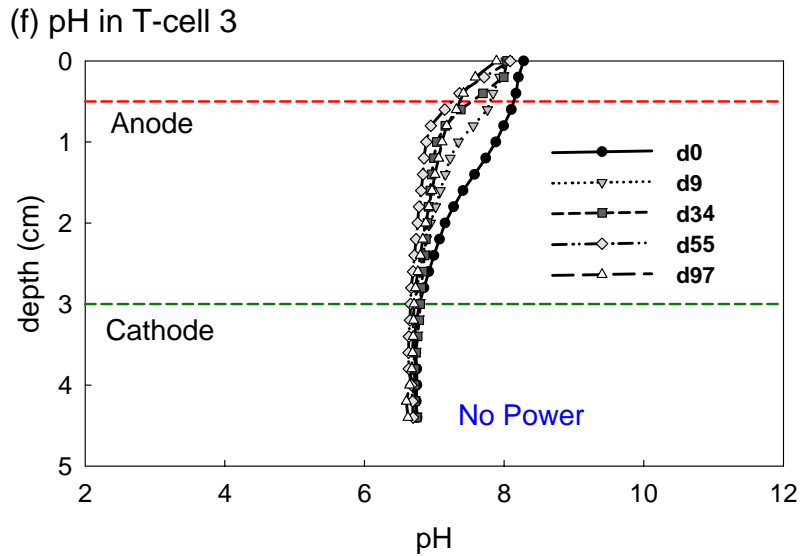
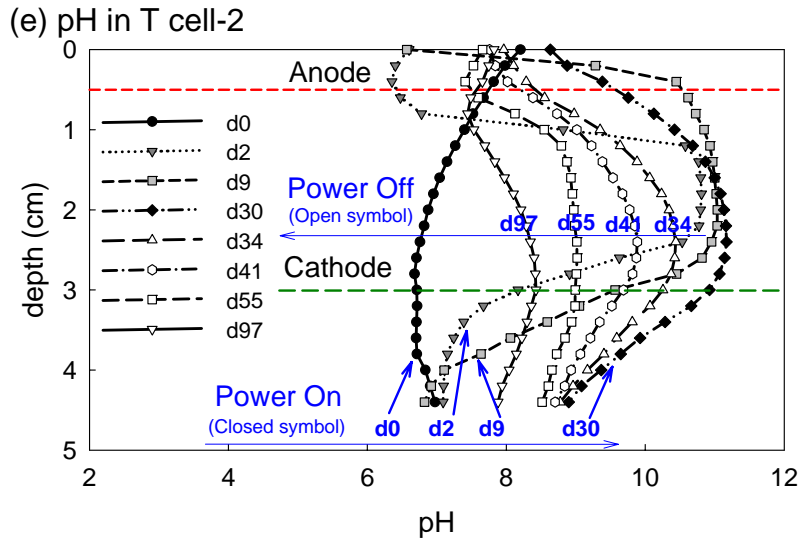


Figure 3-2. (a, b, c) Vertical ORP and (d, e, f) pH profiles developed in sediment and cap containing carbon cloth electrodes (T-cell 1 and T-cell 2) imposed to a 4V external voltage (a~d) or in control sediment (e, f)

T-cell 1: powered connected over ~100 days. T-cell 2: power connected until day 30. T-cell 3: unpowered electrodes control. The horizontal dashed lines indicate the position of electrodes.

Hydrogen production rate and current efficiency

H₂ evolution from the carbon electrode displayed zero-order kinetics. At 4V applied voltage, the electrode surface area normalized rate constant was 5 mmol H₂ m⁻² hr⁻¹ (Figure 3-3a), despite an increase in pH from 7 to 9.5. The zero-order kinetic relationship agrees with a previous report of hydrogen production from carbon-based electrodes[81]. Over 24 hours the current efficiency was about 75% (Figure 3-3b), indicating that 25% of the current flow between the electrodes was not captured as H₂. This was not surprising as H₂ was detected on the anode side of the H-cell, suggesting a diffusion loss through the Nafion membrane. Additionally, O₂ produced at the anode may also diffuse through the membrane [82] and consume electrons at the cathode. Non-Faradic current to maintain charge neutrality at the electrodes may also be a source of current which was not captured as electron equivalents in H₂ gas.

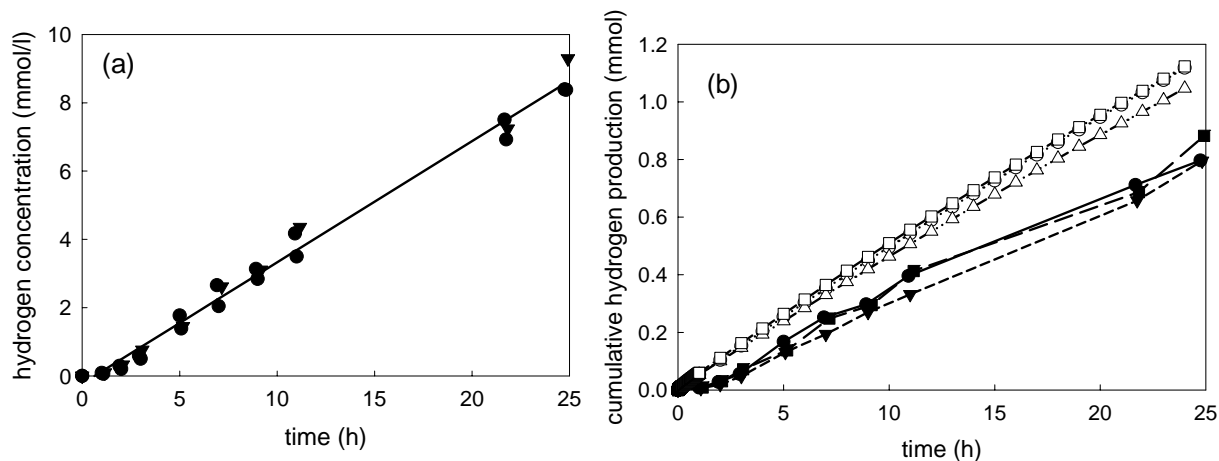


Figure 3-3. Hydrogen production at 4V applied voltage and initial pH 7 in 20 mM NaHCO₃ and 20 mM NaCl solution: (a) hydrogen concentration (b) and cumulative amount.

The three sets of symbols represent triplicate reactors. Solid line in (a) is best fit linear regression. Closed circles in (b) are measured hydrogen and open circles are integral current equivalent.

Influence of voltage and initial pH on hydrogen production

The theoretical equilibrium potential difference between the cathode and the anode necessary for water electrolysis is 1.23V [83]. Therefore hydrogen and oxygen accumulation requires a greater potential difference at the electrodes. In addition, overpotentials at the anode and cathode, resulting from activation and mass-transfer resistive losses as well as ohmic loss across the electrolytic cell, must be overcome for H₂ production to proceed. In order to address these concerns, experiments were performed

to evaluate H₂ production at various applied voltages using carbon cloth electrodes. When applied voltage was in the range of 2 - 5V, the observed current was between 0.5 – 5mA. H₂ production rate was proportional to the applied voltage above 2.5V (Figure 3-4a). There was no statistically significant difference between H₂ production rate at 2.0 and 2.5V. Since applied voltage is the driving force for water electrolysis, the increase in H₂ production rate was not surprising. Similar findings with graphite electrodes are reported [82]. The relationship between applied voltage and H₂ production rate may enable real-time control of electron donor for microbial growth within the sediment cap, creating an impenetrable biobarrier if the contaminant degradation rate is sufficiently high relative to advection and diffusion through the cap [52].

Lower applied voltage produced lower H₂ evolution rates and resulted in smaller pH changes over the course of the experiment (Figure 3-4b). The pH changes are likely to be less of an issue during field applications, as the required rates of H₂ evolution are will be lower for degradation of contaminants present in low concentrations and, as described briefly above, migration of sediment porewater containing natural organic matter and alkalinity creates an elevated buffer capacity [84].

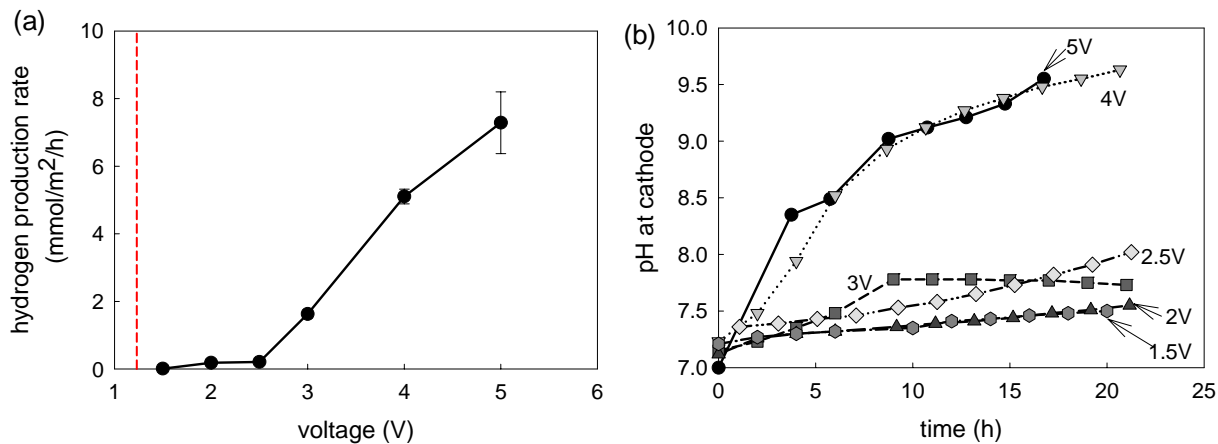


Figure 3-4. Influence of applied voltage on (a) hydrogen production rate and (b) cathode solution pH.

All experiments were conducted at an initial pH=7 in 20mM NaHCO₃ and 20mM NaCl solution over 24 hours. Dashed vertical line in (a) shows the equilibrium potential for water electrolysis. The results are the means of triplicate reactors, and error bars represent standard deviation.

However, the impact of pH on H₂ production rates was examined in the H-cell reactors (Figure 3-5). H₂ production rate was not greatly affected by initial pH at either 4V or 2.5V applied voltage. This result is consistent with the approximately zero-order kinetics for H₂ production despite the pH increase observed with extended reaction times in (Figure 3-4b). However, the impact of pH on H₂ production as well as the change in pH observed with H₂ production should be verified in field samples under conditions which more closely simulate *in situ*.

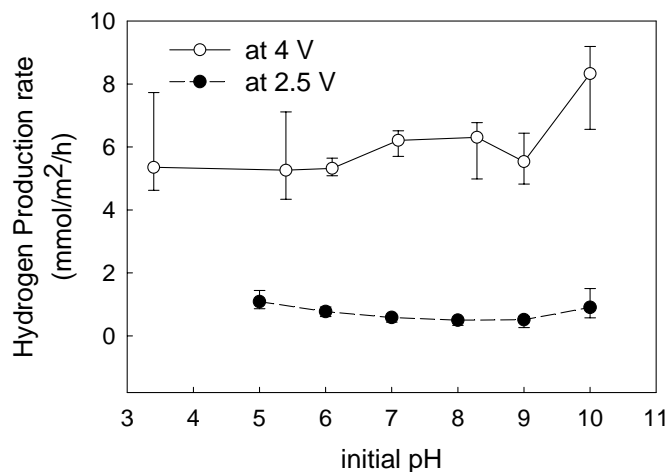


Figure 3-5. Influence of initial pH on hydrogen production rate.

All experiments were conducted at an initial pH=7 in 20mM NaHCO₃ and 20mM NaCl solution over 24 hours. The results are the means of triplicate reactors, and error bars represent standard deviation.

Influence of aqueous chemical species on hydrogen production

Many chemical species which may affect rates and efficiencies of the electrolytic reactions are present in sediment porewater. Among these, electrolyte concentration, presence of divalent cations, and natural organic matter (NOM) were investigated. In reference to Figure 3-6a, the “diluted electrolyte” group and “concentrated electrolyte” group simulated freshwater (I=0.044 N) and seawater (I=1.040 N), respectively [85] and addressed the impact of overpotential changes on H₂ production. The rate of H₂ production increased over an order of magnitude from freshwater to seawater-like conditions and is the result of increasing conductivity in the solution, therefore

reducing the ohmic resistance. The overall result is higher current at a similar electrode potential, which leads to a higher hydrogen production rate. Additionally, depending on the ionic species, they may adsorb to the electrode and alter the kinetics of the H₂-producing reaction through occupation of reactive sites or formation of mineral precipitates. This finding is analogous to those of Call and Logan [86] where H₂ production in MEC increased with catholyte concentration. In practice, the electrode cap operating in high ionic strength porewater would require less energy to achieve similar delivery rates of electron donor and redox gradients through the cap. The ionic strength and species of the sediment porewater will be site-specific and greatly impact remedial design.

Cations may potentially impact remedial design through their precipitation at the electrode. 5mM of calcium and magnesium salts were evaluated for their impact on H₂ production rates (Figure 3-6a). H₂ production was not significantly impacted by the addition of Mg²⁺ and slightly enhanced through the addition of Ca²⁺. Precipitation of solids was observed on the bottom of the cathode chamber but not on the electrode material. These results are different from Franz et al. who observed precipitation and deposition on stainless steel plate cathodes and increased resistance across the cell [87]. This difference is likely the result of different electrode materials, which may alter the double-layer composition as well as kinetics of precipitation reactions. Should cathode

pH affects precipitation reactions, the polarity of the electrodes can be periodically reversed to re-dissolve the precipitates [88].

NOM is a major component of sediment porewater and exert a contribution to conductivity, buffer strength, and reactions at the anode and cathode through electron shuttling [89], and therefore may be expected to affect electrolytic reactions. Humic acid was added to a relatively high concentration of 200mg/L (about 32mg carbon/L). The rate of H₂ production increased statistically significantly ($p=0.04$). The potential reasons for its effect are: (1) contribution to conductivity (by adding 200mg/L humic acid sodium salt, sodium concentration increased about 5mM); (2) humic acid may be adsorbed onto the electrodes and act as electron shuttles [89] or as a donor or acceptor [90].

T-test results indicated that except for the “concentrated electrolyte” group, current efficiency in all other groups was not significantly different from the control (Figure 3-6b).

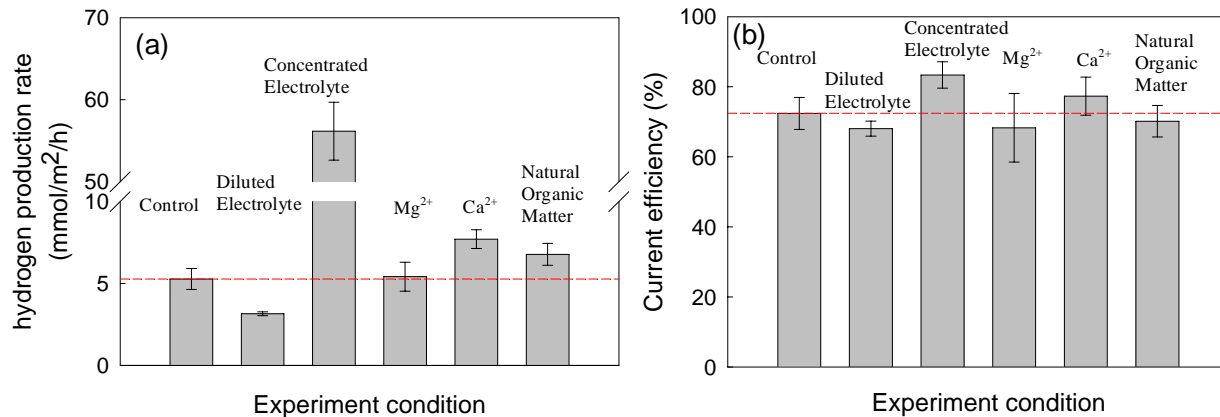


Figure 3-6. Influence of aqueous chemical species on (a) hydrogen production rate and (b) current efficiency.

All experiments were conducted at an initial pH=7 in 20mM NaHCO₃ and 20mM NaCl solution over 24 hours. The results are the means of triplicate reactors, and error bars represent standard deviation. The chemical composition for each group was: Control: 20mM NaHCO₃ and 20mM NaCl; Diluted electrolyte: 20mM NaHCO₃ and 2mM NaCl; Concentrated electrolyte: 20mM NaHCO₃ and 500mM NaCl; Mg²⁺: 20mM NaHCO₃, 20mM NaCl and 5 mM MgCl₂; Ca²⁺: 20mM NaHCO₃, 20mM NaCl and 5mM CaCl₂; Natural organic matter: 20mM NaHCO₃, 20mM NaCl and 200mg/l humic acid sodium salt. The dashed line showed the average results of control group.

3.4 Conclusions

This work demonstrated using carbon cloth as the electrode material, a novel reactive sediment cap can be constructed to manipulate redox condition in sediment cap and

deliver electron donor (hydrogen) for potential contaminants degradation. Reducing conditions was produced at the cathode and oxidizing conditions was produced at the anode. The redox stratification maintained as long as the powered was on and gradually returned to normal conditions once the powered was disconnected. Hydrogen was produced at the cathode and the production rate can be controlled by applied voltage. The electrolyte ionic strength greatly impacted hydrogen production while other common aqueous chemical species did not have significant change hydrogen production rate or current efficiency. These results suggest that electrode-based reactive capping can potentially promote chemical or biological transformations of contaminants within the cap.

Chapter 4. Nitrobenzene sequential reduction/oxidation by graphite electrodes and factors affecting degradation rate^①

Abstract

Carbon electrodes are proposed in reactive sediment caps for *in situ* treatment of contaminants. Emplaced perpendicular to seepage flow, the electrodes provide the opportunity for sequential reduction and oxidation of contaminants. The objectives of this study are to demonstrate degradation of nitrobenzene (NB) as a probe compound for sequential electrochemical reduction and oxidation, and to determine the effect of applied voltage, initial concentration and natural organic matter on the degradation rate. In H-cell reactors with graphite electrodes and buffer solution, NB was reduced stoichiometrically to aniline (AN) at the cathode with nitrosobenzene (NSB) as the intermediate. AN was then removed at the anode, faster than the reduction step. No common AN oxidation intermediate was detected in the system. Both the first order reduction rate constants of NB (k_{NB}) and NSB (k_{NSB}) increased with applied voltage between 2 V and 3.5 V (when the initial NB concentration was 100 μM , $k_{NB} = 0.3 \text{ h}^{-1}$ and $k_{NSB} = 0.04 \text{ h}^{-1}$ at 2 V; $k_{NB} = 1.6 \text{ h}^{-1}$ and $k_{NSB} = 0.64 \text{ h}^{-1}$ at 3.5 V) but stopped increasing beyond the threshold of 3.5 V. When initial NB concentration decreased from 100 to 5

^① This chapter was published in *Environmental Science & Technology* in 2011 under the title "Effect of applied voltage, initial concentration and natural organic matter on sequential reduction/oxidation of nitrobenzene by graphite electrodes"

μM , k_{NB} and k_{NSB} became 9 and 5 times faster, respectively, suggesting that competition for active sites on the electrode surface is an important factor in NB degradation. Presence of natural organic matter (in forms of either humic acid or Anacostia River sediment porewater) decreased k_{NB} while slightly increased k_{NSB} , but only to a limited extent (~factor of 3) for dissolved organic carbon content up to 100 mg/L. These findings suggest electrode-based reactive sediment capping via sequential reduction/oxidation contaminants removal is a potentially robust and tunable technology for *in situ* contaminants degradation.

4.1 Introduction

In situ capping is used to contain contaminated sediments by placing a layer of clean sand or sorbent-amended sand at the sediment-water interface as a barrier for contaminant diffusion to the overlying water column [50, 54, 73]. Reactive sediment capping employs materials that can transform or degrade contaminants within the cap, thereby better preventing their breakthrough from the cap [17, 55]. However, very few, if any, cost-effective materials are available to degrade contaminants within a sediment cap over the long timescales (perhaps decades to centuries) required for *in situ* sediment remediation.

Polarized carbon electrodes were proposed as reactive capping material for engineering desirable redox gradients as well as the delivery of electron donor for contaminant degradation. Contaminants migrating into the cap will be exposed to a reducing environment in the vicinity of the cathode, followed by an oxidizing environment in the vicinity of the anode (the opposite order can also be created by reversing the polarity of the electrodes). Contaminant degradation may occur as a result of microbial activities near each electrode, or due to abiotic reactions at the electrode surfaces. This current study is focused on the use of such a system to degrade contaminants via abiotic redox reactions at the electrodes.

The design of an electrode-based reactive cap for seepage flow conditions requires an understanding of the reaction rates and the impacts of porewater chemistry at the electrode surface. Degradation must be faster than convection through the cap to prevent breakthrough; meanwhile, the reaction rate must also be achievable at reasonably low voltage to minimize energy consumption, as well as pH changes expected from the accumulation of $H^+_{(aq)}$ and $OH^-_{(aq)}$ at the anode and cathode, respectively [17]. The effect of cathode potential on reaction rate, selectivity and efficiency in similar electrochemical devices has been studied [91], but from a practical point of view, applied voltage is more like the controlling parameter in cap design and operation. The applied voltage between the anode and the cathode controls the redox gradient in sediment cap and the evolution rates of electron donor and acceptor [17], but little is known about the voltage effect on contaminant degradation rates on inexpensive carbon electrodes surfaces.

Another open question about the performance of the electrode-based reactive cap is whether initial contaminant concentration will influence the reaction rate constants. A decrease of the 2,4-dichlorophenoxyacetic acid dechlorination rate was reported with increasing substrate concentration using Pd loaded carbon felt cathodes [92]. Similar phenomena also occur in some other heterogeneous catalytic reactions, such as

contaminants degradation on Fe(0) particles surface [93], as a result of the competitive adsorption onto reactive surface sites between the parent and daughter compounds (and also among the parent compound molecules). In real sediments, contaminant concentrations vary by orders of magnitude between the source zone and the downstream plume. The effect of contaminant concentration on reactivity must be determined for site specific feasibility, cap design and operating conditions, and performance.

In sediment systems, natural organic matter (NOM) is likely to affect contaminant degradation rates but this influence has not been examined in electrochemical systems. NOM interacts with environmental contaminants in several ways including electron shuttling [89], covalent binding [94], competitive sorption [95] and solubilization [96]. Carbon electrodes should have high affinity for NOM [97], with the implication that it will adversely affect electrode performance by competitive adsorption. However, interactions such as electron shuttling may increase reactivity [89].

Certain sediment contaminants require sequential reduction/oxidation for complete mineralization, including nitroaromatics, polychlorinated biphenyls (PCBs), and chlorinated hydrocarbons. Sequential electrochemical reduction/oxidation of perchloroethene (PCE) has been demonstrated in groundwater [38]. Nitrobenzene is

another representative of such contaminants. Nitrobenzene oxidation is difficult even under aerobic condition [98, 99] and may lead to toxic dead-end products. [100] In contrast, reduction of nitrobenzene to aniline easily occurs under anaerobic conditions, and aniline can readily undergo oxidative ring cleavage and mineralization to ammonium and CO₂ [101, 102] in an aerobic environment. In addition, the degradation products of nitrobenzene are well-known and easy to measure, the reactions are relatively fast, and it has a relatively low hydrophobicity as compared to other aromatics (thus less adsorption and evaporation loss) which makes it a suitable model compound for this study. Chemical and microbial reduction of nitrobenzene to aniline in a reactive sediment cap containing Fe(0), sorbent, and bacteria has been reported [58]. Nitrobenzene reduction to aniline also occurs in bioelectrochemical systems coupled with acetate oxidation [103]. Complete degradation of nitrobenzene and other nitroaromatics like RDX (hexahydro-1,3,5-trinitro-1,3,5-triazine) and TNT (2,4,6-trinitrotoluene) in a sequential anaerobic/aerobic microbial wastewater treatment process [104] or by sequential oxidation/reduction using IrO₂/TaO₅ doped titanium electrodes [43, 105] have been reported. However, the different role of each stage was not identified.

The objectives of this study are to demonstrate the sequential reduction/oxidation of nitrobenzene using polarized graphite electrodes and determine the effect of applied

voltage, initial contaminant concentration, and NOM on the degradation rate constants. Data from this study will enable better design of reactive sediment caps [17], electrode-based remedial approaches [4], and energy generation from environmentally-deployed electrodes [80].

4.2 Materials and methods

Chemicals

All the chemicals used are reagent grade unless otherwise noted. Nitrobenzene ($\geq 99.5\%$), nitrosobenzene (97%), and aniline (99.9%) were supplied by Sigma-Aldrich (St. Louis, MO). Hydrochloric acid (HCl) solution (37%), sodium phosphate monobasic (NaH_2PO_4) and sodium bicarbonate (NaHCO_3) were supplied by Fisher Scientific (Pittsburgh, PA). Humic acid sodium salt (50-60% as humic acid) was purchased from Acros Organics (Morris Plains, NJ).

Electrode materials

Carbon materials were chosen because of their relatively low cost, resistance to poisoning, and soft and porous texture for easier application in sediment. The carbon cloth electrodes utilized previously were no longer available from the vendor. Instead,

graphite felt (10 cm long × 4 cm wide × 1/4 inch thick, Wale Apparatus Co., Inc., Hellertown, PA) was used as electrodes in this study.

Nitrobenzene degradation reaction

Experiments to study nitrobenzene degradation kinetics were carried out at room temperature ($23 \pm 2^\circ\text{C}$) in two-chamber glass H-cell reactors as described previous chapter. Each chamber contained 60 ml headspace and 250 ml buffer solution (or sediment porewater, or buffer with humic acid, for NOM effect study), and was well mixed using a magnetic stir bar. The buffer solution contained 20 mM NaH_2PO_4 adjusted to pH 6.5 by 5% HCl solution. Such buffer concentration was used in order to match the buffer intensity of Anacostia River (Washington, DC) sediment porewater. Constant voltage was applied using E3620A DC power supplies (Agilent Technologies, Santa Clara CA). In each reactor, one chamber had NB together with buffer and is defined as the working chamber, while the other contains buffer only. The electrode in working chamber was connected to the negative pole of a power supply to serve as cathode during reduction and then switched to the positive pole to serve as anode during oxidation. Real-time electrode potential for the working chamber was measured vs. Ag/AgCl reference electrodes (Electrolytica, Inc., Amherst, NY), and logged using a Model 2700 digital multimeter (Keithley Instruments, Inc., Cleveland, Ohio). Electrode potential is reported as vs. standard hydrogen electrode (SHE). After the voltage was

applied and electrode potential in working chamber became stabilized, 10 mL of NB stock solution (2.5 mM) was added to achieve an initial NB concentration of ~100 μ M, except in the experiments for initial concentration impact, where the concentration of NB was varied.

Sediment porewater simulation

In the NOM effect study, the working chamber of the H-cell reactors were filled with simulated sediment porewater with 20 mM NaH_2PO_4 , or humic acid solution with 20 mM NaH_2PO_4 (both at pH 6.5), instead of pure buffer solution. Simulated sediment porewater was generated by a modified version of the standard method ASTM D3987. In brief, Anacostia River (Washington, DC) sediment (moisture content 46.4 ± 1.7 wt %) was mixed with DI water (1:5 sediment: water weight ratio) in a glass bottle and rotated at 30 rpm for 46 h. The mixture was then centrifuged at 2000xG for 10 min and filtered with a nominal 20~25 μ m filter (Whatman, Piscataway, NJ). The dissolved organic carbon (DOC) content of stimulated porewater was 14.4 mg/l as carbon, reasonably close to actual porewater (24 mg/l). Humic acid (HA) sodium salt was also used as a representative NOM for assessing its impact on reaction rate constants.

Analytical methods

Aqueous concentrations of NB, NSB and AN were quantified by high performance liquid chromatography (HPLC) (Agilent, Santa Clara CA) equipped with a C18 reversed-phase column (15-cm x 4.6-mm, 5 μ m) and UV detector (210 nm). The mobile phase was 50/50 (v/v) methanol/water at 1.0 ml/min. In the experiments with HA, 30/70 (v/v) acetonitrile/water was used as mobile phase to separate peaks of AN from HA. In the experiments with sediment porewater, samples were filtered using a 0.45 μ m syringe filter before HPLC analysis. Headspace H_2 concentration was determined using GC/TCD as previously described [79]. Attempts to identify water soluble oxidation products of AN were conducted using time-of-flight mass spectrometer following HPLC (HPLC-TOF-MS).

4.3 Results and discussions

Nitrobenzene sequential reduction/oxidation

Nitrobenzene can be completely removed by sequential reduction/oxidation with carbon felt electrodes. Figure 4-1 is an example of NB degradation at 3 V applied voltage. Nitrobenzene (NB, $C_6H_5NO_2$) was stoichiometrically reduced to aniline (AN, $C_6H_5NH_2$) via nitrosobenzene (NSB, C_6H_5NO) by cathodic reactions in the electrolytic cell within 20 hours. Phenylhydroxylamin (PHA, C_6H_5NOH), a short-lived intermediate [106] of NSB reduction to AN, was not detected in this study. Following

complete NB reduction to AN, the polarity of the working chamber was reversed and AN was rapidly removed under oxidizing conditions. None of the commonly reported AN oxidation intermediates (catechol [102], benzoquinone or maleic acid [101], dianiline, 4-anilino phenol or azobenzol [107]) were detected by HPLC-TOF-MS. Polymerization products of AN [108] were also not observed. pH in the working chamber was well buffered; at 3 V applied voltage, pH rose from 6.5 to 7 during reduction and decreased to 6.7 at the end of oxidation. Slow NB loss and no products were observed in the control reactor that was not powered (data not shown), indicating that sorption and alkaline hydrolysis were not significant removal mechanisms.

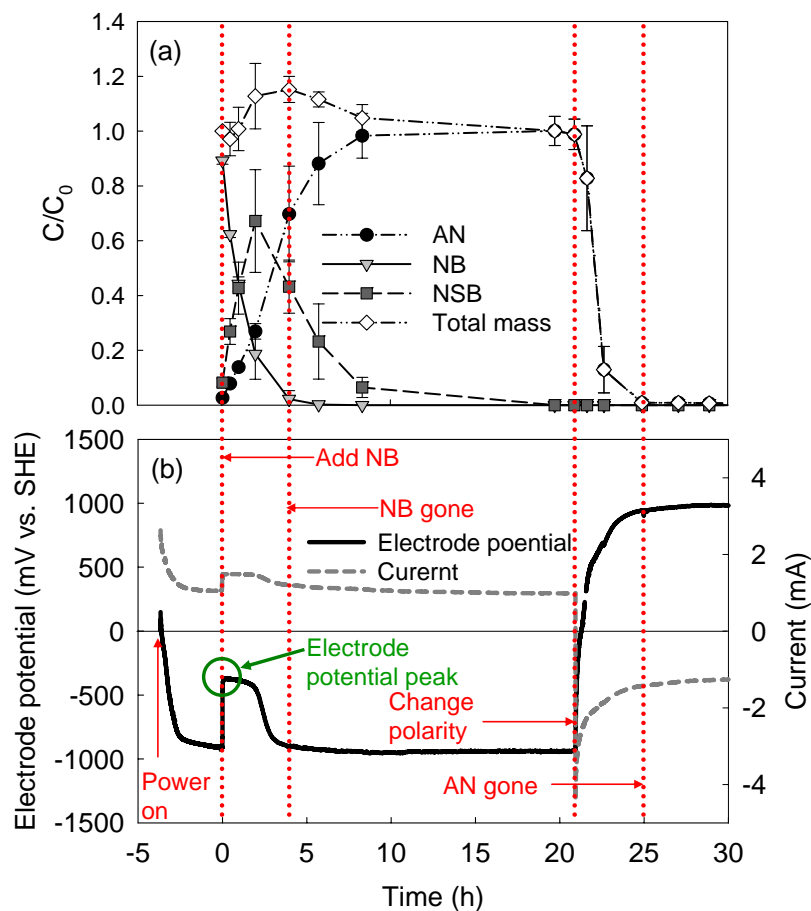


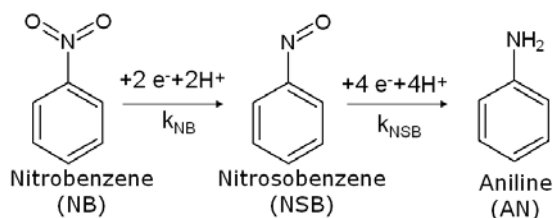
Figure 4-1. Sequential reduction/oxidation of nitrobenzene at 3V applied voltage

(a) Relative molar concentrations of nitrobenzene (NB), nitrosobenzene (NSB) and aniline (AN) with regard to the initial NB added ($100 \mu\text{M}$). The results are the means of triplicate reactors, and error bars represent standard deviation. (b) Working electrode potential (vs. SHE) as a function of time. The circle shows the electrode potential peak. NB was added into pure buffer solution (time zero) after the electrode potential had stabilized. After both NB and NSB were stoichiometrically converted to AN, the polarity of the electrodes were reversed.

Inspection of Figure 4-1b shows that the working electrode potential is an indicator for reaction progression: prior to addition of NB, the only reaction occurring was water electrolysis and the electrode potential stabilized to a baseline (~ -900 mV vs. SHE with an external potential of 3V). The addition of NB (an oxidant) increased the electrode potential to -330 mV, close the NB reduction potential (-356 mV vs. SHE) reported by Wang *et al* [109]. This potential immediately after NB addition is referred as “electrode potential peak” in Figure 4-1b and will be used in following discussion. The potential gradually decreased to its baseline as NB was completely reduced to AN. Reversing the polarity of the electrodes rapidly changed the electrode potential from cathodic to anodic. The potential continued to increase while AN was present and reached a steady value of $\sim +1$ V once AN was completely removed. The potential profile, in conjunction with the concentration profiles with time is useful for analysis in the following sections.

The current data in Figure 4-1b follows a similar trend to the potential: current dropped and got stabilized at 1 mA after power on, and increased instantly to 1.5 mA after NB addition. After NB was totally reduced, current decreased back to 1 mA, and reversed its direction once the polarity was switched. Once AN was totally removed, current reached the steady level of 1 mA (but in opposite direction of flow).

AN oxidation is significantly faster than NB and NSB reduction (Figure 4-1), indicating that the reduction is rate-limiting for sequential reduction/oxidation of NB; therefore, the following degradation study focuses on reduction only. The nearly complete mass balance for NB reduction (Figure 4-1a and Figure 3-2) suggested that the NB reduction pathway can be modeled by the reaction in Equation 4-1 below.



Equation 4-1

The reduction stage of NB removal in Figure 4-1 was replotted in Figure 3-2 to fit the first order reaction kinetics. At 3 V, the NB and NSB reduction rate constant were 0.88 h⁻¹ and 0.36 h⁻¹, respectively. The goodness of fit (R²>0.99) indicated that the sequential first order reactions were suitable to simulate the NB reduction kinetics. The NSB reduction rate constant (k_{NSB}) determined independently from experiments using NSB as the parent compound was similar to the rate constant extracted from experiments with NB as the parent compound (Appendix Figure B-1).

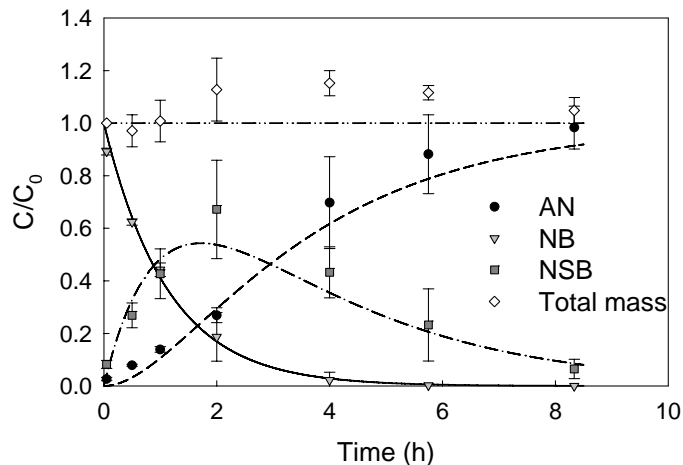


Figure 4-2. First order kinetic model fit for nitrobenzene (NB) reduction to aniline (AN) via nitrosobenzene (NSB) at 3V

Symbols are observed concentration data and lines represent the model fit. The results are the means of triplicate reactors, and error bars represent standard deviation.

Effect of voltage on reduction rate constants

For a reactive cap to mitigate contaminant transport into the overlying water, the contaminant degradation must be faster than the convection through the cap [52]. Since applied voltage is the thermodynamic driving force for the reaction, the observed decontamination rate should increase with increasing voltage, assuming the reaction kinetics is the rate-limiting step. The reduction rate constants of NB and NSB were found to be increased with applied voltage between 2 ($k_{\text{NB}} = 0.3 \text{ h}^{-1}$ and $k_{\text{NSB}} = 0.04 \text{ h}^{-1}$) and 3.5V ($k_{\text{NB}} = 1.6 \text{ h}^{-1}$ and $k_{\text{NSB}} = 0.64 \text{ h}^{-1}$) (Figure 3-3a). However, a higher voltage beyond 3.5V did not cause greater k_{NB} or k_{NSB} , and below 2V no reaction was observed.

The voltage dependence of k_{NB} and k_{NSB} is consistent with the voltage dependence of the electrode potential peak when NB was added (illustrated in Figure 4-1b). The electrode potential peak (Figure 3-3b) decreased as voltage increased up to 3.5 V, but showed no difference between 3.5 V and 4.5 V (the full profile of electrode potential over time under different applied voltage were presented in Appendix Figure B-2). Voltage in excess of 3.5V was likely dissipated by ohmic losses in the electrolyte, rather than for cathodic reduction. Since electrode potential is the determining factor for reduction reaction to take place, the lack of a further decrease in the electrode potential peak with increasing voltage prevented k_{NB} and k_{NSB} from further increase. pH, working electrode potential and current information for each experiment can be found in Appendix Table B-1.

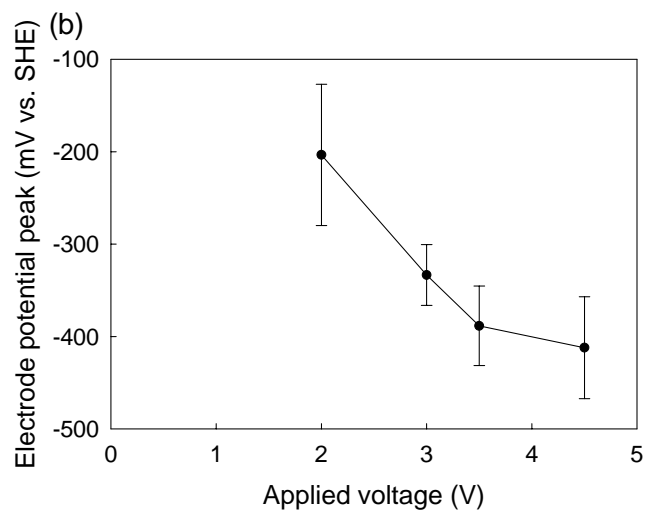
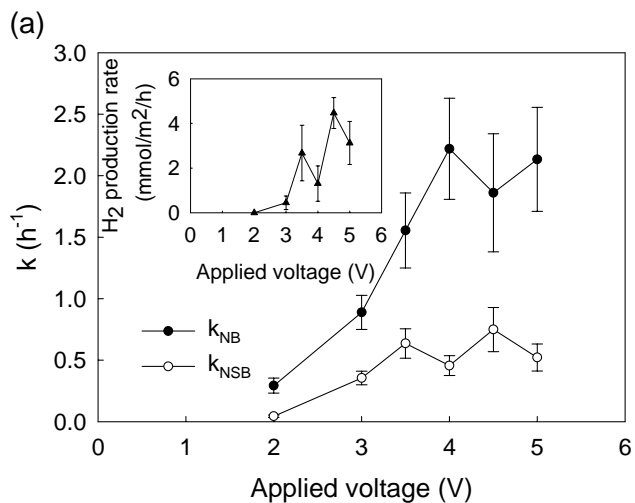


Figure 4-3. Effect of applied voltage on (a) nitrobenzene (k_{NB}), nitrosobenzene (k_{NSB}) reduction rate constants, and hydrogen production rate constant (inset), and (b) electrode potential peaks after NB addition in the working chamber.

Results are the means of triplicate reactors with 100 μM initial nitrobenzene addition. Error bars in (a) represent the 95% confidence interval of the modeled rate constants, and in (b) represent the standard deviation of the triplicate reactors measured.

Effect of initial NB concentration on reduction rate constants

The concentration of sediment contaminants is typically variable through the sediment and cap. Different initial NB concentrations were tested to determine if the observed reaction rate constants were dependent on initial contaminant concentration. Decreasing the initial NB concentration from 100 to 5 μM increased the observed reduction rate constants by a factor of 9 (0.88 h^{-1} to 7.9 h^{-1}) for k_{NB} and 5 for k_{NSB} (0.36 h^{-1} to 1.7 h^{-1}) (Figure 3-4). Similar inverse correlation of initial concentration with reduction rate constant of NB on an Fe(0) surface was attributed to competition for adsorption to a reactive iron surface [93]. In such a circumstance, the observed reduction rates are decided by both reaction kinetics and adsorption kinetics. Another interpretation for this electrochemical system is that since NB is an oxidant higher initial NB concentration lead to higher electrode potential peak (Figure 3-4). The higher (less negative) electrode potential peak decreased the driving force for reaction and therefore slowed down the reaction [110]. The temporal variation of electrode potential for each initial NB concentration is available in Supporting Information (Appendix Figure B-2). pH, working electrode potential and current information for each experiment can be found in Appendix Table B-1.

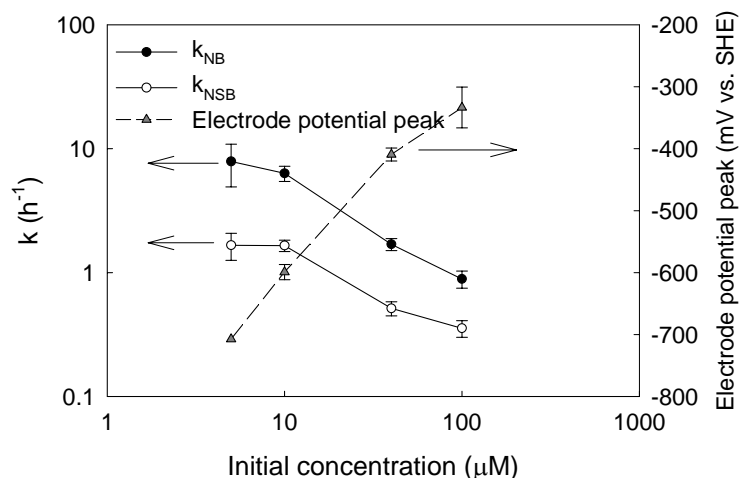


Figure 4-4. Effect of initial nitrobenzene concentration on nitrobenzene (k_{NB}) and nitrosobenzene (k_{NSB}) reduction rate constants, and on electrode potential peaks after NB addition in the working chamber.

Results are means of triplicate experiments at 3V. Error bars for reaction rate constants represent 95% confidence intervals for the modeled values, and for cathode potential peak represent the standard deviation of the triplicate reactors measured.

Effect of NOM on reduction rate constants

The effect of NOM on NB reaction rate constants was examined using simulated sediment porewater (PW) or humic acid (HA) solution (both containing 14.4 mg/l DOC). Figure 3-5a indicates that k_{NB} decreases from 2.2 h^{-1} in no NOM control to 0.7 h^{-1} and 0.8 h^{-1} in the presence of porewater and HA solution, respectively; while in contrast, k_{NSB} was less affected, around 0.4 h^{-1} in all the groups. Figure 3-5a also shows that HA solutions and simulated sediment porewater with the same DOC concentrations have a

similar effect on the NB and NSB reduction rate constants. This suggests that HA may be the key component in porewater responsible for the change of k_{NB} and k_{NSB} . Thus further study on the relationship between the NOM concentration and degradation rate was conducted with HA only. Figure 3-5b shows that very low concentrations of HA (0.44 mg/l DOC) decreased k_{NB} by 2 folds and the effect was not dependent on concentration of added HA over the range of typical DOC concentrations in sediment porewater (several mg/l to ~200 mg/l). This change of k_{NB} is within the range of 1.2 to 10 fold decrease in the reaction rate constant reported for HA effects on NB reduction by Fe(0) [95]. In contrast, k_{NSB} slightly increased with HA concentration, as has been observed for NOM mediated NB chemical reduction by H₂S [89]. NOM did not likely affect the reduction rates by serving as an electron donor, since (1) no matter which source or what concentration of NOM was added, there was no statistically significant difference in electrode potential peak (data not shown) and (2) adding NOM to unpowered reactors could not cause NB reduction (data not shown). Potential explanations of the NOM effect on reduction rates are: (1) NOM may competitively adsorb to the electrode surfaces [95] (accumulation of HA on electrodes surfaces has been observed) and increase the mass transfer resistance of NB or NSB from the bulk solution to the electrodes, thus decreased the reduction rate; or (b) NOM may increase the rate due to electron shuttling [89] between the electrodes and contaminant. However as Figure 3-5 shows, the impacts of NOM on k_{NB} and k_{NSB} were relatively

small (less than a factor of 3) when compared to the impact of applied voltage and initial contaminant concentration (~factor of 10), and therefore were not further investigated. pH, working electrode potential and current information for each experiment can be found in Appendix Table B-1.

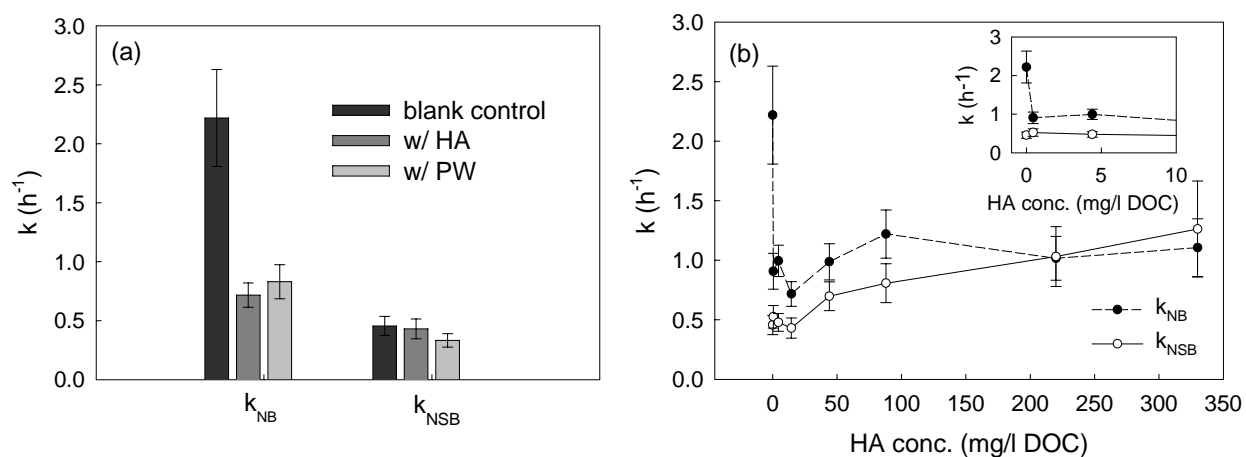


Figure 4-5. Impact of (a) NOM presence and (b) humic acid concentration on nitrobenzene (k_{NB}) and nitrosobenzene (k_{NSB}) reduction rate constants.

The chemical composition for each group in (a) was: blank control: 20 mM NaH_2PO_4 ; w/ HA: HA (14.4 mg/l DOC) and 20 mM NaH_2PO_4 ; w/ PW: simulated sediment porewater (14.4 mg/l DOC) and 20 mM NaH_2PO_4 . The inset in (b) is the scale-up of low concentration data. For both figures, results are means of triplicate experiments with 100 μ M initial nitrobenzene addition at 4 V, and error bars represent the 95% confidence interval of modeled rate constants.

Reaction rate comparison with other studies

The NB reduction rate measured here was comparable to those previously reported using in microbial fuel cells (MFC) [109, 111], however some differences are noteworthy. Wang et al. [109] used acetate oxidation instead of water oxidation (to O₂) at the anode, so we compare reaction rates determined at the same cathode potential instead of at the same total applied voltage. In their study, when the applied voltage was 0.5V, their cathode potential with pre-added NB was -790 mV (without bacteria) or -740 mV (with bacteria). This is much lower than the cathode potential after NB addition at any applied voltage in this study (Appendix Figure B-2). A lower cathode potential would be expected to lead to higher reaction rate. However, k_{NB} determined from their reported concentration vs. time data at this cathode potential is only 0.045 h⁻¹(without bacteria) and 0.2 h⁻¹ (with bacteria); while this study with an abiotic reaction only has a k_{NB} between 0.3 to 2.5 h⁻¹. Although the cathode used in the study by Wang *et al.* was platinumized, the cathode surface area normalized reaction rate in their study (1.1×10^{-3} h⁻¹cm⁻² without bacteria or 1.0×10^{-2} h⁻¹cm⁻² with bacteria) is slower than observed in the present study (between 1.5×10^{-2} h⁻¹cm⁻² and 0.12 h⁻¹cm⁻²). Such comparison suggests that operating the electrodes at lower voltage may slow the desired degradation, but that the total power output can be greatly reduced (0.5V for the study of Wang *et al.*, vs. at least 2V in this study) using a suitable electron donor at the anode. It may be infeasible to continuously providing a suitable electron donor to a sediment cap but, in

the cases of sequential reduction/oxidation, or removing contaminants mixtures requiring different redox conditions, pursuing such coupling is desirable.

Similarly, Li *et al.* [111] used microbial glucose oxidation at the anode to couple with NB reduction at cathode. k_{NB} determined from their reported concentration vs. time data is $\sim 0.8 \text{ h}^{-1}$ (or $1.6 \times 10^{-2} \text{ h}^{-1}\text{cm}^{-2}$) for the initial 3 h and slowed down afterward. Such a reaction rate is close to the low end of the k_{NB} range obtained in this study. The cathode potential at such reaction rate was not reported, but since their cathode was not poised, it should be around the NB reduction potential found in both this study and the study by Wang *et al.* [109]. Their current density at such reaction rate was controlled constantly at 15 A/m^3 (or 165 mA/m^2), while the maximum current density in this study was $125\text{--}375 \text{ mA/m}^2$. Both the reaction and current density observed in this study were similar with these reported in Li's study.

Performance and design of electrode-based reactive cap

We examined how the cap properties (thickness and reactivity) as well as contaminant transport properties (seepage velocity and diffusivity) affected the ability of an electrode-based reactive cap to degrade contaminants moving through by advection and diffusion. Since this model only considers terms which are relevant within a porous electrode, an electrophoretic term for the velocity was not considered. The case study of

NB and the cap parameters used here are included as a metric for comparison to other important sediment contaminants that may have slower rates of reaction.

There are three steps during contaminant abiotic degradation at the electrode surfaces as studied here: diffusion of NB to the electrode surface, reaction of NB at the electrode surface, and diffusion of reaction products from the electrode surface. In the H-cell reactions, we assume that reaction at the electrode surface is the rate controlling step. This is reasonable since the time scale for diffusion in our system ($t_{diff} = L^2 / D$) is approximately 0.2s, assuming a diffusion layer thickness (L) of 10 m and NB diffusivity (D) of $4.4 \times 10^{-10} \text{ m}^2/\text{s}$ [112]. This is much shorter than the timescale for the first order reaction ($t_{rxn} = 1/k$, which is in minutes to hours for NB). Also the oxidation of AN is faster than reduction of NB and NSB (Figure 4-1). Thus the reduction reaction is rate limiting in the well mixed H-cell reactors. The reaction rate may also be assumed to be the rate-limiting step for other, more refractory contaminants with slower degradation kinetics, assuming the diffusivities are in the same magnitude.

In real sediment, within an electrode-based reactive cap, the overall decontamination rate is moderated by contaminant migration in surrounding medium. The steady state contaminant flux to each electrode can be simulated using a one-dimensional advection-diffusion-reaction model [113] with the analytical solution of

$$C(z) = C_0 \exp\left(\frac{v - \sqrt{v^2 + 4Dk}}{2D} z\right) \quad \text{Equation 4-2}$$

Where z is the relative location of the interested point to the bottom of the electrode; C_0 and $C(z)$ are the contaminant concentration in the porewater entering the cap and at position z , respectively; v is the upward sediment porewater average velocity; D is the diffusivity of contaminant; k is observed first order reaction rate constant; h is the electrode thickness.

To make the solution as general as possible, Equation 4-2 can be rewritten in terms of the dimensionless Peclet Number (Pe) and Damkohler number (Da) that can be calculated for any sediment cap and contaminant.

$$Pe = \frac{vh}{D} = \frac{\text{advection rate}}{\text{diffusion rate}} \quad \text{Equation 4-3}$$

$$Da = \frac{kh}{v} = \frac{\text{reaction rate}}{\text{advection rate}} \quad \text{Equation 4-4}$$

Re-writing Equation 4-2 in terms of Pe and Da allows assessment of contaminant removal efficiency (f) for any cap or contaminant in general:

$$f = 1 - \frac{C(h)}{C_0} = 1 - \exp\left(\frac{Pe - \sqrt{Pe^2 + 4DaPe}}{2}\right) \quad \text{Equation 4-5}$$

Figure 6 illustrates the fraction of contaminant removed vs. the Peclet Number for a range of Damkohler numbers. Greater than 80% removal can be achieved with electrode caps having $Da > 5$ at Pe expected in sediments caps ($Pe < 10$, considering the typical sediment flow velocity of several cm/d, electrode thickness of a few cm, and effective diffusivity of 10^{-10} m²/s). It is important to note that Pe and Da are not independent parameters, but rather co-vary with velocity, i.e. Pe number decreases with decreasing porewater velocity, but Da increases with decreasing porewater. Thus, for a given cap dimension, a lower Pe number usually accompanies a high Da . With the assumption of an electrode thickness of 0.635 cm (one layer of the graphite felt used in this study), a NB diffusivity of 4.4×10^{-10} m²/s [112], and the reaction rate constant of 0.5 h^{-1} based on the reactivity data from this study, NB degradation efficiency was predicted to fall between 52% (when porewater velocity was 10 cm/day) and 97% (when porewater velocity was 1 cm/year), shown as the solid line in Figure 3-6. Note diffusivity (D) in water instead of effective diffusivity (D^*) in the porous electrode is used due to lack data for electrode porosity (n) and tortuosity (τ). Since $D^* = Dn\tau$ and $0 < n, \tau < 1$, D is always greater than D^* . Such an approximation therefore leads to underestimate of Pe and thus underestimate of removal efficiency.

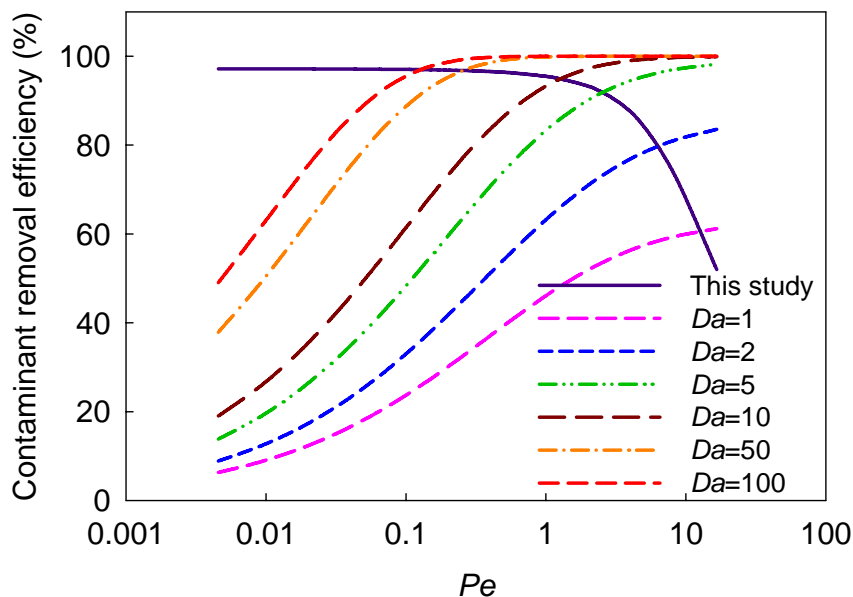


Figure 4-6. Effect of flow conditions (Peclet Number, Pe) on transformation in the sediment cap for a range of reactivity (Damkohler numbers, Da).

The solid line represents the electrode and NB reactivity data in this study ($k=0.5 \text{ hr}^{-1}$, $h=0.635 \text{ cm}$, and $D=4.4 \times 10^{-10} \text{ m}^2/\text{s}$).

Other contaminants may not as easily degraded as NB, and considering that the reaction rate increase with applied voltage are not unlimited, a specific removal efficiency for a particular contaminant may require a degradation rate beyond what the electrode-based reactive cap can provide. In this case, a thicker cap is needed to provide longer hydraulic retention times for the completion of the desired reactions. In addition, though a particular reaction rate may be achievable with a high applied voltage, in many cases it may be desirable to operate at a lower voltage. Then the electrode

thickness may be increased to provide the desired removal efficiency. Operating at low voltage can decrease energy costs and environmental disturbance (e.g., pH change). This is especially true for operation at a voltage which transforms contaminants without hydrogen production (e.g., in Figure 3-3a, at 2V NB and NSB were reduced without hydrogen production). Electrode-based sediments caps will need to be optimized for both design (electrode thickness) and operational (applied voltage) conditions to minimize remediation costs.

It is worth noting that in real sediments mass transfer processes and reactions other than those considered here may also affect the contaminant degradation rates. For example, unlike the NB probe in this study, highly hydrophobic contaminants may strongly adsorb to sediment NOM. Slow desorption from NOM may result in a low contaminant transport rate to the electrode surface, and thus a lower overall removal rate. Also, no electrokinetic term is incorporated in this model, because this model only discusses contaminants behaviors inside the electrode. By ignoring the potential gradient in the porewater inside the electrode, electric potential is considered equal at all positions within the electrode, and electromigration and electroosmosis driven by electric potential gradient become zero. A more complicated model dealing with the heterogeneous potential distribution may be needed for advanced analysis. Other reactions may also need to be considered for the cap design. For instance, hydrogen

produced at the cathode (Figure 3-3a inset) may be utilized by bacteria for contaminant biodegradation. The participation of microbial activity may increase the reactivity (Da) over that of the electrode alone [109]. This is potentially the case for contaminants (such as PCBs) with low abiotic reduction rates, as long as the supplementary biological reduction rate in the presence of low levels of H_2 is high enough to make the electrode-based reactive cap feasible. Either of these conditions would require incorporating mass transfer into the model, or the *in situ* reaction rates, to optimize the design of the cap.

4.4 Conclusions

This work demonstrated graphite felt can be as the electrode material to effectively removal nitrobenzene by sequential reduction/oxidation. The oxidation step is faster than the reduction step. NB reduction can be modeled as a series of two first order reactions, and the reaction rate constants can be controlled by applied voltage between 2V and 3.5V. Lower initial NB concentrations lead to higher reaction rates. The presence of NOM decreased NB reduction rate but increased NSB reduction rate. These results suggest that contaminants requiring sequential reduction/oxidation may be effectively degraded in the electrode-based reactive capping by abiotic electrochemical reactions on electrode surfaces.

Chapter 5. Effect of powered carbon electrodes on 2,4-dichlorophenol biodegradation in sediment slurry^①

Abstract

Microbial degradation of organic contaminants is an important attenuation process for sediment remediation. Placing an electrode-based sediment cap over the contaminated sediment will likely change the intrinsic contaminant biodegradation rates, either by supplying electron donor or acceptor, or by altering the pH in the porewater. Using 2,4-dichlorophenol (DCP) as a probe compound, this study investigated the effect of powered electrodes on the DCP degradation rate in sediment slurry. Degradation rates were measured using both powered and unpowered electrodes, and in active and sterile sediment. DCP was reductively transformed to 4-chlorophenol in sediment slurry with powered or unpowered electrodes. Neither graphite felt nor carbon paper cathodes induced abiotic electrochemical DCP dechlorination at low applied voltage (2-3 V for graphite felt, 2.5-3.5 V for carbon paper) in either biologically-active or sterile sediment, confirming that observed DCP degradation was biological. DCP removal rates ranged from 1-20 $\mu\text{M}/\text{day}$ in unamended sediment to 50-200 $\mu\text{M}/\text{day}$ in sediment amended with nutrients (vitamins and trace metals). Comparing DCP removal rates for

^① This chapter is under preparation for possible publication.

powered and unpowered electrodes in sediment slurries, it was found that graphite felt electrodes did not change DCP removal rates in nutrient-amended sediment slurry and carbon paper electrodes decreased DCP removal rate in unamended sediment slurry. Additional batch studies on the effects of hydrogen concentration and porewater pH on DCP biodegradation rate were performed to better understand how the powered electrodes may impact DCP biodegradation rate. An increase of either hydrogen concentration or pH was found to depress the dechlorination rate in unamended sediment slurries without electrodes, suggesting the observed negative effect of powered electrodes on DCP biodegradation rate may be caused by hydrogen production and increase of sediment pH near the cathode. The results of this study suggest electrode-based sediment cap does not benefit natural attenuation of DCP which is degradable in the sediment without any intervention.

5.1 Introduction

Biodegradation of contaminants in sediment and sediment caps is essential for sediment management. It has been demonstrated that in a laboratory scale cinder/granular iron sediment cap, the presence of nitrobenzene degrading bacteria can improve nitrobenzene degradation compared to in abiotic situation [58]. Also, aerobic bacteria in sand cap over coal tar-contaminated river sediment can reduce polycyclic aromatic hydrocarbons (PAHs) concentrations in water flowing through the sediment and cap with the supply of oxygen and nutrients [56]. In another study with a simulated bioreactive sand cap, a mixed bacterial consortium transformed tetrachloroethene to cis-1,2-dichloroethene and vinyl chloride, and by adding soluble electron donor, complete dechlorination to ethane was achieved [114]. These examples demonstrate the importance of electron donor/acceptor in microbial sediment remediation.

We hypothesize that an electrode-based sediment cap may be used to facilitate contaminant biodegradation. As discussed in previous chapters, hydrogen and oxygen produced in the electrode-based reactive caps may be utilized as electron donor and acceptor, respectively, by certain bacteria for contaminant biodegradation. Also, direct microbial respiration of the anode and cathode as electron acceptor and donor,

respectively, may also be involved in bioremediation. The coupling of contaminant oxidation or reduction to microbial respiration of electrodes has been studied previously; for example, PAHs oxidation coupled with microbial respiration of an anode as the electron acceptor [5], U(VI) [4] and nitrate reduction [3] coupled with microbial respiration of the cathode as the electron donor. For some contaminants like chlorinated hydrocarbons, sequential microbial reductive dechlorination at the cathode followed by microbial oxidation at the anode may be a good approach for these highly refractory contaminants.

Incorporating biodegradation into the electrode-based reactive cap is also beneficial for refractory contaminants where abiotic reactions afforded by the electrochemical reaction are not fast enough to prevent breakthrough in the cap. Even if the desired degradation rate is achievable by the abiotic reaction alone, the participation of microbes may decrease required abiotic reaction rate and thus decrease required applied voltage and consequently reduce operating cost (lower the required voltage), and unintended effects like local pH change around the electrodes.

Studies on electrode-stimulated degradation of important sediment contaminants have been recently reported. It has been demonstrated that carbon electrodes can enhance PAHs degradation and increase the number of PAHs degrading genes in sediment

slurries and in sand sediment caps [45]. Both naphthalene and phenanthrene degradation rates were faster in ElectroBioReactors (sediment slurries with 3.5V powered electrodes) than in killed control (sterile sediment slurries with 3.5V powered electrodes) and in anaerobic control (anaerobic sediment slurries without power). Also, in sand sediment caps with 2V applied voltage, phenanthrene concentrations near the anode (normalized to unaffected parts of the cap) were 11-16% less than observed in an unpowered control, and naphthalene concentrations around the anode area (also normalized to unaffected parts of the cap) were 3% more and 20% less, respectively, in the duplicate powered caps, than the unpowered control. Similarly, polychlorinated biphenyl (PCB) removal was improved using titanium electrodes in sediment-water microcosms [46]. While only negligible PCB loss was observed in sterilized sediment slurry with 1.5V or without power over 88days, ~15% loss was observed in unpowered active sediment slurry, and up to 64% loss was achieved in powered active sediment slurry. More PCB loss was observed in lower applied voltage (1.5V) than high voltage (2.2V and 3.0 V).

With the above two reports suggesting powered electrodes in sediment environment may change contaminant biodegradation, it is interested to study if powered electrodes will also promote biodegradation of other contaminants. In this study, 2,4-dichlorophenol (DCP) degradation in a sediment slurry with powered and unpowered

carbon electrodes was measured to determine if powered electrodes can change DCP degradation rate. Chlorophenols are an important class of environmental contaminants with extensive usage as biocides and wood preservatives.

DCP was chosen because the degradation products are well known and easy to measure; also, microbial degradation rates of DCP were moderate (naturally occurring biodegradation of chlorophenols typically have half-lives between 2 and 70 days [115]), not too high to make electrochemical reaction unnecessary and not too low so it can provide enough experimental observation within relatively short period (days to weeks); DCP has moderate hydrophobicity and therefore exhibits relatively low adsorption and evaporative losses.

Biodegradation of DCP in sediment with 10% hydrogen as the electron donor has been studied with 4-chlorophenol as the only product [116]. Another study suggested 100 kPa hydrogen can stimulate dechlorination of DCP in unacclimated sediment [117]. Electrochemical dechlorination of chlorophenols has been achieved in various laboratory electrochemical cells [35, 118-120]. The combination effect of electrodes and microbial activity can potentially improve chlorophenol removal with pure culture bacteria [121] and bacteria enrichment from wastewater treatment plant [122]. However,

biodegradation of chlorophenols with electrodes in actual sediments has not been examined.

Once confirmed that powered electrodes could change DCP biodegradation rates, further studies were conducted to better understand why powered electrodes have such impact. Specifically, hydrogen accumulation and pH shift caused by water electrolysis were hypothesized as the potential explanations for the influence of electrodes on degradation. Thus, DCP biodegradation in sediment slurries without electrodes were studied with different hydrogen and pH levels simulating the conditions observed in presence of powered electrodes.

The hypotheses tested in this study were: (1) applying powered electrodes to sediment will yield a higher degradation rate compared to sediment without powered electrodes and electrodes without microorganisms, and (2) hydrogen and pH are two important factors influenced by the electrodes that impact DCP degradation rates.

5.2 Materials and methods

Chemicals

2,4-dichlorophenol, 4-chlorophenol, 2-chlorophenol were supplied by Acros (Geel, Belgium). Phenol, methanol, toluene, acetic acid (glacial), ammonia dihydrogen phosphate ($\text{NH}_4\text{H}_2\text{PO}_4$), hydrochloric acid (HCl) solution (37%) and sodium hydroxide (NaOH) were supplied by Fisher Scientific (Pittsburgh, PA).

Electrode materials

Carbon materials were chosen because of their relatively low cost, resistance to poisoning, and its flexible and porous texture for easy application. This study used both the same graphite felt as in previous chapter (10 cm long \times 4 cm wide \times 1/4 inch thick, Wale Apparatus Co., Inc., Hellertown, PA), as well as another carbon material, carbon paper (10 cm long \times 2.5 cm wide, BASF Fuel Cell, Inc., Somerset, NJ), in order to examine the effect of different electrode materials on DCP biodegradation. Pd/Nb mesh (1"OD \times 3"L, Scribner Associates Inc., Southern Pines, NC) was used as anode to lower the energy consumption dissipated in the anode side, which is not the focus of this study.

Sediment source and properties

Sediment used in this study was collected from Anacostia River in Washington, DC. Sediment was stored in plastic bottles under ~2 cm of site water at 4°C in dark until use. Major contaminants present in the Anacostia River include PAHs, PCBs and metals [123]. The properties of the sediment and porewater are listed in Appendix C. In this

study, the sediment was added into the buffer (20 mM $\text{NH}_4\text{H}_2\text{PO}_4$ at pH 7) to achieve 1% dry solids slurry. The concentration of 2,4-DCP in observed Anacostia River sediment and porewater is 330 $\mu\text{g}/\text{kg}$ and 10 $\mu\text{g}/\text{L}$, respectively [123]. But for the ease of detection, a higher concentration of 2,4-DCP ($\sim 80 \mu\text{M}$) was dosed into the slurry in this study.

DCP degradation in H-cell reactors

DCP degradation experiments were conducted at room temperature ($23 \pm 2^\circ\text{C}$) in H-cell reactors as described in previous chapters. Each chamber of the H-cell reactors contained 60 ml of headspace and 250 ml of electrolyte (sediment slurry as catholyte, $\text{NH}_4\text{H}_2\text{PO}_4$ buffer as anolyte), and was well mixed using a magnetic stir bar. About 1/3 of the sediment slurry was pre-inoculated anaerobically with a chlorophenol mixture ($\sim 80 \mu\text{M}$ of 2,4-DCP, 2-CP, 4-CP and phenol, the mixture was introduced to the sediment slurry as 2 ml stock solution in methanol) without the presence of electrodes, 1/3 was pre-inoculated with a chlorophenol mixture with powered electrodes, and 1/3 was fresh, non-inoculated sediment. Thus, original bacteria in Anacostia river sediment, bacteria adapted to DCP, and bacteria adapted to powered electrode were all present in the slurry. In order to test whether nutrient level would impact the DCP degradation rate in powered and unpowered conditions, nutrient-amended experiments were conducted by adding 0.05% vitamin and mineral solution to the slurries. The

compositions of the nutrient solutions are listed in Appendix C. All the reactors were assembled in anaerobic hood filled with nitrogen gas, and continuously mixed at 300 rpm by magnetite stir bars at room temperature.

Constant voltage was applied to the reactors using an E3620A DC power supplies (Agilent Technologies, Santa Clara CA). Sterile controls with powered electrodes were made by autoclaving the sediment slurry three times at 120 °C for 20 min each time. No power controls were made with embedded but unpowered electrodes and active sediment slurry. Triplicate reactors were used for the experimental group and no power control, and duplicates were used in the sterile control.

DCP degradation was tested under different applied voltages between 2V and 3.5V. At each voltage, 0.4 ml of 50 mM 2,4-DCP stock solution in 1:1 methanol/water was injected into the cathode chamber to achieve an initial concentration of ~80 µM before the power was turned on, and re-spiked when the DCP had completely degraded. In nutrient-amended experiments, each time before changing the tested voltage, the sediment slurry from the previous experiment was centrifuged at 6000 rpm for 6 min, washed once with the $\text{NH}_4\text{H}_2\text{PO}_4$ buffer to remove the accumulated products that may be toxic to the bacteria, and re-suspended by the buffer with vitamin and mineral solution for the next set of experiments. The concentrations of chlorophenols in re-

suspended sediment after wash were negligible. In unamended slurry experiments, the sediment was not washed. NaOH or HCl was added into the cathode chambers to keep pH neutral if catholyte pH was found lower than 6.5 or higher than 8.

DCP degradation in batch reactors without electrodes

DCP dechlorination batch experiments were conducted in duplicate serum bottle reactors. Each bottle includes 55 ml sediment slurry (1% dry solids) with $\text{NH}_4\text{H}_2\text{PO}_4$ buffer (same as used in H-cell reactors) with 20 ml anaerobic headspace. About 1/3 of the sediment slurry was pre-inoculated anaerobically with the chlorophenol mixture (same as described above) without the presence of electrodes, 1/3 was obtained from the H-cell reactors, and 1/3 was fresh, non-inoculated sediment. Thus, original bacteria in Anacostia river sediment, bacteria adapted to DCP, and bacteria adapted to electrode-induced pH and hydrogen level were all present in the slurry. All the reactors were assembled in anaerobic hood filled with nitrogen gas, and continuously mixed at 300 rpm by magnetite stir bars in room temperature during the experiments. DCP was dosed as described above.

Four constant pH levels were tested for DCP degradation: pH 7, pH 6.5, pH 7.5, and pH 8. Another test with pH increased from 7 to 8 over three days and then lowered to 7 on the fourth day was also conducted to mimic the temporal fluctuation in pH observed in

powered H-cell reactors). HCl or NaOH was added as needed to maintain the desired pH over the course of the experiment. Four headspace hydrogen concentrations were tested for DCP degradation: 0%, 5%, 25% and 50%. Pure hydrogen gas was injected into the headspace as needed to maintain the desired concentration for the duration of the experiment.

Analytical methods

Sediment slurry samples (1 ml per sample, duplicates samples per reactor) were taken over time and the pH was measured using a pH probe (Fisher Scientific, Pittsburgh, PA). The DCP in each sample was then extracted using 0.5 ml toluene. The extraction efficiency for DCP and 4-CP at pH 7 were 84% and 73%, respectively. DCP extraction efficiency did not significantly difference when pH of the slurry varied from 6.5, 7, 7.5 to 8 ($p=0.56$ for single factor analysis of variance), but 4-CP extraction efficiency decreased from 83% at pH 6.5 to 80% at pH 8 ($p=0.004$). After extraction, a 0.2 ml aliquot of toluene was mixed with 0.2 ml methanol, and analyzed by high performance liquid chromatography (HPLC) (Agilent, Santa Clara CA) equipped with a C18 reversed-phase column (15-cm x 4.6-mm, 5 μ m) and UV detector (280 nm). The mobile phase was 60:40:2 methanol: water: acetic acid initially at 1 ml/min, start increasing at 4.5 min until reached 1.5 ml/min at 6 min, and maintain at 1.5 ml/min for another 6 min.

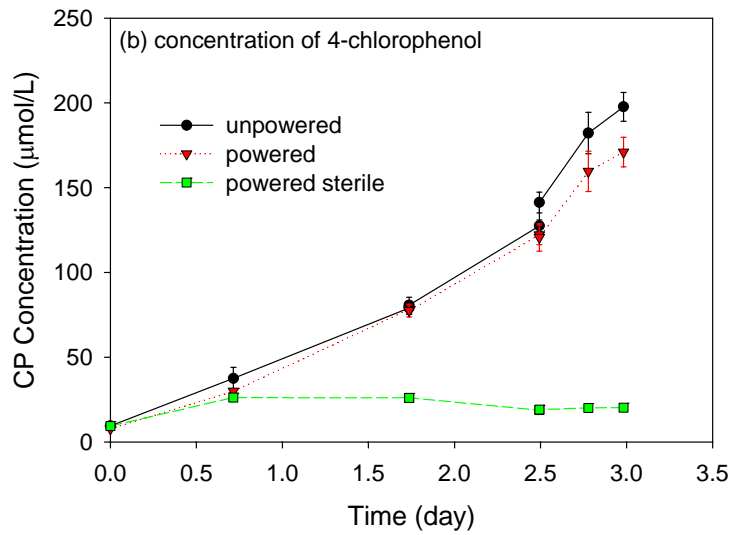
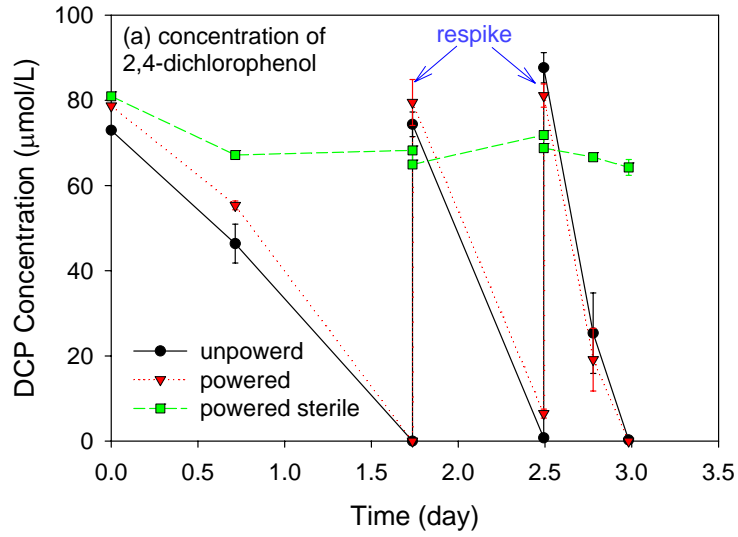
Headspace H₂, CH₄ and CO₂ concentrations were determined by GC/TCD as described in previous chapters.

5.3 Results and discussions

DCP degradation in nutrient-amended sediment slurry with graphite felt electrodes

Figure 5-1 shows representative data for 2,4-dichlorophenol (DCP) degradation in sediment slurry with graphite felt electrodes with 2V applied voltage. Over three subsequent spikes of DCP, 4-chlorophenol (CP) was the only dechlorination product. 2-chlorophenol and phenol were not observed. DCP removal rates were similar in slurry with and without power. The powered, sterile slurry did not exhibit DCP removal. The same trend was also observed for CP production, indicating that the main mechanism of DCP dechlorination was microbial degradation rather than direct electrochemical degradation. The hydrogen concentration provides additional support for microbial degradation rather than an abiotic mechanism. The hydrogen concentration in the sterile, powered control was high due to water electrolysis, but was low in the powered sediment slurry. This suggests that the produced hydrogen in powered sediment was consumed by microbial activity. The unpowered slurry also had a low level of hydrogen, most likely from hydrogen-producing bacteria. Methane concentration was similar in powered and unpowered sediment with live cultures, suggesting that

methanogens were present in both communities. No methane was detected in the sterile control as expected.



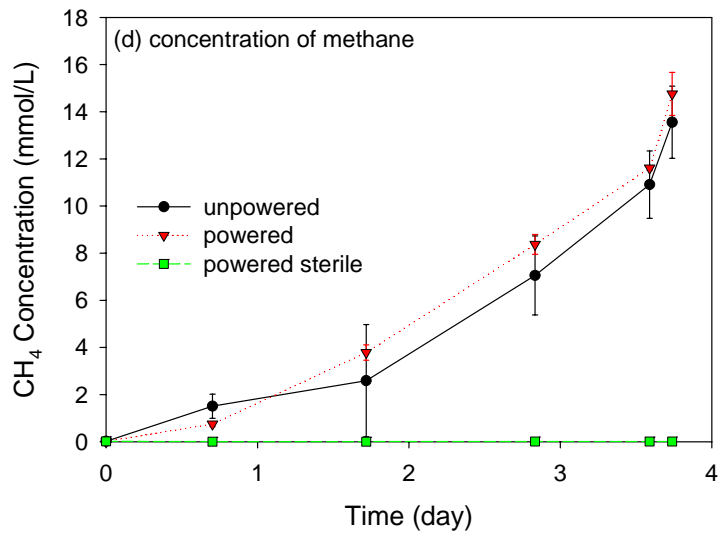
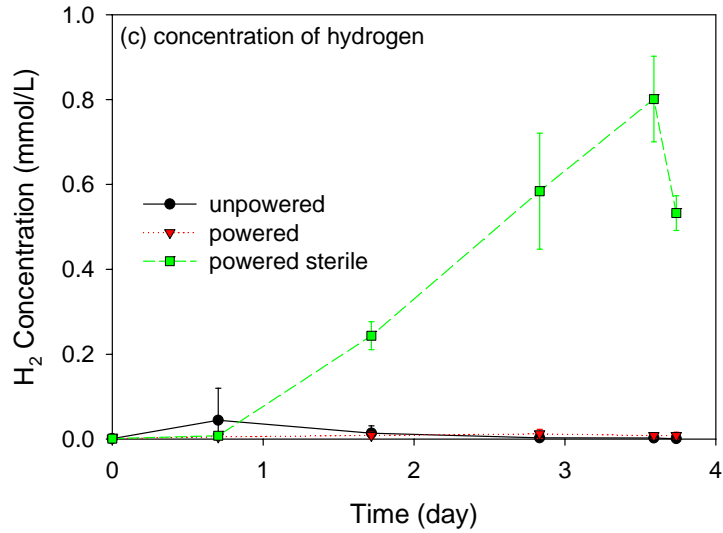


Figure 5-1. (a) removal of 2,4-dichlorophenol (DCP), production of (b) 4-chlorophenol (CP) (c) hydrogen, and (d) methane in nutrient-amended unpowered sediment slurry, sediment slurry powered with graphite felt electrodes at 2V applied voltage, and a powered but sterilized sediment slurry

The results are the means of duplicate or triplicate reactors, and error bars represent standard deviation.

Effect of voltage on DCP degradation rate in nutrient-amended sediment slurry with graphite felt electrodes

The effect of applied voltage on DCP degradation rate was tested at 2V, 2.5V and 3V, as illustrated in Figure 5-2. Degradation at each voltage was tested over at least two spikes of DCP. A T-test indicates that there is no statistically significant difference in DCP removal rates in slurries with powered and unpowered electrodes for any DCP spike ($p > 0.05$) except for the 1st spike where the DCP removal rates in powered and unpowered slurry were 45.9 ± 0.1 and 42.3 ± 0.3 $\mu\text{M}/\text{day}$, respectively ($p = 0.0015$). DCP removal rate in the sterile control was negligible and no significant increase of 4-CP concentration was observed. DCP degradation rate was unaffected by applied voltage in either biotic or abiotic reactors, suggesting that electrochemical dechlorination did not occur over the range of the applied voltage tested (2-3 V). DCP removal was higher in later spikes in the presence of live cultures with powered or unpowered electrodes. Since sediments were washed (as described in the Material and Method section) before each voltage change, such higher removal rate in later spikes suggests that the microbial communities needed time to recover and re-establish after sediment washing.

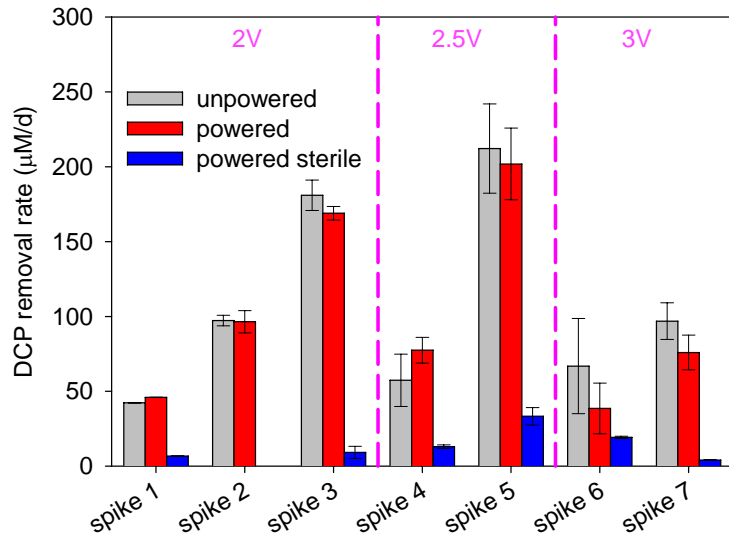
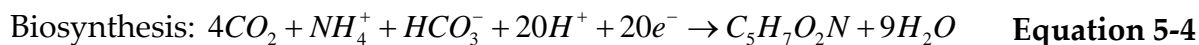
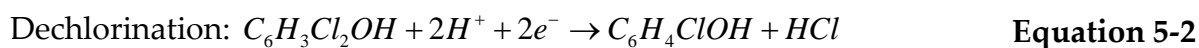
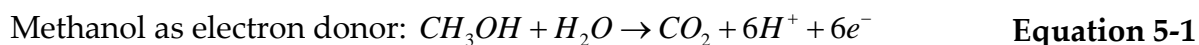


Figure 5-2. Effect of applied voltage on 2,4-dichlorophenol (DCP) degradation in nutrient-amended sediment slurry with graphite felt electrodes

DCP was added to the slurries in seven consecutive spikes, and sediment was washed before changing the applied voltage. The results are the means of duplicate or triplicate reactors, and error bars represent standard deviation.

The results from DCP degradation studies in sediment slurries with graphite electrodes (Figure 5-1 and Figure 5-2) indicate the presence of powered electrodes neither significantly promoted nor depressed DCP biodegradation in the tested sediment slurry. One potential reason is that the DCP biodegradation rate in the nutrient-amended sediment was already high enough that it was relatively unaffected by electrodes, i.e. the required organisms, electron donor and nutrients are already sufficient for biodegradation and thus did not gain extra benefit from the electrodes. It is noticed that

~ 20 mM of methanol was added into the slurries in order to spike DCP, and methanol could provide electrons (Equation 5-1) for DCP biodegradation (Equation 5-2), although some electrons would be consumed in methanogenesis (Equation 5-3) and biosynthesis (Equation 5-4) instead of dechlorination). Thus the degradation rate of the dosed ~80 uM DCP was not affected by the presence of powered electrodes.



Also, another group of experiments was conducted in sediment slurries without nutrient-amendment in order to investigate the effect of powered electrodes under less favorable conditions for biodegradation of DCP. Since graphite felt cathodes did not appear to stimulate abiotic electrochemical dechlorination of DCP, another cathode material, carbon paper was tested in these DCP-removal experiments.

DCP degradation in unamended sediment slurry with carbon paper electrodes

In unamended sediment slurry, the DCP removal rate with powered carbon paper electrodes was not as high as the unpowered control (Figure 5-3), suggesting that the presence of powered electrodes was detrimental to DCP biodegradation. The powered,

sterile control showed some DCP removal, but no dechlorination products were observed, indicating the observed DCP loss was most likely loss due to adsorption onto the electrodes or reactor walls. The applied voltage had no effect on the DCP removal rate in the powered reactor, also suggesting electrochemical DCP degradation was not occurring. Since the sediment was not washed before changing the applied voltage, the DCP removal rate in the unpowered slurry increased with each additional spike, probably due to the adaption of dechlorinators to DCP over time. Although the concentration of methanol introduced into the slurries did not change, DCP biodegradation rates in the unamended sediment were at least one magnitude slower than in nutrients-amended slurry (Figure 5-2 and Figure 5-3), suggesting the biodegradation was limited by the availability of nutrients necessary for microbial activities.

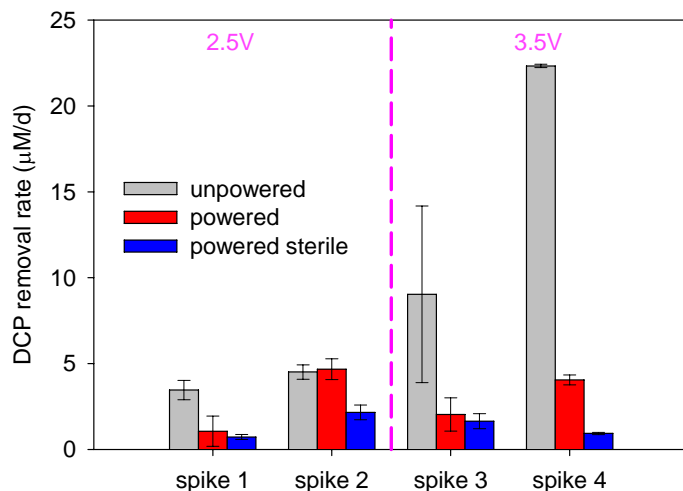


Figure 5-3. Effect of applied voltage on 2,4-dichlorophenol (DCP) degradation in unamended sediment slurry with carbon paper electrodes

DCP was added to the slurries in four consecutive spikes, and sediment was NOT washed before changing the applied voltage. The results are the means of duplicate reactors, and error bars represent standard deviation.

The results in Figure 5-2 and Figure 5-3 suggest that, with the applied voltage insufficient to drive electrochemical DCP degradation, the presence of powered electrodes either did not improve, or even depressed DCP biodegradation. This disproves our initial hypothesis that powered electrodes may provide electron donors and stimulate microbial dechlorination of DCP. Thus, further studies were conducted to investigate factors introduced by the electrodes that may influence the DCP degradation rates.

Powered electrodes in the sediment slurry system can alter several geochemical parameters related to microbial activity. These include redox potential, hydrogen concentration and pH. Changing redox potential is in fact one of the hypothesized benefits of electrode-stimulated biodegradation: creating a reduced environment around the cathode and an oxidative environment around the anode should facilitate electron transfer in contaminant transformation. Hydrogen concentration can have two potentially opposing effects: produced hydrogen can serve as the electron donor for the dechlorinators and thus stimulate DCP degradation, but it can also serve as electron donor for competing bacteria and thus depresses DCP degradation [124-126]. The effect of pH change is even more complicated. The dechlorinators may only be active in certain pH range; the form of DCP existing in the aqueous phase (protonated or deprotonated) depends on pH; and the availability of nutrients are directly related to pH level (some metals precipitate at high pH and some elements change chelating form). Thus, DCP degradation at different hydrogen and pH levels were determined to help explain the effect of powered electrodes on DCP biodegradation.

Effect of hydrogen concentration on DCP biodegradation in sediment slurry

Figure 5-4a shows the DCP biodegradation over time at different headspace hydrogen concentrations. In general, adding H₂ to the reactors lead to higher residual DCP

concentrations or a lower rate of reaction. DCP can be totally removed in 11 days without hydrogen addition. Adding 5% hydrogen in the headspace generally did not change the removal rate, but lead to a low concentration of residual DCP ($\sim 5 \mu\text{M}$) which could not be further removed over 20 days. A similar trend was observed with a higher hydrogen level (25%), with $\sim 20 \mu\text{M}$ residual DCP. Adding a high concentration of hydrogen (50%), on the other hand, lead to slower DCP removal rates, but also the complete removal of DCP within 20 days.

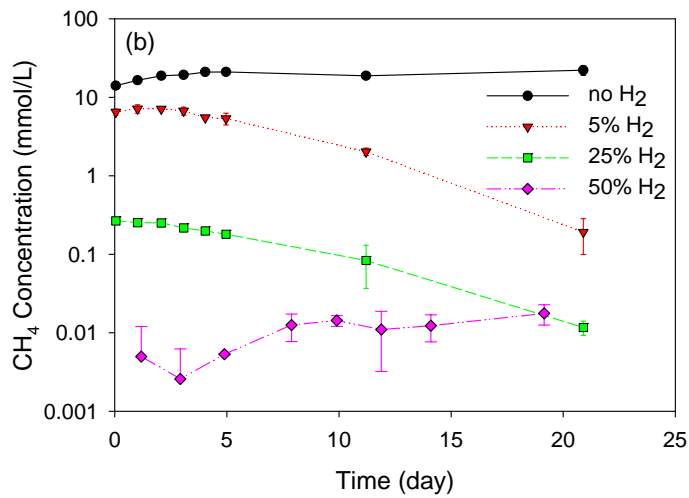
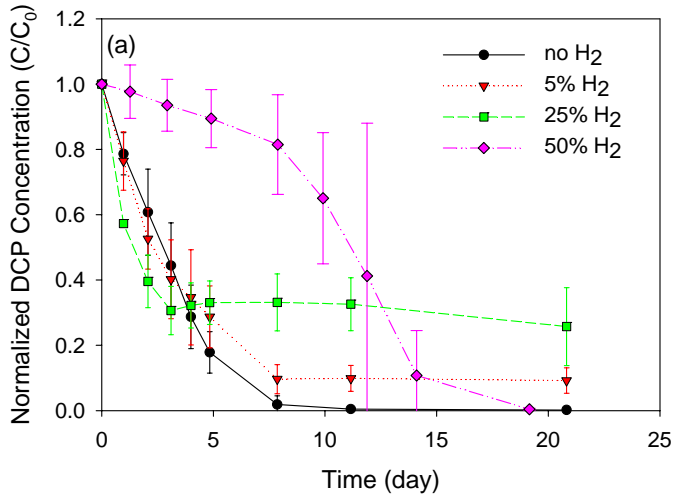


Figure 5-4. Effect of headspace hydrogen concentration on (a) 2,4-dichlorophenol (DCP) degradation and (b) methane production in unamended sediment slurry without electrode

DCP concentrations were normalized to initial DCP concentration (~80 μM). Hydrogen was injected into the headspace as needed to keep the desired constant concentration over the duration of the experiment. The results are the means of duplicate reactors, and error bars represent standard deviation.

Overall, results in Figure 5-4a suggest that hydrogen negatively impacted DCP dechlorination, conflicted with the reported studies showing hydrogen can improve DCP biodegradation [116, 117], but the reason for such difference is unclear. It seems the methanol introduced into the sediment sample during DCP spiking this study is enough to support dechlorination, thus adding 5% or 25% hydrogen to the sediment slurry did not change the initial degradation rate. One potential explanation for the observation that the DCP residual was proportional to the hydrogen concentration is that, other bacteria in the slurry were competing with dechlorinators for nutrients (as suggested for the electrode reactions mentioned above where nutrients in unamended sediment were a limiting factor for DCP biodegradation). When DCP concentration was high, the side reactions could not outcompete dechlorination so the DCP removal rate was not affected by hydrogen concentration; but as the DCP concentration decreased and could not maintain a high population of dechlorinators, the numbers of other bacteria increased and the dechlorinators lost their privilege for maintaining dechlorination, so DCP was no longer degraded. A high level of hydrogen (50%) seems to depress the activity of the whole microbial community, as evidenced by the low methane production (Figure 5-4b), thus a slow but complete DCP removal was achieved.

It is important to note that, unlike previous studies on the effects of hydrogen on dechlorination [124-126], methanogenesis in this study was not a key side reaction

competing for hydrogen with dechlorinators. As shown in Figure 5-4b, methanogenesis was also depressed by hydrogen: the concentration of methane decreased with increasing hydrogen concentration. The reason for this observation is unclear.

Effect of pH on DCP biodegradation in sediment slurry

Figure 5-5a shows DCP biodegradation under different pH conditions. Dechlorination started later at pH 6.5 than at pH 7, but both achieved totally removed in 10 days. Under all other pH conditions (pH 7.5, pH 8, and pH oscillating between 7 and 8), no dechlorination was observed. These results, however, contradict several previous reports that a higher pH (generally around 8) favors chlorophenols dechlorination by both pure culture [127], mixed culture from lakes [128], soil [129], and aerobic digesters [130]. The reason for such a difference is unknown.

There are three possible explanations for the observed pH effect: (1) a larger portion of DCP is deprotonated at higher pH (the pKa of DCP is 7.85) and the dechlorinating organisms cannot utilize this charged form; (2) the activities of either the dechlorinating organisms, or other bacteria in collaboration with dechlorinators are depressed at higher pH; or (3) certain nutrients become (partially) unavailable at high pH.

First consider the pH effect on DCP speciation. Although it is reported that low pH values increased the amount of DCP adsorbed to bacterial cells [131], the deprotonated form of DCP is still expected to be bioavailable, inferred from studies with complete DCP microbial dechlorination at pH higher than its pKa [117, 128, 130, 132, 133]. Also, at pH 7.5 or 8, or oscillating between 7 and 8, since there are still some protonated DCP molecules available for the bacteria, the dechlorination rate should not be negligible as was seen here. Thus, DCP speciation should not be the main reason for the observed pH effect. pH effect on DCP and 4-CP extraction efficiencies were also considered unrelated to the observed degradation rate change, since at all tested pH level, the extraction efficiencies were all similar, as shown in Figure C-1 in Appendix C.

Next consider the pH effect on bacteria. It is generally considered that dechlorination can occur in the range of pH 6-8 [134]. If it is the case for this study, then it is more possible that pH indirectly affected dechlorination by changing other species in the microbial community, rather than directly affecting the activity of dechlorinators. Methane production (Figure 5-5b) had many similarities with dechlorination: at pH 7, both process were at highest levels; at pH 6.5, both process started slow but got significant improved after 5 days; there is rarely change in methane concentration at pH oscillating conditions, and very slow increase at pH 8, suggesting high pH indeed depressed methanogenesis. It is reported that pH had a greater impact on methane

production than dechlorination of tetrachloroethylene in mixed soil bacteria culture [135]. Methanogens may provide essential nutrients to the dechlorinators, as suggested by the fact that the presence of methanogens inhibitor would also inhibit dechlorination of perchloroethene [136]. If this is also true for DCP dechlorination in this study, limited DCP biodegradation at high pH may be explained as a result of the depressed methanogens activity. This hypothesis partially explains why there was no dechlorination at pH 8 and pH oscillating conditions, but can not explain why at pH 7.5, methane production was active (Figure 5-5b) but dechlorination was not observed.

The pH effect on nutrients availability was tested in another set of experiments on nutrient amended sediment slurries (Figure 5-5c). After adding nutrients into the sediment slurry, the DCP biodegradation rate in sediment slurry was greatly increased compared to unamended conditions at pH 7.5. More importantly, the degradation rate at pH 7.5 was similar to that at pH 7 or pH 6.5. These results suggest that in unamended sediment at higher pH, some key nutrients may not be available to the bacteria, (e.g., precipitation) and nutrient amendment may supplement some nutrient loss caused by pH rise.

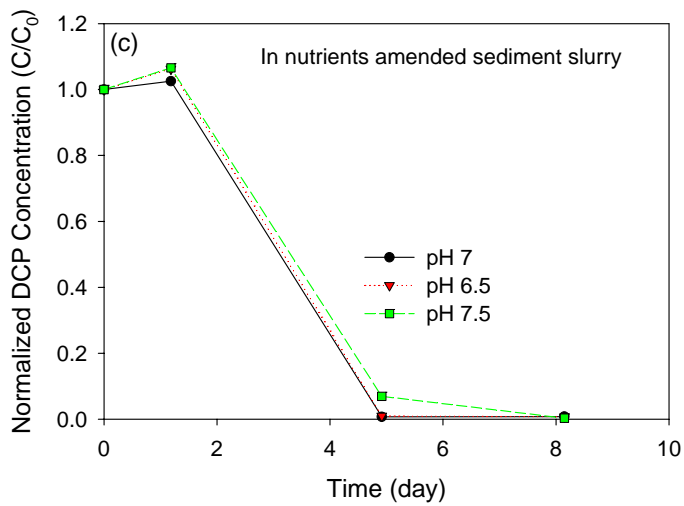
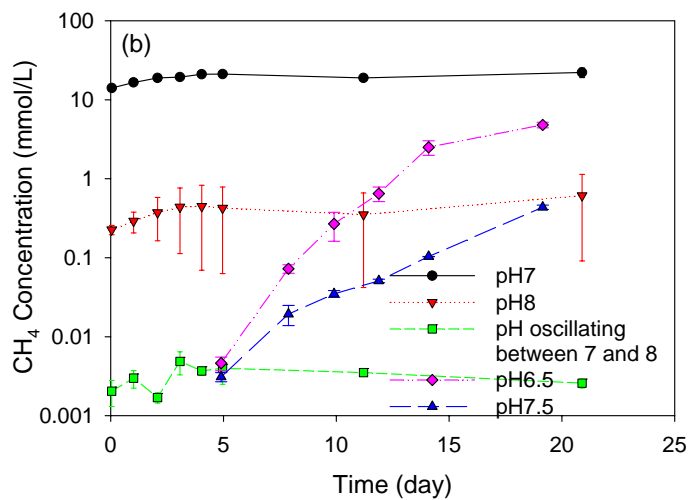
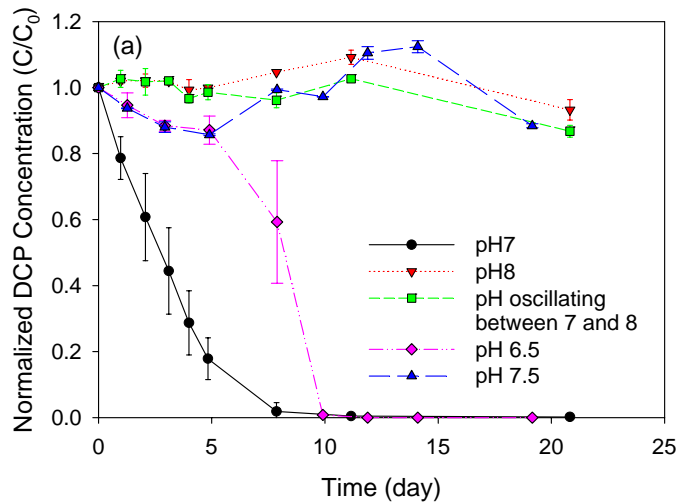


Figure 5-5. Effect of pH on (a) 2,4-dichlorophenol (DCP) degradation and (b) methane production in unamended sediment slurry, and (c) DCP degradation in nutrient-amended sediment slurry without electrode

DCP concentrations were normalized to initial DCP concentration ($\sim 80 \mu\text{M}$). HCl or NaOH was added as needed to keep desired constant pH over the experiment. The results are the means of duplicate reactors, and error bars represent standard deviation.

5.4 Conclusions and Implications for Sediment Capping

This work demonstrated that 2,4-dichlorophenol can be reductively transformed to 4-chlorophenol in sediment slurries with carbon electrodes powered by applied voltage that is insufficient to induce abiotic electrochemical dechlorination. However, applying powered electrodes to sediment did not yield a higher degradation rate of DCP in the tested sediment than observed with unpowered electrodes. In the absence of added nutrients, the powered electrode decreased the rate of DCP biodegradation. The powered electrodes may change the biodegradation rate by altering sediment pH and hydrogen concentration: hydrogen produced by water electrolysis may lower the beneficial microbial activities in sediment, while pH rise near the cathode can greatly depress the dechlorination rate.

This study shows different results than the previous studies that demonstrate enhancement of biodegradation of PAHs [45] and PCBs [46] in sediment in the presence of powered electrodes. The reason for the different observations is unclear. The lower reactivity in powered sediment compared to unpowered sediment may be caused by insufficient catalytic activity of the electrode materials used, inadequate applied voltage supplied to the electrodes, especially high microbial activity of the sediment used in this study, high concentration of methanol introduced into the system, or high biodegradability of DCP. The previous mentioned two studies on powered electrode improving biodegradation in sediment did not provide information on hydrogen formation in their systems. pH shift near electrode surfaces were also observed in these studies, but apparently did not prove detrimental to the microbial activity, or the negative effect of pH was compensated by other positive effects of the powered electrode. However, the study with PCB showed that the removal percentage decreased with increasing applied voltage from 1.5V to 3V [46]. Their findings may be the result elevated hydrogen concentration or pH changes at high voltage that hindered biodegradation, as observed in this study.

Although the negative effect of powered electrodes on DCP biodegradation provide important information on decision-making level, revealing there are scenario when the electrode-based cap does not work well, as an scientific exploration, it is more

interesting to find when the electrode-based cap do work. DCP is not a good probe compound to demonstrate the improvement of sediment *in situ* biodegradation stimulated by powered electrodes, or the Anacostia River sediment is not good model sediment. In retrospect, it would have been better to examine the biodegradation of DCP in the sediments first and assess the impact of the various perturbations introduced by electrodes (e.g. H₂, and pH changes) on microbial activity first. In that way, the conclusion that powered electrodes probably would not work well for this probe compound in the tested sediment can be draw without even moving to the electrode-based degradation experiments, and the following study can be focused on other contaminants and/or other sediment source.

The results in this study suggest that the electrode-based sediment cap does not benefit natural attenuation of more easily degradable compounds like DCP, and when essential nutrients are plentiful. Hydrogen as electron donor provided by the cap might only be needed for removing refractory compounds with low intrinsic degradation rates. Also, this work suggests that to maintain desirable biological activity, effective pH control methods, for example adding pH buffering chemicals when constructing the cap, may be necessary.

Chapter 6. Electrode-based selective oxidation of bromide in mining brines from hydraulic fracturing sites^①

Abstract

Mining brine produced from hydraulic fracturing of shale gas has raised a number of environmental and human health issues. An important health concern associated with the brine is its high bromide concentration (~1g/L). If the brine is discharged to receiving waters that serve as drinking water sources, the bromide in it can lead to the formation of carcinogenic brominated disinfection byproducts (DBPs) during water treatment. However, the co-existence of other ions in the mining brine, especially chloride as high as 30-200 g/L, makes bromide removal technically challenging. This study investigated the feasibility of using electrodes for selective bromide removal from mining brine. In this process, bromide is selectively oxidized to form bromine, without causing chloride and water oxidation. The bromine can then be outgassed from the solution and recovered. Results of this study suggested it is possible to selectively remove bromide from the brine with a relatively fast rate (~10 h⁻¹m⁻² for produced water and ~60 h⁻¹m⁻² for flowback water), and with an acceptable current efficiency (60-90%) at reasonable energy costs (6 kJ/g Br). Although the presence of chloride and other brine

^① This chapter is under preparation for possible publication.

components decreased the bromide removal rate compared to synthetic bromide solutions, the process parameters measured suggest that selective bromide removal from mining brines is feasible utilizing mature technologies used in the chlor-alkali process.

6.1 Introduction

Hydraulic fracturing for mining natural gas trapped in shales produces large amounts of brine with exceptionally high salt content that can reach 5 times that of sea water [10]. Management of the brines associated with gas extraction is important for sustainable development of the shale gas mining industry. The fracturing fluid flowing back out of the shale after fracturing includes both a high flow rate, short duration “flowback water” and a low flow rate, long duration “produced water” [11]. Total dissolved solids (TDS) in the brine are primary constituents of concern in onshore operations. Although TDS does not present a direct threat to humans and ecosystems, the presence of high TDS limits potential reuse of mining brine in irrigation, livestock or wildlife watering, and other various uses (e.g., vehicle washing and power plant makeup water). Also, mining brine contains constituents which are a health concern, including dispersed and dissolved organic compounds (e.g., heavy and light hydrocarbons, phenols, ketones), chemical additives (surfactants, biocides, scale inhibitors and corrosion inhibitors), bacteria, metals (e.g., zinc, lead, manganese, iron, and barium) and naturally occurring radioactive material [137]. Thus, the brine needs to be properly treated before reuse or discharge to protect groundwater and surface water resources. Traditional mining brine treatment includes oil-water separation by skimming, flotation or other treatments, and suspended solids removal by settling or filtration [137].

Besides the components in mining brine discussed above, the presence of bromide also draws special interest. When the brine is discharged to surface water, the bromide may become a potential detrimental factor. If the receiving water is used for water supply with chlorination used for disinfection, bromide becomes the precursor for many brominated carcinogenic disinfection byproducts (DBPs) [12]. For example, the Monongahela River in southwestern Pennsylvania received gas mining brine from the Marcellus Shale, and in drinking water utilities using it as the source water, associated concurrent increase of brominated DBPs, TDS and bromide concentration have already been observed [13, 14]. Thus, it will likely be necessary to lower the bromide level in shale gas mining prior to discharge to protect surface and ground water quality.

However, available techniques for effectively remove bromide in mining brine are limited. There are some bromide removal methods proposed for drinking water treatment, such as silver-doped activated carbon aerogels adsorption [70] and aluminum coagulation [71]. However the brackish nature of the mining flowback water and produced water makes selective bromide removal difficult because of the presence of overwhelming high concentration of chloride (magnitudes higher than bromide) and other ions. These ions compete with bromide removal and generally render these approaches ineffectual. Another option is to remove bromide together with all other TDS in the desalination process. However the available techniques (e.g., thermal

distillation, ion exchange, reverse osmosis, forward osmosis, nanofiltration, ultrafiltration, electrodialysis, reverse electrodialysis, electrodeionization and capacitive deionization) are all prohibitively energy intensive [10], especially when the target is only to remove bromide and the presence of other ions is not problematic. The estimated of energy consumptions for reverse osmosis, capacitive deionization and thermal distillation used in general desalination processes, as well as the energy consumption of selective electrolysis proposed in this study, are compared in Table 6-1. The detailed calculation of energy consumption is shown in Appendix D.

Table 6-1. Theoretical minimum energy consumption for different technologies

Method	Energy consumption (kJ/g Br)
Electrolysis (remove Br ⁻ selectively)	1.3
Reverse osmosis (remove TDS)	11
Capacitive deionization (remove TDS)	412
Thermal distillation (remove TDS)	2142

Note: assuming use brine with the chemical composition as shown in Table 1-2

Electrolytic oxidation is an effective method to convert chloride into chlorine (Equation 1-2), and this process has been utilized in chlor-alkali industry for decades with brine or seawater as the chloride source. Since halogens have many common characteristics, an analogous process of electrolytic oxidizing bromide to bromine can be applied for bromide removal and bromine production from the bromide containing mining brine (Equation 1-1).



This method may be competitive for treating mining brine, because the high salinity in brine provide natural electrolyte for the electrochemical reaction, and thus lowers the energy consumption. However, precise electrode potential control is necessary for selective bromide removal, because the standard bromide oxidizing potential is only 0.27 V lower than the chloride oxidizing potential (Equation 1-2 and Equation 1-1, the potentials are vs. standard hydrogen electrode (SHE)) [16].

A similar process was developed to directly oxidize bromide to bromine by electrodes both in drinking water source treatment [66-68] and for bromine production from bromide-containing brine [63-65]. However, the former only treat relatively clean water with very low bromide concentration (~200 ppb), while the later focused on bromine production and does not address the need for low residual bromide concentration of the processed brine. It is thus unclear whether such electrolytic treatment can be successfully applied in treating a chemically complicated mining brine to achieve a low bromide concentration to decrease the DBPs formation potential.

For the purpose of preventing brominated DBP formation, electrolytic bromide removal can be performed either in the brine before discharge or in the drinking water treatment plant before chlorination. In practice, bromide removal from brine has several advantages: (1) The high TDS in brine provides natural electrolyte support for the electrolytic reaction and thus reduces energy consumption over what would be expected for relatively low ionic strength drinking water with greater ohmic losses. (2) The volume of brine discharge is much less than drinking water to be treated, thus smaller reactors and electrodes are needed if bromide is removed from brine. (3) If the treated brine is discharged into surface water with high flow rate, the bromide concentration in the treated brine does not have to be as low as in drinking water treatment, because dilution will further reduce the bromide concentration in receiving water. (4) DBPs are not regulated in brine discharge, but are strictly regulated in drinking water, thus DBPs formation during electrolyzing the brine is not a concern but needs to be carefully avoided when electrolyzing drinking water. It is therefore a better option to remove bromide at the point of brine discharge instead of drinking water treatment.

The objective of this work is to evaluate the feasibility of selective bromide removal from mining brine by electrolysis, and to make preliminary estimates for the energy cost of a scaled up process for treating mining brine. Specifically, the feasibility of

selective bromide removal in the presence of chloride was determined, and the bromide removal rate at different chloride concentration and in real mining brine was measured.

6.2 Materials and methods

Chemicals

All the chemicals used were reagent grade unless otherwise noted. Sodium chloride (NaCl), sodium sulfate (Na₂SO₄), potassium bromide (KBr), potassium bromide (KBr), soluble starch, potassium dichromate (K₂Cr₂O₇), eriochrome black T, disodium ethylenediamine tetraacetate dehydrate (C₁₀H₁₄N₂Na₂O₈·2H₂O), magnesium chloride hexahydrate (MgCl₂·2H₂O), ammonium chloride (NH₄Cl), sodium carbonate (Na₂CO₃), sodium bicarbonate (NaHCO₃), triethanolamine (C₆H₁₅NO₃), sodium hydroxide (NaOH), sulfuric acid (H₂SO₄) and hydrochloric acid (HCl) were supplied by Fisher Scientific (Pittsburgh, PA). Sodium persulfate (Na₂S₂O₈) was purchased from Acros (Geel, Belgium). Calcium carbonate (CaCO₃, special reagent low in heavy metals, alkalis, and magnesium), ammonium hydroxide (NH₄OH), was purchased from Aldrich Chemical (Milwaukee, MI).

Electrode materials

Graphite materials were historically used in chlor-alkali processes as the anode because of their low cost and resistance to poisoning. The graphite felt used in nitrobenzene

study was found not selective enough for bromide over chloride and thus was not used. In this study solid graphite rods, were chosen as the anode. Pd/Nb mesh (1"OD x 3"L, Scribner Associates Inc., Southern Pines, NC) was used as cathode to lower the energy consumption dissipated in the cathode side.

Mining brine

Flowback water sample and produced water sample were collected from Southwestern Pennsylvania. Both samples are stored at 4 °C until use. Samples were filtered with 20 µm filter (Grade 41 ashless quantitative filter paper, Whatman, Piscataway, NJ) before using in bromide removal experiments. Properties of the brines including hardness, alkalinity, pH, conductivity, total dissolved solid (TDS) and dissolved volatile solids (DVS), dissolved organic and inorganic carbon content (DOC and DIC) were determined using standard analytical methods as described below. For the experiments with softened brine, excess amount of Na₂SO₄, Na₂CO₃ and NaOH was added to brine to precipitate hardness. Then the brine was filtered again and adjusted back to initial pH before use.

Linear voltammetry

Linear voltammetry of bromide and chloride oxidation on graphite electrodes was carried out using a potentiostat (mode 2049, AMEL Instrument, Milano, Italy) to

demonstrate the possibility of stimulate bromide oxidation without chloride and water oxidation, and to determine the proper anode potential for selective bromide oxidation. For these initial experiments graphite rods (0.25"OD x 3"L, GraphiteStore.com, Inc., Buffalo Grove, IL) were used as both working and counter electrodes. The electrode potential was scanned between 0 and 2V against Ag/AgCl reference electrodes (Electrolytica, Inc., Amherst, NY) at a scan rate of 50 mV/s. Tested electrolytes include buffer solution (5 mM phosphorous buffer at pH 7), pure bromide solution (buffer + 0.5M KBr), pure chloride solution (buffer + 0.5M NaCl) and a combined bromide/chloride solution (buffer + 0.5M KBr + 0.5M NaCl). During scans, the electrolytes were constantly mixed by magnetite stir bar at 500 rpm at room temperature.

Selective bromide removal from synthetic water and mining brine

A series of experiments was carried out at room temperature ($23\pm 2^{\circ}\text{C}$) in H-cell reactors as described in previous chapters. Each chamber contained 90 ml of headspace and 220 ml of electrolyte (synthesized or actual brine solution), and was well mixed using a magnetic stir bar. In these experiments graphite rods (1"OD x 3"L, Graphite Engineering & Sales Co., Greenville, MI) anodes and Pt/Nb mesh (1"OD x 3"L, Scribner Associates Inc., Southern Pines, NC) cathodes were used with Ag/AgCl as the reference electrodes. The anode potential was poised at 1V vs. Ag/AgCl by the potentiostat. Duplicate H-cells

were used for each experiment to determine reproducibility. Bromide removal experiments were conducted in bromide solution with different chloride concentrations, flowback water, and produced water. Air was constantly bubbled into the anode chamber to strip the formed bromine (Br₂) out of the chamber. The outlet gas was directed to a separate bottle containing 2.5 g/L KI to collect the produced bromine for quantitative analysis.

Calculation of bromide removal rate, current efficiency and energy consumption

The bromide concentration in solution was monitored over 6.5 hours, and was fitted using a first-order kinetic model. For all experiments, R²>0.98 was achieved for the model fits. The first order kinetic rate constant was used to compare the rates achievable under the various electrolyte conditions used.

Current efficiency was calculated using Equation 3-1 and Equation 6-4.

$$\text{Current efficiency} = \frac{C_{Br^-,initial} - C_{Br^-,end}}{\text{Current equivalent of Br}} \text{ (dimensionless)} \quad \text{Equation 6-3}$$

Where

$$\text{Current equivalent of Br} = \frac{\int_0^{t_{total}} Idt}{F} \times \frac{MW}{Vol} \text{ (g/L)} \quad \text{Equation 6-4}$$

I is the cell current (A); *t*_{total} is the total reaction time (s) ; *F* the Faradic constant (96485 C/mol); *MW* is the molecular weight of bromine element (80 g/mol); *Vol* is the volume of electrolyte in anode chamber (0.22 L).

Energy consumption was calculated using Equation 6-5.

$$\text{Energy consumption} = \frac{\int_0^{t_{\text{total}}} V I dt}{(C_{Br^-, \text{initial}} - C_{Br^-, \text{end}}) Vol} \text{ (J/g)} \quad \text{Equation 6-5}$$

V is the cell voltage (V).

Analytical methods

Mining brine properties: hardness of the brine was determined by EDTA titration (standard method 2340C); alkalinity was determined by H_2SO_4 titration to pH 4.3 (standard method 2320B); pH and conductivity were determined by pH and conductivity probe; TDS and DVS were determined by heating water sample at 104°C and 550°C, respectively; DOC and DIC were measured by O.I. Analytical 1010 liquid TOC analyzer (College Station, TX).

Bromide and chloride concentration in the electrolyte were determined by ion chromatography (IC) (Dionex, Sunnyvale, CA) using an AS14A column and conductivity detector. The mobile phase was 8 mM Na_2CO_3 /1 mM $NaHCO_3$ at 1.0 ml/min. Bromine captured by KI adsorption is reduced to bromide and was also quantified by IC. Bromine remaining in the H-cells was determined by titrating the electrolyte with $Na_2S_2O_3$ and the KI-starch indicator. The total produced bromine

concentration was calculated as the sum of bromine captured in KI and bromine remaining in the electrolyte.

6.3 Results and discussion

Linear voltammetry and proof of bromide selective oxidation

Although there is a 0.27 V gap between the standard potential for bromide oxidation (1.09 V vs. SHE) and chloride oxidation (1.36 V vs. SHE), in practical this gap may be negligible. The standard potentials are determined for 1 M conditions, while higher concentrations of bromide and chloride will lead to lower potentials. Since the mining brine contains at least an order of magnitude higher concentration of chloride than bromide, the reduction potential gap between bromide and chloride oxidation reaction is reduced. For example, when chloride and bromide are at their respective median concentration in mining brine (76 g/L and 1.2 g/L, Table 1-2 in Chapter 1), the theoretical chloride and bromide oxidation potential become, 1.34 V and 1.20 V, respectively, leading to the theoretical gap only 0.14 V. Moreover, the electrodes may have different overpotential for bromide and chloride oxidation, if the overpotential for bromide oxidation is greater than for chloride oxidation, the practical gap will become even smaller. Thus, special attention is needed to avoid the chlorine side reaction.

Another important side reaction is water electrolysis. Theoretically oxygen production starts at lower potential (0.82 V vs. SHE) than bromine production at pH 7. Although many commonly used electrode materials have large overpotentials for oxygen generation, and in practice oxygen production does not occur under 2V, it is still necessary to verify whether oxygen production is an important side reaction with the graphite electrodes used in this study. And if oxygen and chlorine production did start about the same potential as bromine production, selective bromide removal would become unfeasible because the high concentration of water and chloride would make the rates of the two side reactions faster than bromide oxidation.

To demonstrate the possibility of selective bromide oxidation without chloride and water oxidation, and to determine the proper anode potential for selective bromide oxidation, linear voltammetry of buffer solution (5 mM phosphorous buffer at pH 7), 0.5M bromide in buffer, 0.5M chloride in buffer and a combined 0.5M bromide/0.5M chloride solution in buffer was conducted, as shown in Figure 6-1. The onset of bromide oxidation occurred at ~0.85V vs. Ag/AgCl (~1.1 V vs. SHE), chloride oxidation was at ~1.25V vs. Ag/AgCl (~1.5V vs. SHE), and water oxidation was not observed in the potential range tested. Compared to the theoretical potential, it appears that the graphite electrodes used in this study require a very low or negligible overpotential for bromide oxidation, a moderate overpotential for chloride oxidation, and a significant

overpotential for oxygen production. Thus, bromine formation is favored over chlorine and oxygen formation at low potential. The behavior of the combined Br⁻/Cl⁻ solution was the same as the Br⁻ solution before the onset of chlorine production, and only had higher current than the Br⁻ solution after chlorine production started, suggesting the presence of chloride did not interfere with bromide oxidation at low potential. Since there is ~0.5V gap between bromide oxidation and chloride oxidation, and even a greater gap between bromide oxidation and water oxidation, selective bromide removal in chloride-rich solution is possible.

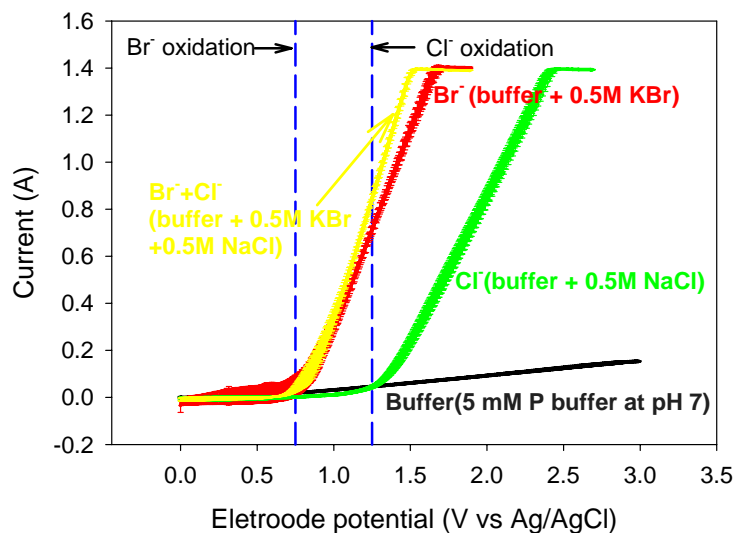


Figure 6-1. Linear voltammetry of Br⁻ and Cl⁻ solutions with graphite rod electrodes

Solutions were constantly stirred by magnetite bars at 500 rpm at room temperature.

Voltammetry conditions: scan rate: 50 mV/s; step width: 100 ms; step height: 5 mV.

Error bars represent standard deviations of 5 replicate scans for each solution.

While the linear voltammetry suggested bromide can be selectively oxidized in the presence of an equal molar concentration of chloride, the electrolysis of chloride and bromide solution in H-cell reactors (Figure 6-2) further verified the potential of this method for selective bromide removal when chloride exists at significantly higher concentrations than bromide, typical for mining brine. Concentrated chloride solution (76 g/L) was poised at 1V vs. Ag/AgCl electrode for 20 hours. No chlorine generation was detected using $\text{Na}_2\text{S}_2\text{O}_3$ titration, and both the cell voltage and current were constantly low, further evidencing that no chloride oxidation was taking place. However, once a relatively low concentration (1.2 g/L) of bromide was added into the electrolyte, there was an immediate jump in both cell voltage and current, and the electrolyte turned to a yellow-green color, suggesting bromide was oxidized to form bromine. The voltage and current gradually decreased and returned to the initial level as bromide was consumed. These results suggest, even at high concentration and prolonged reaction time, chloride cannot be oxidized at the poised potential (1V vs. Ag/AgCl electrode) while bromide at a much lower concentration can be selectively oxidized when the anode potential is carefully controlled.

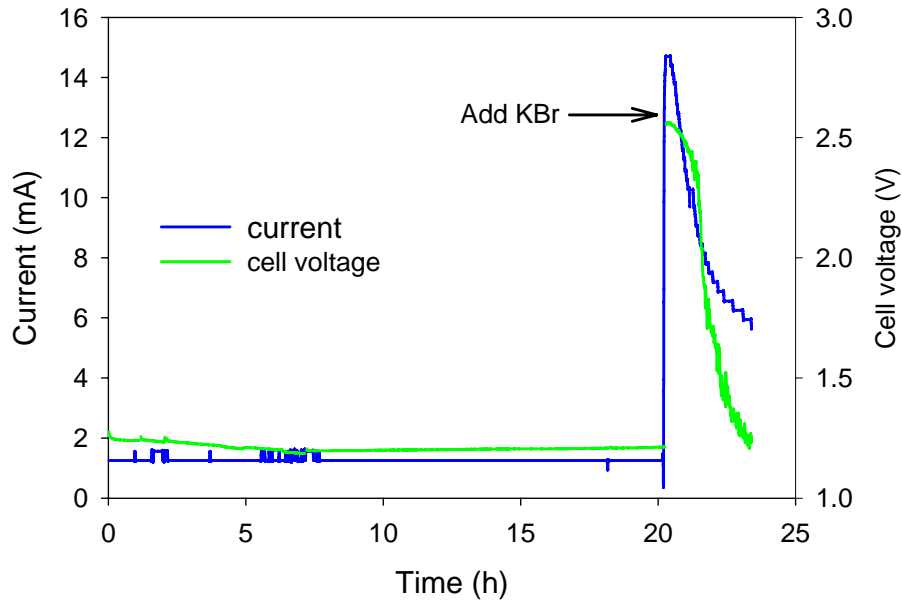


Figure 6-2. Current and cell voltage profile in H-cell reactor with 76 g/L chloride solution before and after adding 1.2 g/L bromide

Cell voltage was measured between the graphite anode and the Pt/Nb cathode. The anode was poised at 1V vs. Ag/AgCl electrode. Initial electrolyte was NaCl only, and KBr was added after 20 hours.

Effect of chloride concentration on bromide removal

The removal of bromide from synthetic brine containing 1.2 g/L bromide and different chloride concentrations was measured to determine the effect of chloride concentration on bromide oxidation. The bromide concentration used here was selected based on the median concentration found in mining brine (Table 1-2 in Chapter 1), and the chloride concentration was selected to represent low, median and high concentration in mining

brine. Chloride at the same mass concentration of bromide (1.2 g/L) was also tested. Figure 6-3 is an example profile of the measured bromine and bromide concentration over time. Within 6.5 hours, all the bromide in the electrolyte was oxidized to bromine and removed from the solution by air stripping. The current efficiency was 80%, and no chlorine was detected in the KI adsorption solution.

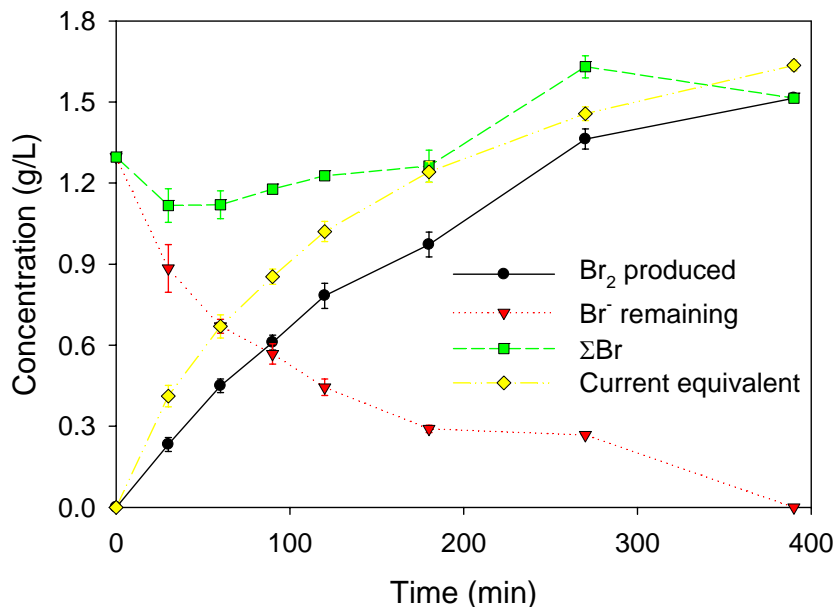


Figure 6-3. Bromide removal in 1.2 g/L Br⁻ + 76 g/L Cl⁻ solution by graphite rod anode poised at 1V vs. Ag/AgCl electrode

The results are the means of duplicate reactors, and error bars represent standard deviation.

The measured bromide removal rate constant vs. chloride concentration is shown in Figure 6-4. The data indicate that chloride significantly decreased the bromide removal rate, but the effect is non-linear. When chloride is present in the electrolyte at the same amount of bromide, the bromide removal rate was reduced by 30% compared to the absence of chloride. However, when chloride concentration was further increased, the decrease in the bromide removal rate was much less severe. Except for the no chloride situation, there is a linear relationship between chloride concentration and bromide removal rate. Given that the adsorbed chloride is not oxidized, the reason for chloride depressing bromide removal rate may be competitive adsorption on the anode surface. However, the presence of chloride ions also has a positive impact on the overall process. The presence of chloride increases the electrolyte conductivity, thereby reducing the energy consumption for bromide removal by a factor of 6 to 11. In practice, the savings on energy use will likely compensate for the lower reaction rate, although a lower reaction rate necessitates longer retention times and hence larger reactors (higher capital) for a given flow rate. The current efficiency for bromide removal was relatively unaffected by chloride concentration.

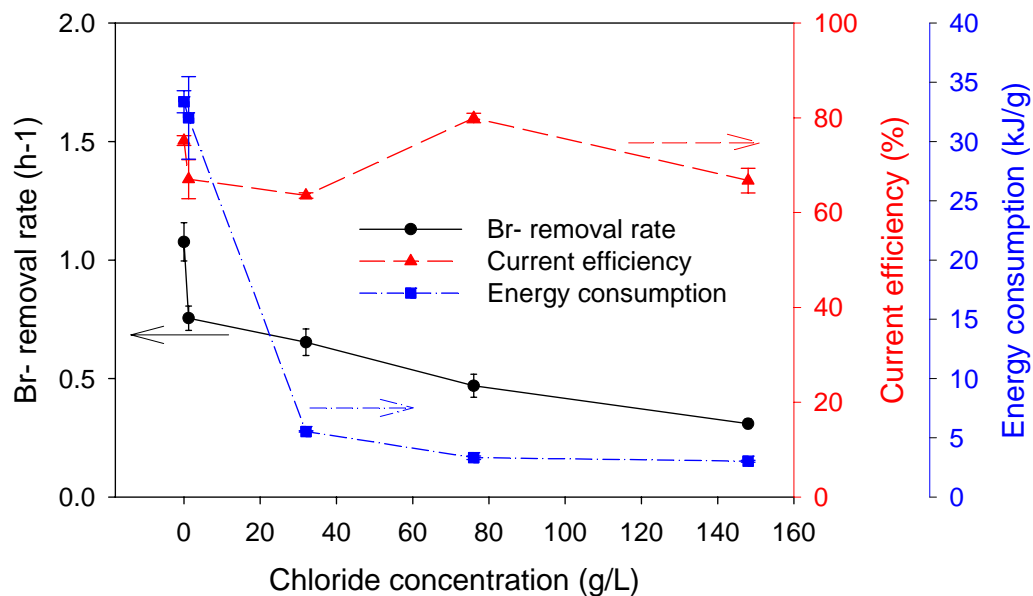


Figure 6-4. Effect of chloride concentration on bromide removal rate, current efficiency and energy consumption in synthesized brine by graphite rod anode poised at 1V vs. Ag/AgCl electrode

Bromide concentration is 1.2 g/L. The results are the means of duplicate reactors, and error bars represent standard deviation.

Bromide removal from mining brine

Two kinds of mining brine (one flowback water sample, one produced water sample) were tested for selective bromide removal by electrolysis. The properties of the brine samples are summarized in Table 6-2.

Table 6-2. Properties of brine samples

	Flowback water sample	Produced water sample
Total dissolved solids (g/L)	46.4±0.3 ^c	184.6±1.1 ^c
Dissolved volatile solids (g/L)	4.7±0.3 ^c	15.4±0.6 ^c
pH	6.93	4.74
Conductivity (mS/cm)	86±18 ^c	287±18 ^c
Alkalinity (mg/L as CaCO ₃)	402	7
Hardness (mg/L as CaCO ₃)	9	60
Dissolved organic carbon (mg/L)	26.7	16.9
Dissolved inorganic carbon (mg/L)	47.2	1.2
Chloride (g/L)	23	110
Bromide (g/L)	0.26/1.2 ^d	1.7

Notes:

- a. Not measured, value calculated based on solution makeup.
- b. ND: not determined.
- c. Average of triplicate measurements ± standard deviation.

The original bromide concentration in flowback water sample is 0.24 g/L; in the bromide removal experiment it was amended with KBr up to 1.2 g/L in order to compare the result with other tested water samples.

Since there is a linear relationship between chloride concentration and the bromide removal rate when chloride concentration is not zero (Figure 6-4), the bromide removal rate in synthetic brine with the same concentration in the two mining brine samples can be estimated, and they were compared with the bromide removal rate measured in real brine samples. Figure 6-5 compares the bromide removal rate, energy consumption and current efficiency in flowback water, produced water and synthetic brine (pure bromide and chloride solution). The bromide removal rate was 44% lower than in synthetic brine for flowback water, and 84% lower for produced water (Figure 6-5a), suggesting that besides bromide, other components in mining brine are also having a negative impact

on the bromide removal rate. The flowback and produced water samples were softened in order to verify if the negative impact was due to the presence of hardness. The softened brine had similar removal rates compared to original brines, suggesting hardness was not responsible of decreasing the bromide removal rate. pH, alkalinity or DIC (HCO_3^- and CO_3^{2-}) is probably not the reason, either, since in all the experiments, regardless of the properties of the water used as electrolyte, the pH of the electrolyte dropped to ~2.5 with 30 minutes, diminishing any pH, alkalinity or DIC differences in initial brine samples. Table 6-3 lists several chemical species that may exist in the mining brine. Although their concentrations are low, their standard oxidation potential are all lower than bromide, thus they preferentially react on the anode and compete with bromide oxidation. However, further study on which chemical components in the brine samples other than chloride are responsible for the decrease in bromide removal rate were not conducted.

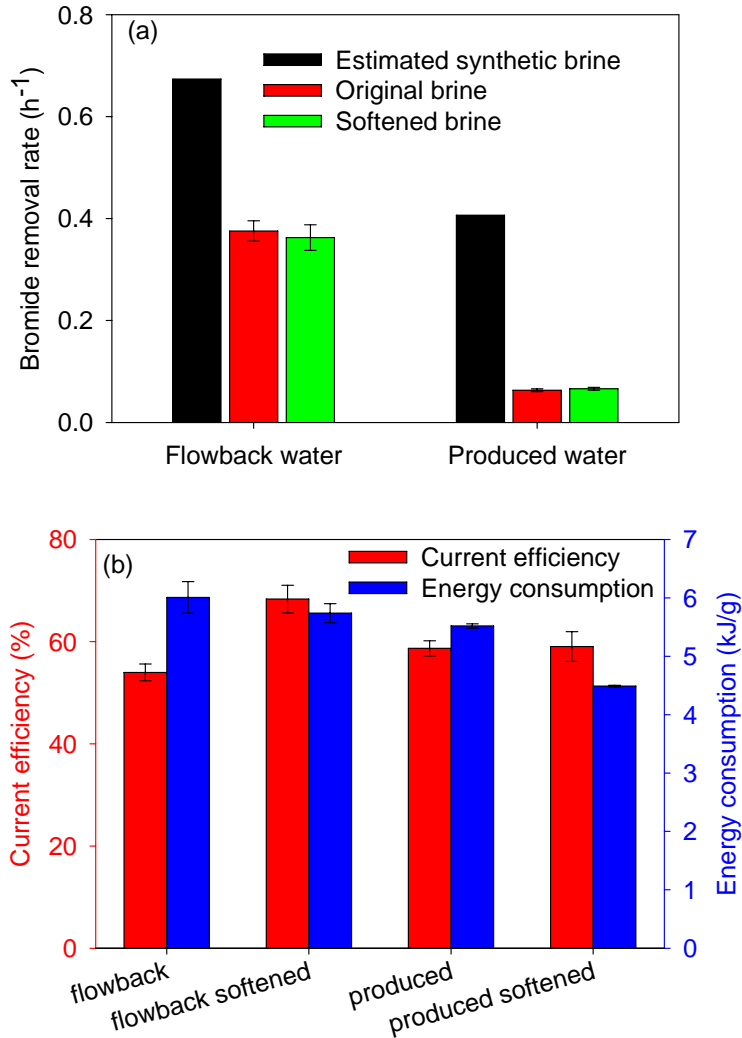


Figure 6-5. Bromide removal rate (a), current efficiency and energy consumption (b) in synthetic brine, flowback water and produced water by graphite rod anode poised at 1V vs. Ag/AgCl electrode

The estimated removal rates in synthesized brine are interpolated from the relationship between chloride concentration and bromide removal rate (Figure 6-4) based on the measured chloride concentration in each brine sample. The other results are the means of duplicate reactors, and error bars represent standard deviation.

Table 6-3. Species with lower standard equilibrium potential (E^0) than bromide that may exist in mining brine

(data from [16] and [138]; data in [138] were converted from equilibrium potentials at pH=7 to standard states (pH=0) to compare with data from [16]; also pH observed in the anolyte was below 2). E^0 for bromide oxidation is 1.09 V vs. SHE)

Species	Oxidation half reaction	E^0 (V vs. SHE)
formic acid	$HCOOH \rightleftharpoons CO_2 + 2H^+ + 2e^-$	-0.017
HS^-	$HS^- \rightleftharpoons S + H^+ + 2e^-$	-0.064
Acetic acid	$CH_3COOH + 2H_2O \rightleftharpoons 2CO_2 + 8H^+ + 8e^-$	0.123
Ethanol	$CH_3CH_2OH \rightleftharpoons CH_3CHO + 2H^+ + 2e^-$	0.216
Lactic acid	$CH_3CH(OH)OH \rightleftharpoons CH_3COCOOH + 2H^+ + 2e^-$	0.223
HS^-	$HS^- + 4H_2O \rightleftharpoons SO_4^{2-} + 9H^+ + 8e^-$	0.245
	$HS^- + 3H_2O \rightleftharpoons HSO_3^- + 6H^+ + 6e^-$	0.297
Succinic acid	$HOOCCH_2CH_2COOH \rightleftharpoons HOOCCH=CHCOOH + 2H^+ + 2e^-$	0.38
I^-	$2I^- \rightleftharpoons I_2 + 2e^-$	0.536
	$3I^- \rightleftharpoons I_3^- + 2e^-$	0.536
$FeCO_3$	$FeCO_3 + 2H_2O \rightleftharpoons Fe(OH)_3 + CO_2 + H^+ + e^-$	0.613
Fe^{2+}	$Fe^{2+} \rightleftharpoons Fe^{3+} + e^-$	0.771
Mn^{2+}	$Mn^{2+} \rightleftharpoons Mn^{4+} + 2e^-$	0.798
I^-	$I^- + H_2O \rightleftharpoons HIO + H^+ + 2e^-$	0.987
	$I^- + 2H_2O \rightleftharpoons IO_3^- + 6H^+ + 6e^-$	1.085

Energy consumption and current efficiency in all tested brine solutions are close to the levels in synthetic brine (Figure 6-5b and Figure 6-4). These results suggest that electrodes can selectively and effectively remove bromide in mining brine which

contains one or two orders of magnitude higher chloride concentration than bromide, at lower removal rate than in pure solution but with similar energy consumption and current efficiency. Further, results from different water samples suggest that such treatment has considerable tolerance to various properties of the brine.

Engineering considerations

The bromide removal rates achieved in this study ranged from 0.4 h^{-1} for flowback water to 0.06 h^{-1} for produced water. When normalized to the electrode surface area (64 cm^2), the removal rate is $\sim 60 \text{ h}^{-1}\text{m}^{-2}$ in flowback water and $\sim 10 \text{ h}^{-1}\text{m}^{-2}$ in produced water.

Using a configuration of an electrolyzer used in the chlor-alkali process and results obtained from these experiments, the required size of electrolyzers suitable for bromide removal from mining brine was estimated. A first-order reaction for bromide removal in a continuous stirred tank reactor was used, assuming that the reaction rate constant would not change even when the bromide concentration has decreased to trace amount.

This assumption should be verified in future studies. It is also assumed that the slow step in the process was bromide oxidation rather than removal of the produced bromine.

Electrolyzer design criteria for the chlor-alkali process are not available. However, a list of characteristics of several chlor-alkali industrial facilities is available [139]. From this

list, the median electrode area per cell is $\sim 3 \text{ m}^2$, and the cell volume is $\sim 0.5 \text{ m}^3$. If such an electrolyzer is used for bromide removal, and the treatment target is to reduce bromide concentration from 1 g/L ($10^6 \mu\text{g/L}$) to $50 \mu\text{g/L}$ (allowable bromide level for drinking water sources regulated in California), the retention time (t) required for electrolysis is

$$\ln\left(\frac{C}{C_0}\right) = -k_s S t$$

$$\Rightarrow t = \frac{-\ln(C/C_0)}{k_s S} = \frac{-\ln(50/10^6)}{60 \text{ h}^{-1} \text{ m}^{-2} \times 3 \text{ m}^2} = 0.055 \text{ h} = 3.3 \text{ min for flowback water}$$

$$\text{Or } t = \frac{-\ln(C/C_0)}{k_s S} = \frac{-\ln(50/10^6)}{10 \text{ h}^{-1} \text{ m}^{-2} \times 3 \text{ m}^2} = 0.33 \text{ h} = 20 \text{ min for produced water}$$

Where C and C_0 are influent and effluent bromide concentration, respectively; k_s is the surface area normalized reaction rate ($60 \text{ h}^{-1} \text{ m}^{-2}$ or $\sim 10 \text{ h}^{-1} \text{ m}^{-2}$); S is the electrode surface area.

An estimate of the required reactor volume can be made based on the flow rates of brine generation. The flow rate of brine varies from as high as $10,000$ barrels /day at the initial stage of fracturing to as low as 2 barrel /day after 50 days [11], which is 0.3 - $1600 \text{ m}^3/\text{day}$. Thus the total volume of reactors needed is:

$1600\text{m}^3 / \text{day} \times 0.055\text{h} \times \text{day} / 24\text{h} = 3.7\text{m}^3$ for the high flow rate flowback water and

$0.3\text{m}^3 / \text{day} \times 0.33\text{h} \times \text{day} / 24\text{h} = 4.1 \times 10^{-3}\text{m}^3$ for low flow rate produced water

These calculations indicate that several electrolyzers, each with a size of 0.5 m^3 are needed to run in parallel to treat the flowback water at the highest rate (in the case of peak flow 10000 barrels /day, 8 reactors are needed), while one electrolyzer of 0.5 m^3 volume would be sufficient for handling the low flow rate produced water. The results also show that the low bromide removal rate in produced water can be compensated using a longer retention time to achieve the required treatment goal because the flow rate of produced water is low.

The cell current during electrolysis of each water sample decreased from $\sim 100\text{ mA}$ to $\sim 20\text{ mA}$ as the reaction proceeded, but generally the integrated average is about 20 mA , and thus the current density is about 3 A/m^2 . This is much lower than the current density used in chlor-alkali cells ranging in several kA/m^2 [140].

The energy consumption observed in bromide removal in this study is generally at the level of 6 kJ/g Br , not including energy needed for bromine stripping. Not surprisingly, this is higher than the theoretical minimal energy consumption as calculated in Appendix D and summarized in Table 6-1 because the current efficiency is not 100%

and overpotential exists in practice. When converted the observed energy consumption to chlorine equivalent, it is about 3760 kWh/ ton Cl. This value is higher than the energy consumption in membrane chlor-alkali cells used in the industry (2600-2800 kWh /ton Cl) [140] but within the same magnitude. The higher energy consumption for bromide removal than in the chlor-alkali process is not surprising because: (1) the NaCl concentration in the feed brine in chlor-alkali process is 285-315 g/L [140], while the bromide concentration in the mining brine is only ~1 g/L, and the efficiency decreases with decreasing substrate concentration; (2) in order to make the effluent bromide concentration as low as possible, the electrolysis needs to be performed until the electrolyte is almost exhausted (several mg/L or even $\mu\text{g/L}$ level), while this is not necessary in chlor-alkali process (the recommended minimum NaCl concentration in the depleted brine is 170 g/L) [140].

The domestic commercial price for bromine is not available, and the exported elemental bromine can be used to identify price trends. In 2010m the average value of exported bromine (including cost, insurance and freight) was \$1760/ton [141]. The average wholesale price for electricity in PJM West Pennsylvania in 2010 was \$54.04/MWh [142], which is about 1.5×10^{-5} /kJ. Thus the energy cost for electrolysis bromide removal is about 1.5×10^{-5} /kJ $\times 6\text{kJ/g} = 9 \times 10^{-5}$ /g = \$90/ton. Using these estimations, recovering the produced bromine could help offset the cost of brine treatment.

Another issue yet to be discussed is about bromine separation. Once bromine is formed, it may transform into HBrO, BrO⁻, Br⁻, and Br₃⁻, according to Equation 6-6 to Equation 6-8:



The formation of these species will reduce current efficiency and mass of bromine collected. Maintaining acidic conditions will help avoid these reactions. Below pH 5, Br₂ is the dominate species while the sum of HBrO, BrO⁻, Br⁻, and Br₃⁻ are less than 15% of the total bromine [143]. In this study, the pH of the anolyte dropped to 2 within 30 min of electrolysis, regardless of the initial pH of water sample used, and thus is sufficient to maintain bromine form. However, in a flow-through system, if the retention time is too short to induce sufficient pH decrease, an additional procedure may be necessary to further decrease pH of the brine, such as extend the retention time or addition of acid. The cost for these procedures would need to be accounted when evaluating the economics of this bromide removal process.

6.4 Conclusions

This work demonstrates that it is both thermodynamically and kinetically feasible to use electrodes to selectively remove bromide from mining brine without generating chlorine or oxygen. The presence of high concentrations of chloride and other unknown components in the brine decreases the bromide removal rate, but the reaction remains fast enough for effective treatment. The energy consumption of this process is comparable with industrial chlorine production in the chlor-alkali process, and the industrial chlor-alkali electrolyzers used can meet the treatment requirements for bromide removal in the mining brine in terms of both electrode surface area and reactor volume. These results suggest that it is promising to utilize the electrode-base system for treating mining brine with high bromide level.

Chapter 7. Conclusions, implications, contributions, and suggestions for future research

The research presented in this dissertation focused on evaluating the feasibility and performance of electrode-based technologies for treating contaminated sediments *in situ*, and for the selective removal of bromide from industrial brines. Results from these experimental studies and subsequent analysis provide valuable insights into the potential use of electrode-based treatment for these important environmental issues. A summary of the key findings and implications of those findings for each application is presented, along with the key contributions that this research provides. Finally, future research needs in each area are given.

7.1 Electrode-based reactive sediment cap

7.1.1 Summary and conclusions

In situ capping is an effective remediation strategy for sediment contamination. Compared to traditional sand and sorbent-amended caps, reactive caps capable of transforming contaminants may improve remediation efficiency. However, it is not known whether carbon or other electrode materials can assure long-term contaminant degradation in a sediment cap. An electrode-based reactive cap using carbon electrodes

powered at low voltage as the reactive material is proposed in this study to stimulate abiotic and/or biotic contaminant degradation *in situ*. The work presented in this thesis evaluated the feasibility of such electrode-based reactive caps for sediment remediation, and determined the key environmental factors affecting cap performance.

Conclusions from this work include:

- A reactive sediment cap with powered carbon electrodes may induce and maintain a redox gradient in Anacostia River sediment.
- Powered carbon electrodes can support hydrogen production that may serve as an electron donor for contaminant degradation.
- Powered carbon electrodes can abiotically induce sequential reduction/oxidation of nitrobenzene.
- Powered carbon electrodes do not improve the biodegradation rate of 2,4-dichlorophenol in Anacostia River sediment.
- Varying voltage between the electrodes provides a control mechanism for hydrogen production and abiotic contaminant degradation rates.
- The electrode-based sediment cap is relatively robust across a broad range of aqueous geochemical conditions.

7.1.2 Engineering implications

Important engineering implications of electrode-based sediment capping technology include:

- Electrode-based sediment remediation can provide effective abiotic degradation of selected contaminants, suggesting that this approach may be suitable for some contaminants, e.g. those that inhibit natural attenuation due to their toxicity and/or high concentration in the sediment.
- The same electrode material was reused for experiments over several years in this study without decreases in reactivity. This indicates its potential for long term use of carbon materials *in situ*.
- Electrode-stimulated reactions (especially water electrolysis) may significantly increase or decrease pH at the cathode and anode, respectively. These changes may impact local microbial ecology and contaminant biodegradation potential. Effective pH control through addition of buffer materials to the cap may be necessary in certain scenarios.
- The electrode-based sediment remediation approach is relatively robust. It appears to be effective across a broad range of aqueous geochemical conditions. It may be ideally suited for marine and brackish systems because the natural ionic strength provides a sufficiently conductive supporting electrolyte that will

decrease energy costs. However, results from the bromide oxidation experiments (in chapter 6) suggest that cautions may be needed to avoid chlorine production at the anode in chloride-rich waters.

- Stimulation of biodegradation of DCP by powered electrodes was not observed in this study. This result contrasts previous reports of enhanced biodegradation of PAHs and PCBs, and suggests the need to identify the suitability of electrode-based caps for enhancing contaminant biodegradation on a case-by-case basis. Success will likely depend on the contaminant of interest and on the geochemistry of the sediment porewater.

7.1.3 Contributions and benefits

The electrode-based reactive sediment cap is an innovative integration of a previously studied electrochemical contaminant degradation technology into sediment caps to intercept and degrade contaminants *in situ*. This study proposes a solution for maintaining and fine-tuning cap reactivity through simple adjustment of voltage between carbon electrodes. The major contributions of this work are:

- It provided valuable information for the expected performance of the electrode-based reactive cap in real sediment applications. Although the capability of electrodes to treat contaminants has been well documented before, this study

systematically evaluated the effect of environmentally relevant factors on the electrochemical reaction rates of selected contaminants.

- It verified for the first time that carbon electrodes can be used to engineer a redox gradient in a sediment and cap, deliver electron donor, and degrade selected contaminants under a variety of aqueous geochemical conditions.
- It demonstrated the ability to control the reactivity by simply adjusting the applied voltage.
- It provided valuable information on when to expect the electrode-based system to be advantageous for contaminant control and when it may not be.
- It provided an estimation of the relationships between site conditions, electrode cap reactivity and contaminant removal rates and percentage. This can be used to aid in future designs and to identify necessary operation parameters for site conditions.

Findings in this dissertation are useful for engineers searching for an alternative remediation approach when conventional technologies such as traditional capping are not effective. It offers the scientific community an enhanced understanding of the reactivity of electrodes in environmental media. The body of work is a good starting point for further developing a field scale application.

7.1.4 Suggestions for future research

The research presented in this dissertation suggests the following directions for future investigation:

- How will powered electrodes affect contaminant biodegradation under other experimental conditions (different contaminants, sediments, electrodes, applied voltage, etc.)? Despite the inability to promote DCP biodegradation in this study, considering the two examples of biodegradation enhancement of contaminants observed in sediment [45, 46] and numerous examples of bio-electrodegradation of contaminants in other matrices [4, 5, 38, 91, 103, 121, 122, 144, 145], it is concluded that the effect of powered electrodes on biodegradation is case-specific. The unexpected results observed in this study may be caused by the high microbial activity of the sediment used in this study, or the high biodegradability of probe compound. Also, conducting the DCP biodegradation experiments at conditions where abiotic electrochemical reduction is also happening might suggest different results, with higher applied voltage and/or electrode materials with higher catalytic activity. Thus, it is worthy trying other refractory contaminants under other experiment conditions to confirm the effect of powered electrodes in biodegradation, and to determine all of the factors that affect success.

- How will the electrode-based sediment cap behave under flow conditions representative for sediment pore water seepage? All the tests in this study, as well as the other electrode-stimulated sediment remediation studies reported [45, 46], are based on stagnant conditions. This is reasonable for the very low flow conditions typical in sediment, but even a low seepage rate (e.g. 0.5 cm/d) may provide continuous nutrients and buffer intensity input, flush out accumulated degradation products, and stabilize redox and pH stratification. Thus, the cap may perform better and have less of an impact on the local microenvironment with sediment pore water seepage compared to stagnant conditions. Understanding the impact of flow on performance is important to evaluate the feasibility of the electrode-based sediment cap.
- Which electrode materials will be suitable for the electrode-based sediment cap? Which electrode properties are required to achieve and maintain the good performance of such a cap? Many electrode materials may be applied for reactive capping. In this study carbon electrodes were selected because of their low cost, high surface area, and durability. Three types of electrodes were tested. Carbon cloth is ideal for maintaining a redox gradient and for hydrogen generation; graphite felt is good for nitrobenzene degradation but not for dichlorophenol degradation; and carbon paper is also not suitable for

dichlorophenol degradation. A systematic study of electrode properties required for effective specific contaminant degradation, and the criteria for selecting electrodes materials, will help to identify the right material for site-specific remediation needs. Possible parameters for electrode materials to evaluate include cost, specific surface area, affinity to target contaminants, thermodynamic (overpotential) and kinetic (reaction rate) properties for contaminants degradation, and life time (e.g., permeability and reactivity after sediment bacterial colonization and organic matter fouling, tolerance to catalyst poisoning of sediment species such as sulfide, and material loss by self oxidation).

7.2 Electrode-based selective bromide removal in mining brines

7.2.1 Summary and conclusions

Elevated levels of bromide in flowback water and produced water generated in shale gas hydraulic fracturing are of environmental concern and can lead to formation of brominated disinfection by-products (DBPs) when discharged into water utilized as a public drinking water source. Current water treatment technologies cannot selectively remove bromide from the mining brine when high concentrations of chloride and other ions exist. In this thesis an electrode-based treatment was evaluated for its ability to

selectively oxidize bromide to bromine, which can then be removed from brine by air stripping. The major conclusions of this work are:

- Selective electrolytic oxidation of bromide can be achieved with accurate potential control, thereby avoiding chloride and water oxidation.
- Selective bromide removal can be realized in synthetic brines as well as real flowback and produced water samples.
- The presence of high concentrations of chloride and other unspecified oxidizable species in flowback and produced waters lowers bromide removal rates over synthetic brine.
- Bromide removal from mining brines (flowback and produced water) at typical flow rates can be achieved using electrolyzers that are currently used in the chlor-alkali process and with similar energy consumption.

7.2.2 Engineering implications

Important engineering implications from this study for the use of electrodes to selectively remove bromide from mining brines include the following:

- Based on the rates of bromide oxidation measured here, the electrolyzers do not have to be large ($\sim 0.5 \text{ m}^3$) to treat flowback water and produced water. The

hydraulic retention time will scale with chloride concentration and potentially with other components in the water.

- Primary treatment (e.g. settling, softening, activated carbon adsorption) of the brine to remove co-contaminants before electrolysis may be desirable to improve bromide removal. Pretreatments may also decrease the potential for corrosion and scaling in the electrolyzers and reduce energy consumption.
- Bromine produced with this method is a valuable commodity. This study did not focus on how to effectively collect and purify produced bromine, but recovering the produced bromine can partially offset the cost of brine treatment.

7.2.3 Contributions and benefits

This study demonstrates an economically feasible approach to remove bromide from mining brine in the presence of high concentration of chloride. Although halogen ion oxidation from brine has been developed for decades in the chlorine and bromine industry, this study is the first to apply the electrode-based bromide oxidation technology in mining brine, targeting at high levels of bromide removal and low residual bromide concentrations. The major contributions of this work are:

- It verified that bromide in brine can be removed by electrolysis, and that selective bromide oxidation can be achieved with accurate anode potential control.
- It demonstrated the ability to achieve high levels of bromide removal and low residual bromide concentrations in real flowback and produced water, providing valuable information for future deployment of field-scale electrode-based bromide removal.
- It provided a promising method to convert bromide in brine into a valuable commodity, bromine.
- It provides an approach not only for hydraulic fracturing generated brine, but one that may also be applicable to other industrial brines or brackish waters containing bromide.

The findings obtained in this study provide valuable information for industries with mining brines management problems. It also offers the scientific community insight into some of the aqueous geochemical factors that impact anode reactions and creates a starting point for further developing a field scale application.

7.2.4 Suggestions for future research

The research presented in this dissertation suggests the following directions for future investigation:

- Is there a better way to supply power and control the electrode potential for selective bromide oxidation? When applying the proposed bromide removal treatment at a natural gas hydraulic fracturing site, industrial scale methods for accurately controlling electrode potential will need to be developed. It is easy to control the anode potential to avoid chloride and water oxidation at the laboratory scale using a potentiostat, but whether it is feasible to use the same equipment in the field with large scale reactors is unknown. Potentiostats used in the laboratory are typically expensive and delicate, which may not be suitable for industrial usage. Thus, finding a better instrument for supplying power becomes a primary issue in field application. In the chlor-alkali industry, electricity is supplied to the electrolyte in a constant current mode, which can be provided simply and cheaply using standard power supplies. For the treatment of brine from each site having distinct physical and chemical characteristics, it might also be possible to use a constant current mode but still ensure appropriate anode potential. To achieve this, lab trials using the site water and scaled down electrolyzers similar to those used in the chlor-alkali process are

needed to determine an appropriate current density which ensures that the anode potential is in the right range, and that this current density value can be applied in field with a power supply. If this is proven reliable, the use of potentiostats can be avoided.

- What effluent bromide concentration can be achieved in field scale electrolyzers using economically acceptable design and operating conditions? How can the electrode surface area to reactor volume ratio, hydraulic retention time, temperature, mixing conditions, and reactor design (e.g. single large reactor or multiple small reactors, reactors connected in parallel or series) be optimized for bromide removal at a reasonable cost? Can diluting the produced water with natural water (if applicable) by a couple of times increase the bromide removal rate in produced water (and if it is necessary)? Will the bromide removal rate and energy cost be stable over long time operation? Answering these questions is essential for the application of electrode-base bromide removal in mining brine in field.

Reference

1. U.S. Environmental Protection Agency *Contaminated sediment management strategy (EPA-823-R-98-001)*; Washington, D.C., 1998.
2. U.S. Environmental Protection Agency *Cleaning up the nation's waste sites: markets and technology trends (EPA 542-R-04-015)*; Washington, D.C., 2004.
3. Gregory, K. B.; Bond, D. R.; Lovley, D. R., Graphite electrodes as electron donors for anaerobic respiration. *Environ. Microbiol.* **2004**, *6*, (6), 596-604.
4. Gregory, K. B.; Lovley, D. R., Remediation and recovery of uranium from contaminated subsurface environments with electrodes. *Environ. Sci. Technol.* **2005**, *39*, (22), 8943-8947.
5. Zhang, T.; Gannon, S. M.; Nevin, K. P.; Franks, A. E.; Lovley, D. R., Stimulating the anaerobic degradation of aromatic hydrocarbons in contaminated sediments by providing an electrode as the electron acceptor. *Environ. Microbiol.* **2010**, *12*, (4), 1011-1020.
6. Vogel, T. M.; Criddle, C. S.; McCarty, P. L., Transformations of halogenated aliphatic compounds. *Environ. Sci. Technol.* **1987**, *21*, (8), 722-736.
7. Bedard, D. L., A case study for microbial biodegradation: anaerobic bacterial reductive dechlorination of polychlorinated biphenyls-from sediment to defined medium. *Annual Review of Microbiology* **2008**, *62*, 253-270.
8. Harkness, M. R.; McDermott, J. B.; Abramowicz, D. A.; Salvo, J. J.; Flanagan, W. P.; Stephens, M. L.; Mondello, F. J.; May, R. J.; Lobos, J. H.; Carroll, K. M.; Brennan, M. J.; Bracco, A. A.; Fish, K. M.; Warner, G. L.; Wilson, P. R.; Dietrich, D. K.; Lin, D. T.; Morgan, C. B.; Gately, W. L., In situ stimulation of aerobic PCB biodegradation in Hudson River sediments. *Science* **1993**, *259*, (5094), 503-507.
9. Himmelheber, D. W.; Taillefert, M.; Pennell, K. D.; Hughes, J. B., Spatial and temporal evolution of biogeochemical processes following in situ capping of contaminated sediments. *Environ. Sci. Technol.* **2008**, *42*, (11), 4113-4120.
10. Gregory, K. B.; Vidic, R. D.; Dzombak, D. A., Water management challenges associated with the production of shale gas by hydraulic fracturing. *Elements* **2011**, *7*, (3), 181-186.
11. Acharya, H. R. *Cost effective recovery of low-TDS frac flowback water for re-use (DE-FE0000784)*; U.S. Department of Energy, 2011.
12. World Health Organization, Environmental health criteria 216: disinfectants and disinfectant byproducts. In Geneva, 2000.
13. Handke, P. *Trihalomethane speciation and the relationship to elevated total dissolved solid concentrations affecting drinking water quality at systems utilizing the Monongahela*

River as a primary source during the 3rd and 4th quarters of 2008; Pennsylvania Department of Environmental Protection: Harrisburg PA, 2009.

14. States, S.; Casson, L.; Cyprych, G.; Monnell, J.; Stoner, M.; Wydra, F., Bromide in the allegheny river and thms in pittsburgh drinking water: a link with marcellus shale drilling. In *American Water Works Association -- Water Quality Technology Conference* Phoenix, AZ, 2011.

15. ORSANCO Minutes from the ORSANCO commission meetings for October 2011 (available at <http://www.orsanco.org/commission-minutes>). (July 5th),

16. Lide, D. R., *CRC handbook of chemistry and physics*. 92nd Edition ed.; CRC Press: Boulder, Colorado, 2011.

17. Sun, M.; Yan, F.; Zhang, R.; Reible, D. D.; Lowry, G. V.; Gregory, K. B., Redox control and hydrogen production in sediment caps using carbon cloth electrodes. *Environ. Sci. Technol.* **2010**, *44*, (21), 8209-8215.

18. Sun, M.; Reible, D. D.; Lowry, G. V.; Gregory, K. B., Effect of applied voltage, initial concentration and natural organic matter on sequential reduction/oxidation of nitrobenzene by graphite electrodes. *Environ. Sci. Technol.* **2012**, *46*, (12), 6174-6181.

19. U.S. Environmental Protection Agency *Recent developments for in situ treatment of metal contaminated soils*; Washington, D.C., 1996.

20. U.S.Army Environmental Center *In situ electrokinetic remediation of metal contaminated soils technology status report*; 2000.

21. Kornilovich, B.; Mishchuk, N.; Abbruzzese, K.; Pshinko, G.; Klishchenko, R., Enhanced electrokinetic remediation of metals-contaminated clay. *Colloid Surf. A-Physicochem. Eng. Asp.* **2005**, *265*, (1-3), 114-123.

22. Saichek, R. E.; Reddy, K. R., Electrokinetically enhanced remediation of hydrophobic organic compounds in soils: A review. *Crit. Rev. Environ. Sci. Technol.* **2005**, *35*, (2), 115-192.

23. Raats, M. H. M.; van Diemen, A. J. G.; Lavèn, J.; Stein, H. N., Full scale electrokinetic dewatering of waste sludge. *Colloids Surf., A* **2002**, *210*, (2-3), 231-241.

24. Li, T. P.; Yuan, S. H.; Wan, J. Z.; Lin, L.; Long, H. Y.; Wu, X. F.; Lu, X. H., Pilot-scale electrokinetic movement of HCB and Zn in real contaminated sediments enhanced with hydroxypropyl-beta-cyclodextrin. *Chemosphere* **2009**, *76*, (9), 1226-1232.

25. Virkutyte, J.; Sillanpää, M.; Latostenmaa, P., Electrokinetic soil remediation - critical overview. *Sci. Total Environ.* **2002**, *289*, (1-3), 97-121.

26. Acar, Y. B.; Alshawabkeh, A. N., Principles of electrokinetic remediation. *Environ. Sci. Technol.* **1993**, *27*, (13), 2638-2647.

27. Chung, H. I.; Lee, M., A new method for remedial treatment of contaminated clayey soils by electrokinetics coupled with permeable reactive barriers. *Electrochim Acta* **2007**, *52*, (10), 3427-3431.

28. Jackman, S. A.; Maini, G.; Sharman, A. K.; Sunderland, G.; Knowles, C. J., Electrokinetic movement and biodegradation of 2,4-dichlorophenoxyacetic acid in silt soil. *Biotechnol. Bioeng.* **2001**, *74*, (1), 40-48.
29. Yang, G. C. C.; Hung, C.-H.; Tu, H.-C., Electrokinetically enhanced removal and degradation of nitrate in the subsurface using nanosized Pd/Fe slurry. *J. Environ. Sci. Health., Part A* **2008**, *43*, (8), 945-951.
30. O'Connor, C. S.; Lepp, N. W.; Edwards, R.; Sunderland, G., The combined use of electrokinetic remediation and phytoremediation to decontaminate metal-polluted soils: A laboratory-scale feasibility study. *Environ. Monit. Assess.* **2003**, *84*, (1-2), 141-158.
31. Mulligan, C. N.; Yong, R. N.; Gibbs, B. F., Remediation technologies for metal-contaminated soils and groundwater: an evaluation. *Engineering Geology* **2001**, *60*, (1-4), 193-207.
32. Probst, R. F.; Hicks, R. E., Removal of contaminants from soils by electric fields. *Science* **1993**, *260*, (5107), 498-503.
33. Ho, S. V.; Sheridan, P. W.; Athmer, C. J.; Heitkamp, M. A.; Brackin, J. M.; Weber, D.; Brodsky, P. H., Integrated in situ soil remediation technology: the Lasagna process. *Environ. Sci. Technol.* **1995**, *29*, (10), 2528-2534.
34. Feleke, Z.; Araki, K.; Sakakibara, Y.; Watanabe, T.; Kuroda, M., Selective reduction of nitrate to nitrogen gas in a biofilm-electrode reactor. *Water Res.* **1998**, *32*, (9), 2728-2734.
35. Chen, J.-L.; Wang, J.-Y.; Wu, C.-C.; Chiang, K.-Y., Electrocatalytic degradation of 2,4-dichlorophenol by granular graphite electrodes. *Colloids Surf., A* **2011**, *379*, (1-3), 163-168.
36. Kuroda, M.; Watanabe, T.; Umedu, Y., Simultaneous oxidation and reduction treatments of polluted water by a bio-electro reactor. *Water Sci. Technol.* **1996**, *34*, (9), 101-108.
37. Farmer, J. C.; Bahowick, S. M.; Harrar, J. E.; Fix, D. V.; Martinelli, R. E.; Vu, A. K.; Carroll, K. L., Electrosorption of chromium ions on carbon aerogel electrodes as a means of remediating ground water. *Energy & Fuels* **1997**, *11*, (2), 337-347.
38. Lohner, S. T.; Becker, D.; Mangold, K.-M.; Tiehm, A., Sequential reductive and oxidative biodegradation of chloroethenes stimulated in a coupled bioelectro-process. *Environ. Sci. Technol.* **2011**, *45*, (15), 6491-6497.
39. Alshawabkeh, A. N.; Sarahney, H., Effect of current density on enhanced transformation of naphthalene. *Environ. Sci. Technol.* **2005**, *39*, (15), 5837-5843.
40. Shimomura, T.; Sanford, R. A., Reductive dechlorination of tetrachloroethene in a sand reactor using a potentiostat. *J. Environ. Qual.* **2005**, *34*, (4), 1435-1438.
41. Al-Abed, S. R.; Fang, Y. X., Influences of pH and current on electrolytic dechlorination of trichloroethylene at a granular-graphite packed electrode. *Chemosphere* **2006**, *64*, (3), 462-469.

42. Gilbert, D.; Sale, T.; Petersen, M., Electrolytic reactive barriers for chlorinated solvent remediation (e-barriers). In *In Situ Remediation of Chlorinated Solvent Plumes*, Stroo, H. W. a. H., Ed. Springer: New York, 2008; pp 573-589
43. Gilbert, D. M.; Sale, T. C., Sequential electrolytic oxidation and reduction of aqueous phase energetic compounds. *Environ. Sci. Technol.* **2005**, *39*, (23), 9270-9277.
44. Sale, T.; Petersen, M.; Gilbert, D. *Electrically induced redox barriers for treatment of groundwater*; ESTCP Final Report: 2005.
45. Yan, F.; Reible, D. D., PAH degradation and redox control in an electrode enhanced sediment cap. *J. Chem. Technol. Biotechnol.* **2012**, *ASAP*.
46. May, H. D.; R.Sowers, K.; Chun, C.; Payne, R., Integrating microbial biostimulation and electrolytic aeration to degrade POPs. In *Contaminated Sediments: New Tools and Approaches for in-situ Remediation - Session IV*, The Hazardous Waste Clean-Up Information (CLU-IN) Web Site (http://www.clu-in.org/conf/tio/sediments4_021411/): 2011.
47. U.S. Environmental Protection Agency *Contaminated sediment remediation guidance for hazardous waste sites (EPA-540-R-05-012)*; Washington, D.C., 2005.
48. Azcue, J. M.; Zeman, A. J.; Mudroch, A.; Rosa, F.; Patterson, T., Assessment of sediment and porewater after one year of subaqueous capping of contaminated sediments in Hamilton Harbour, Canada. *Water Sci. Technol.* **1998**, *37*, (6-7), 323-329.
49. Wang, X. Q.; Thibodeaux, L. J.; Valsaraj, K. T.; Reible, D. D., Efficiency of capping contaminated bed sediments in situ. I, Laboratory-scale experiments on diffusion-adsorption in the capping layer. *Environ. Sci. Technol.* **1991**, *25*, (9), 1578-1584.
50. Jacobs, P. H.; Forstner, U., Concept of subaqueous capping of contaminated sediments with active barrier systems (ABS) using natural and modified zeolites. *Water Res.* **1999**, *33*, (9), 2083-2087.
51. Zimmerman, J. R.; Ghosh, U.; Millward, R. N.; Bridges, T. S.; Luthy, R. G., Addition of carbon sorbents to reduce PCB and PAH bioavailability in marine sediments: Physicochemical tests. *Environ. Sci. Technol.* **2004**, *38*, (20), 5458-5464.
52. Murphy, P.; Marquette, A.; Reible, D.; Lowry, G. V., Predicting the performance of activated carbon-, coke-, and soil-amended thin layer sediment caps. *J. Environ. Eng.* **2006**, *132*, (7), 787-794.
53. Weber, W. J.; Tang, J. X.; Huang, Q. G., Development of engineered natural organic sorbents for environmental applications. 1. Materials, approaches, and characterizations. *Environ. Sci. Technol.* **2006**, *40*, (5), 1650-1656.
54. McDonough, K. M.; Murphy, P.; Olsa, J.; Zhu, Y. W.; Reible, D.; Lowry, G. V., Development and placement of a sorbent-amended thin layer sediment cap in the Anacostia River. *Soil. Sediment. Contam.* **2007**, *16*, (3), 313-322.
55. Choi, H.; Agarwal, S.; Al-Abed, S. R., Adsorption and simultaneous dechlorination of PCBs on GAC/Fe/Pd: mechanistic aspects and reactive capping barrier concept. *Environ. Sci. Technol.* **2009**, *43*, (2), 488-493.

56. Hyun, S.; Jafvert, C. T.; Lee, L. S.; Rao, P. S. C., Laboratory studies to characterize the efficacy of sand capping a coal tar-contaminated sediment. *Chemosphere* **2006**, *63*, (10), 1621-1631.
57. Himmelheber, D. W.; Pennell, K. D.; Hughes, J. B., Natural attenuation processes during in situ capping. *Environ. Sci. Technol.* **2007**, *41*, (15), 5306-5313.
58. Sun, H.; Xu, X.; Gao, G.; Zhang, Z.; Yin, P., A novel integrated active capping technique for the remediation of nitrobenzene-contaminated sediment. *J. Hazard. Mater.* **2010**, *182*, (1-3), 184-190.
59. Venkatesh, S.; Tilak, B. V., Chlor-alkali technology. *Journal of Chemical Education* **1983**, *60*, (4), 276-278.
60. Pletcher, D., *Industrial electrochemistry*. 1st ed.; Chapman and Hall: London, UK, 1982.
61. Dow, H. H. Process of extracting bromine. U.S. Patent 460370, Sep 29, 1891.
62. Kesner, M. Bromine and bromine compounds from the dead sea. Chapter 3: How is bromine produced? <http://www.weizmann.ac.il/sci-tea/Brombook/pdf/chapter3.pdf> (July, 8, 2012),
63. Yalçın, H.; Koç, T.; Pamuk, V., Hydrogen and bromine production from concentrated sea-water. *Int. J. Hydrogen Energy* **1997**, *22*, (10-11), 967-970.
64. Qi, J.; Savinell, R., Analysis of flow-through porous electrode cell with homogeneous chemical reactions: application to bromide oxidation in brine solutions. *J. Appl. Electrochem.* **1993**, *23*, (9), 873-886.
65. Qi, J.; Savinell, R., Development of the flow-through porous electrode cell for bromide recovery from brine solutions. *J. Appl. Electrochem.* **1993**, *23*, (9), 887-896.
66. Kimbrough, D. E.; Suffet, I. H., Electrochemical removal of bromide and reduction of THM formation potential in drinking water. *Water Res.* **2002**, *36*, (19), 4902-4906.
67. Kimbrough, D. E.; Suffet, I. H., Electrochemical process for the removal of bromide from California state project water. *Journal of Water Supply Research and Technology-Aqua* **2006**, *55*, (3), 161-167.
68. Bo, L. Electrolytic cell and process for removal of bromide ions and disinfection of source waters using silver cathode and/or dimensionally stable anode (DSA): a process for the reduction of disinfectant/disinfection byproducts in drinking water. U.S. Patent 7384564, Jun 10, 2008.
69. Martinez-Huitle, C. A.; Brillas, E., Electrochemical alternatives for drinking water disinfection. *Angew. Chem. Int. Ed.* **2008**, *47*, (11), 1998-2005.
70. Sánchez-Polo, M.; Rivera-Utrilla, J.; Salhi, E.; von Gunten, U., Removal of bromide and iodide anions from drinking water by silver-activated carbon aerogels. *J. Colloid Interface Sci.* **2006**, *300*, (1), 437-441.
71. Ge, F.; Zhu, L. Z., Effects of coexisting anions on removal of bromide in drinking water by coagulation. *J. Hazard. Mater.* **2008**, *151*, (2-3), 676-681.

72. U.S. Environmental Protection Agency *The incidence and severity of sediment contamination in surface waters of the United States, national sediment quality survey*; Washington, DC, 2004.
73. Palermo, M., Maynard, S., Miller, J., and Reible, D., Guidance for in situ subaqueous capping of contaminated sediments. In Great Lakes National Program Office, Chicago, 1998.
74. National Research Council, *A risk-management strategy for PCB-contaminated sediments*. National Academies Press: Washington, D.C., 2001.
75. Reible, D.; Hayes, D.; Lue-Hing, C.; Patterson, J.; Bhowmik, N.; Johnson, M.; Teal, J., Comparison of the long-term risks of removal and in situ management of contaminated sediments in the Fox River. *Soil. Sediment. Contam.* **2003**, *12*, (3), 325-344.
76. U.S. Environmental Protection Agency, EPA's monitored natural attenuation policy. *The Army Lawyer* **1998**, *308*, (85).
77. Himmelheber, D. W.; Thomas, S. H.; Loffler, F. E.; Taillefert, M.; Hughes, J. B., Microbial colonization of an *in situ* sediment cap and correlation to stratified redox zones. *Environ. Sci. Technol.* **2009**, *43*, (1), 66-74.
78. Brendel, P. J.; Luther, G. W. I., Development of a gold amalgam voltammetric microelectrode for the determination of dissolved Fe, Mn, O₂, and S(-II) in porewaters of marine and freshwater sediments. *Environ. Sci. Technol.* **1995**, *29*, (3), 751-761.
79. Liu, Y.; Majetich, S. A.; Tilton, R. D.; Sholl, D. S.; Lowry, G. V., TCE dechlorination rates, pathways, and efficiency of nanoscale iron particles with different properties. *Environ. Sci. Technol.* **2005**, *39*, (5), 1338-1345.
80. Reimers, C. E.; Tender, L. M.; Fertig, S.; Wang, W., Harvesting energy from the marine sediment-water interface. *Environ. Sci. Technol.* **2001**, *35*, (1), 192-195.
81. Sun, M.; Sheng, G. P.; Zhang, L.; Xia, C. R.; Mu, Z. X.; Liu, X. W.; Wang, H. L.; Yu, H. Q.; Qi, R.; Yu, T.; Yang, M., An MEC-MFC-coupled system for biohydrogen production from acetate. *Environ. Sci. Technol.* **2008**, *42*, (21), 8095-8100.
82. Logan, B. E.; Call, D.; Cheng, S.; Hamelers, H. V. M.; Sleutels, T. H. J. A.; Jeremiasse, A. W.; Rozendal, R. A., Microbial electrolysis cells for high yield hydrogen gas production from organic matter. *Environ. Sci. Technol.* **2008**, *42*, (23), 8630-8640.
83. Benjamin, M. M., *Water chemistry*. McGraw Hill: 2002; p 648.
84. Khaitan, S.; Dzombak, D. A.; Lowry, G. V., Chemistry of the acid neutralization capacity of bauxite residue. *Environmental Engineering Science* **2009**, *26*, (5), 873-881.
85. Holland, H. D., *The chemistry of the atmosphere and oceans* John Wiley & Sons Inc: New York, 1978; p 154.
86. Call, D.; Logan, B. E., Hydrogen production in a single chamber microbial electrolysis cell lacking a membrane. *Environ. Sci. Technol.* **2008**, *42*, (9), 3401-3406.
87. Franz, J. A.; Williams, R. J.; Flora, J. R. V.; Meadows, M. E.; Irwin, W. G., Electrolytic oxygen generation for subsurface delivery: effects of precipitation at the cathode and an assessment of side reactions. *Water Res.* **2002**, *36*, (9), 2243-2254.

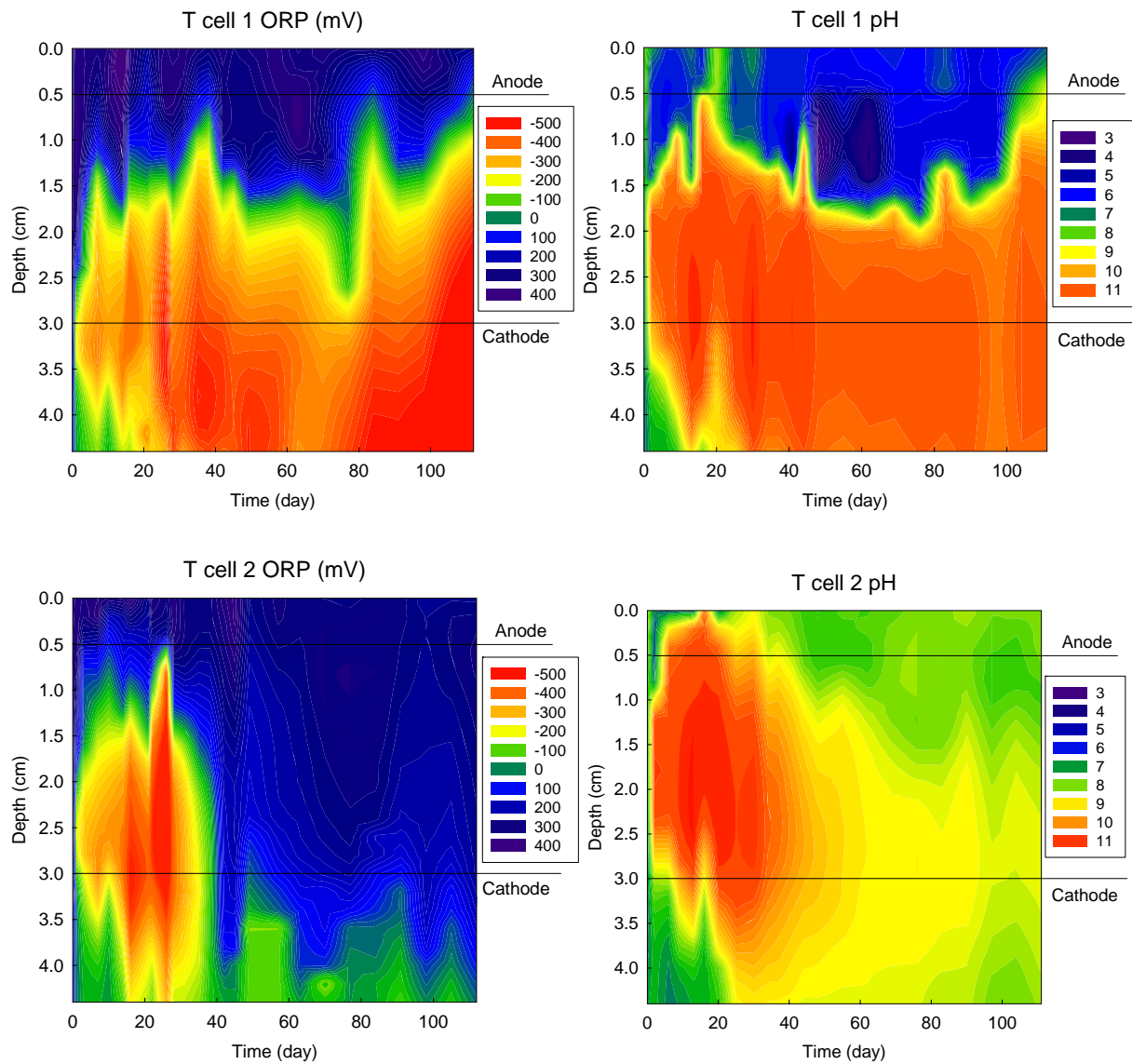
88. Petersen, M. A.; Sale, T. C.; Reardon, K. F., Electrolytic trichloroethene degradation using mixed metal oxide coated titanium mesh electrodes. *Chemosphere* **2007**, *67*, (8), 1573-1581.
89. Dunnivant, F. M.; Schwarzenbach, R. P.; Macalady, D. L., Reduction of substituted nitrobenzenes in aqueous solutions containing natural organic matter. *Environ. Sci. Technol.* **1992**, *26*, (11), 2133-2141.
90. Motheo, A. J.; Pinhedo, L., Electrochemical degradation of humic acid. *Sci. Total Environ.* **2000**, *256*, (1), 67-76.
91. Aulenta, F.; Canosa, A.; Reale, P.; Rossetti, S.; Panero, S.; Majone, M., Microbial reductive dechlorination of trichloroethene to ethene with electrodes serving as electron donors without the external addition of redox mediators. *Biotechnol. Bioeng.* **2009**, *103*, (1), 85-91.
92. Tsyganok, A. I.; Otsuka, K., Selective dechlorination of chlorinated phenoxy herbicides in aqueous medium by electrocatalytic reduction over palladium-loaded carbon felt. *Appl. Catal., B* **1999**, *22*, (1), 15-26.
93. Arnold, W. A.; Roberts, A. L., Pathways and kinetics of chlorinated ethylene and chlorinated acetylene reaction with Fe(0) particles. *Environ. Sci. Technol.* **2000**, *34*, (9), 1794-1805.
94. Eriksson, J.; Frankki, S.; Shchukarev, A.; Skyllberg, U., Binding of 2,4,6-trinitrotoluene, aniline, and nitrobenzene to dissolved and particulate soil organic matter. *Environ. Sci. Technol.* **2004**, *38*, (11), 3074-3080.
95. Keum, Y.-S.; Li, Q. X., Reduction of nitroaromatic pesticides with zero-valent iron. *Chemosphere* **2004**, *54*, (3), 255-263.
96. Chiou, C. T.; Kile, D. E.; Brinton, T. I.; Malcolm, R. L.; Leenheer, J. A.; MacCarthy, P., A comparison of water solubility enhancements of organic solutes by aquatic humic materials and commercial humic acids. *Environ. Sci. Technol.* **1987**, *21*, (12), 1231-1234.
97. Kilduff, J. E.; Karanfil, T.; Weber, W. J., Competitive Interactions among Components of Humic Acids in Granular Activated Carbon Adsorption Systems: Effects of Solution Chemistry. *Environ. Sci. Technol.* **1996**, *30*, (4), 1344-1351.
98. Preuss, A.; P.G.Rieger, Anaerobic transformation of 2,4,6-trinitrotoluene. In *Biodegradation of nitroaromatic compounds*, Spain, J. C., Ed. Plenum Press: New York, 1995.
99. Rieger, P. G.; H.J.Knachmuss, Basic knowledge and perspectives on biodegradation of 2,4,6-trinitrotoluene and related nitroaromatic compounds in soil. In *Biodegradation of nitroaromatic compounds*, Spain, J. C., Ed. Plenum Press: New York, 1995.
100. Nishino, S. F.; Spain, J. C., Degradation of nitrobenzene by a *Pseudomonas pseudoalcaligenes*. *Appl. Environ. Microbiol.* **1993**, *59*, (8), 2520-2525.
101. Kirk, D. W.; Sharifian, H.; Foulkes, F. R., Anodic oxidation of aniline for waste water treatment. *J. Appl. Electrochem.* **1985**, *15*, (2), 285-292.
102. Lyons, C. D.; Katz, S.; Bartha, R., Mechanisms and pathways of aniline elimination from aquatic environments. *Appl. Environ. Microbiol.* **1984**, *48*, (3), 491-496.

103. Mu, Y.; Rozendal, R. A.; Rabaey, K.; Keller, J. r., Nitrobenzene removal in bioelectrochemical systems. *Environ. Sci. Technol.* **2009**, *43*, (22), 8690-8695.
104. Dickel, O.; Haug, W.; Knackmuss, H.-J., Biodegradation of nitrobenzene by a sequential anaerobic-aerobic process. *Biodegradation* **1993**, *4*, (3), 187-194.
105. Wani, A. H.; O'Neal, B. R.; Gilbert, D. M.; Gent, D. B.; Davis, J. L., Electrolytic transformation of ordinance related compounds (ORCs) in groundwater: Laboratory mass balance studies. *Chemosphere* **2006**, *62*, (5), 689-698.
106. Sternson, L. A.; DeWitte, W. J., High-pressure liquid chromatographic analysis of aniline and its metabolites. *Journal of Chromatography A* **1977**, *137*, (2), 305-314.
107. Li, Y.; Wang, F.; Zhou, G.; Ni, Y., Aniline degradation by electrocatalytic oxidation. *Chemosphere* **2003**, *53*, (10), 1229-1234.
108. Matsushita, M.; Kuramitz, H.; Tanaka, S., Electrochemical oxidation for low concentration of aniline in neutral pH medium: application to the removal of aniline based on the electrochemical polymerization on a carbon fiber. *Environ. Sci. Technol.* **2005**, *39*, (10), 3805-3810.
109. Wang, A.-J.; Cheng, H.-Y.; Liang, B.; Ren, N.-Q.; Cui, D.; Lin, N.; Kim, B. H.; Rabaey, K., Efficient reduction of nitrobenzene to aniline with a biocatalyzed cathode. *Environ. Sci. Technol.* **2011**, *45*, (23), 10186-10193.
110. Newman, J.; Thomas-Alyea, K. E., *Electrochemical systems*. 3rd ed.; Wiley-Interscience: New York, 2004; p 203-240.
111. Li, J.; Liu, G.; Zhang, R.; Luo, Y.; Zhang, C.; Li, M., Electricity generation by two types of microbial fuel cells using nitrobenzene as the anodic or cathodic reactants. *Bioresour. Technol.* **2010**, *101*, (11), 4013-4020.
112. Smeltzer, J. C.; Fedkiw, P. S., Reduction of nitrobenzene in a parallel-plate reactor. *Journal of The Electrochemical Society* **1992**, *139*, (5), 1358-1366.
113. Schwarzenbach, R. P.; Gschwend, P. M.; Imboden, D. M., *Environmental organic chemistry*. 2nd ed.; Wiley-Interscience: 2002; p 1006-1009.
114. Himmelheber, D. W.; Pennell, K. D.; Hughes, J. B., Evaluation of a laboratory-scale bioreactive in situ sediment cap for the treatment of organic contaminants. *Water Res.* **2011**, *45*, (17), 5365-5374.
115. Susarla, S.; Yonezawa, Y.; Masunaga, S., Reductive transformations of halogenated aromatics in anaerobic estuarine sediment: kinetics, products and pathways. *Water Res.* **1998**, *32*, (3), 639-648.
116. Warner, K. A.; Gilmour, C. C.; Capone, D. G., Reductive dechlorination of 2,4-dichlorophenol and related microbial processes under limiting and non-limiting sulfate concentration in anaerobic mid-Chesapeake Bay sediments. *FEMS Microbiol. Ecol.* **2002**, *40*, (2), 159-165.
117. Zhang, X.; Wiegel, J., Sequential anaerobic degradation of 2,4-dichlorophenol in freshwater sediments. *Appl. Environ. Microbiol.* **1990**, *56*, (4), 1119-1127.

118. Dabo, P.; Cyr, A.; Laplante, F.; Jean, F.; Menard, H.; Lessard, J., Electrocatalytic dehydrochlorination of pentachlorophenol to phenol or cyclohexanol. *Environ. Sci. Technol.* **2000**, *34*, (7), 1265-1268.
119. Skadberg, B.; Geoly-Horn, S. L.; Sangamalli, V.; Flora, J. R. V., Influence of pH, current and copper on the biological dechlorination of 2,6-dichlorophenol in an electrochemical cell. *Water Res.* **1999**, *33*, (9), 1997-2010.
120. Cheng, I. F.; Fernando, Q.; Korte, N., Electrochemical dechlorination of 4-chlorophenol to phenol. *Environ. Sci. Technol.* **1997**, *31*, (4), 1074-1078.
121. Strycharz, S. M.; Gannon, S. M.; Boles, A. R.; Franks, A. E.; Nevin, K. P.; Lovley, D. R., Reductive dechlorination of 2-chlorophenol by *Anaeromyxobacter dehalogenans* with an electrode serving as the electron donor. *Environ. Microbiol. Rep.* **2010**, *2*, (2), 289-294.
122. Zhang, X.-N.; Huang, W.-M.; Wang, X.; Li, H.; Lu, H.-Y.; Lin, H.-B., Biofilm-electrode process with high efficiency for degradation of 2,4-dichlorophenol. *Environ. Chem. Lett.* **2010**, 1-6.
123. Miller, C. V.; Klohe, C. A. *Summary of water- and sediment-quality data for Anacostia River well sites sampled in July-August 2002*; U.S. Department of the Interior and U.S. Geological Survey: Baltimore, Maryland, 2003.
124. Smatlak, C. R.; Gossett, J. M.; Zinder, S. H., Comparative kinetics of hydrogen utilization for reductive dechlorination of tetrachloroethene and methanogenesis in an anaerobic enrichment culture. *Environ. Sci. Technol.* **1996**, *30*, (9), 2850-2858.
125. Yang, Y.; McCarty, P. L., Competition for hydrogen within a chlorinated solvent dehalogenating anaerobic mixed culture. *Environ. Sci. Technol.* **1998**, *32*, (22), 3591-3597.
126. Löffler, F. E.; Tiedje, J. M.; Sanford, R. A., Fraction of electrons consumed in electron acceptor reduction and hydrogen thresholds as indicators of halorespiratory physiology. *Appl. Environ. Microbiol.* **1999**, *65*, (9), 4049-4056.
127. Stanlake, G. J.; Finn, R. K., Isolation and characterization of a pentachlorophenol-degrading bacterium. *Appl. Environ. Microbiol.* **1982**, *44*, (6), 1421-1427.
128. Ning, Z.; Kennedy, K. J.; Fernandes, L., pH dependency of 2,4-chlorophenol dechlorination by acclimated anaerobic granules. *Water SA* **1998**, *24*, (2), 153-156.
129. Chang, B.-V.; Yeh, L.-N.; Yuan, S.-Y., Effect of a dichlorophenol-adapted consortium on the dechlorination of 2,4,6-trichlorophenol and pentachlorophenol in soil. *Chemosphere* **1996**, *33*, (2), 303-311.
130. Armenante, P. M.; Kafkewitz, D.; Jou, C. J.; Lewandowski, G., Effect of pH on the anaerobic dechlorination of chlorophenols in a defined medium. *Appl. Microbiol. Biotechnol.* **1993**, *39*, (6), 772-777.
131. Sinclair, G. M.; Paton, G. I.; Meharg, A. A.; Killham, K., Lux-biosensor assessment of pH effects on microbial sorption and toxicity of chlorophenols. *FEMS Microbiol. Lett.* **1999**, *174*, (2), 273-278.

132. Armenante, P. M.; Kafkewitz, D.; Lewandowski, G.; Kung, C.-M., Integrated anaerobic-aerobic process for the biodegradation of chlorinated aromatic compounds. *Environ. Prog.* **1992**, *11*, (2), 113-122.
133. Armenante, P. M.; Kafkewitz, D.; Lewandowski, G. A.; Jou, C.-J., Anaerobic-aerobic treatment of halogenated phenolic compounds. *Water Res.* **1999**, *33*, (3), 681-692.
134. Fennell, D. E. G., J. M., Microcosms for site-specific evaluation of enhanced biological reductive dehalogenation. In *Dehalogenation: Microbial Processes and Environmental Applications*, Häggblom, M. M., Bossert, I. D., Ed. Kluwer Academic Publishers: Boston, MA, 2003.
135. Zhuang, P.; Pavlostathis, S. G., Effect of temperature, pH and electron donor on the microbial reductive dechlorination of chloroalkenes. *Chemosphere* **1995**, *31*, (6), 3537-3548.
136. Fathepure, B. Z.; Boyd, S. A., Reductive dechlorination of perchloroethylene and the role of methanogens. *FEMS Microbiol. Lett.* **1988**, *49*, (2), 149-156.
137. Veil, J. A.; Puder, M. G.; Elcock, D.; Redweik, R. J. *A white paper describing produced water from production of crude oil, natural gas and coal bed methane*; U.S. Argonne National Laboratory: 2004.
138. Madigan, M.; Martinko, J., *Brock biology of microorganisms* 11th ed.; Prentice Hall, Inc. : Upper River Saddle, NJ, 2006.
139. Mantell, C. L., *Industrial electrochemistry*. 1st ed.; McGraw-Hill: New York, 1931.
140. T. F. O'Brien; T. V. Bommaraju; Hine, F., *Handbook of chlor-alkali technology*. Springer: New York, NY 2005.
141. Ober, J. A. *2010 Minerals Yearbook: bromine*; U.S. Geological Survey: 2011.
142. U.S. Energy Information Administration, Electricity wholesale market data (<http://www.eia.gov/electricity/wholesale/index.cfm>). In September 20, 2012 ed.; 2012.
143. Cettou, P.; Robertson, P. M.; Ibl, N., On the electrolysis of aqueous bromide solutions to bromate. *Electrochim Acta* **1984**, *29*, (7), 875-885.
144. Sakakibara, Y.; Kuroda, M., Electric prompting and control of denitrification. *Biotechnol. Bioeng.* **1993**, *42*, (4), 535-537.
145. Thrash, J. C.; Van Trump, J. I.; Weber, K. A.; Miller, E.; Achenbach, L. A.; Coates, J. D., Electrochemical stimulation of microbial perchlorate reduction. *Environ. Sci. Technol.* **2007**, *41*, (5), 1740-1746.

Appendix A. Supplementary materials for Chapter 3



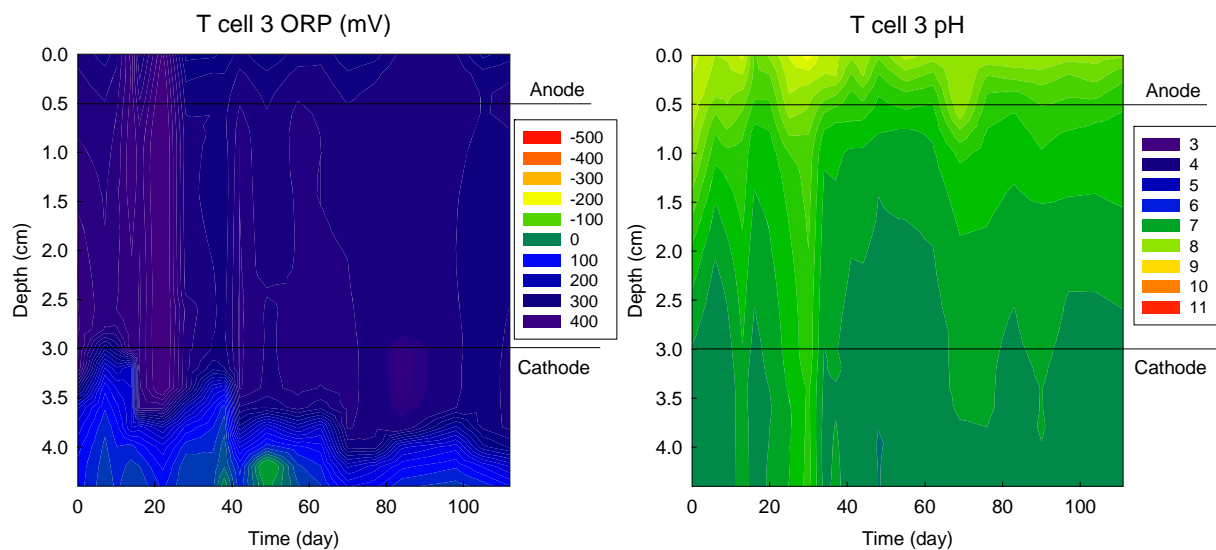


Figure A-1 Vertical ORP (left) and pH (right) profiles over time developed in sediment and cap containing carbon cloth electrodes

T-cell 1 and T-cell 2 were imposed to a 4 V external voltage. T-cell 3 was in control sediment with unpowered electrode. Depth zero was the water-sand interface. The horizontal black lines indicate the position of electrodes.

Appendix B. Supplementary materials for Chapter 4

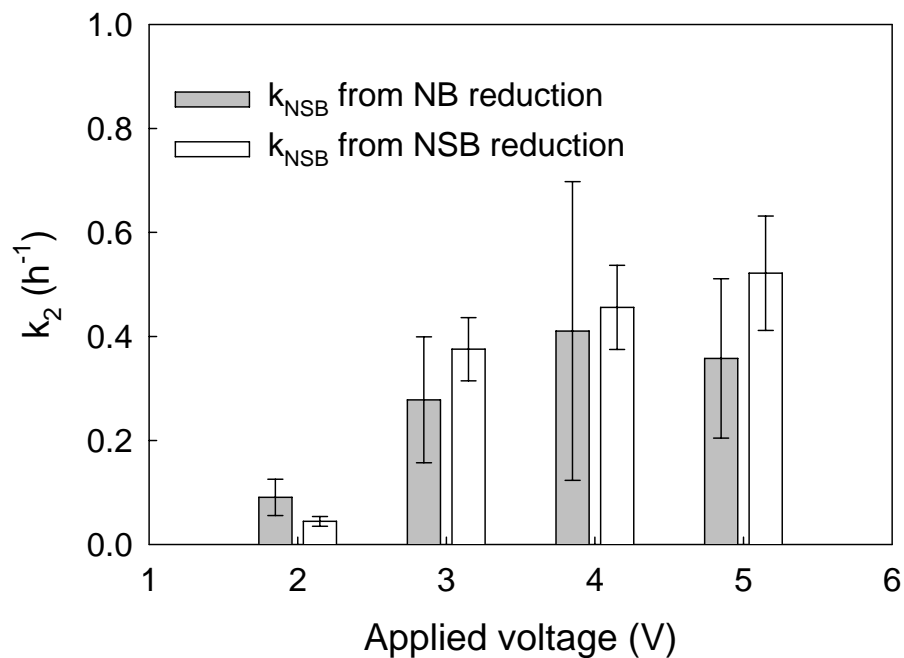


Figure B-1 Modeled first-order NSB reduction rate (k_{NSB}) from NB reduction (similar experiments as Figure 1) and NSB reduction (separate experiments with NSB directly added into reactors)

NB or NSB initial concentration were both 100 μM . Results from the average of triplicates and error bars represent the 95% confidence interval of the modeled rate constants

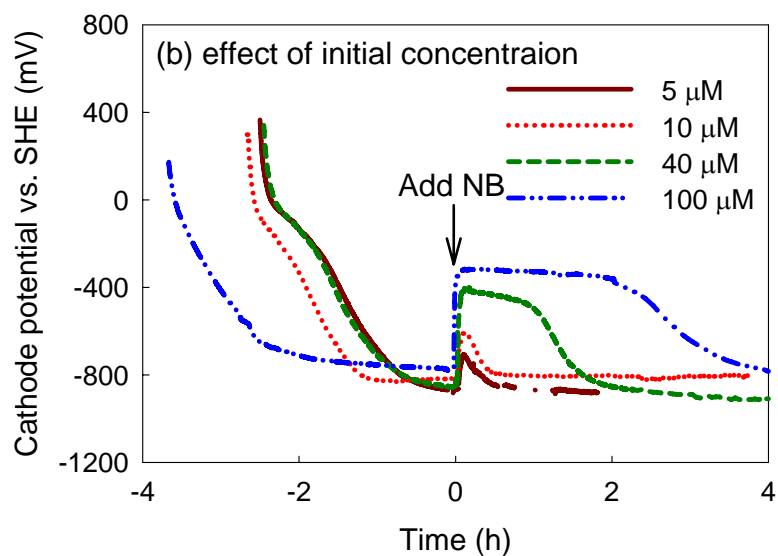
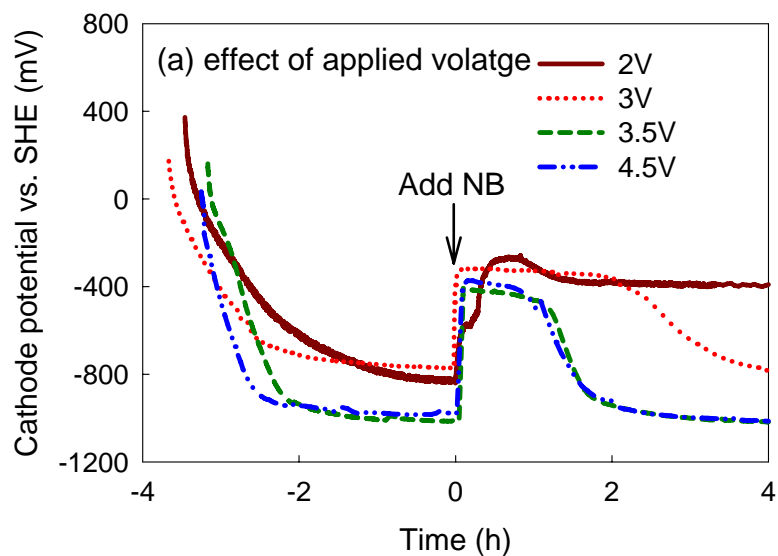


Figure B-2 Electrode potential in the working chamber vs. time during NB reduction at (a) different applied voltage (initial NB 100 μM) and (b) different initial NB concentration (at 3 V)

Each line is a representative from triplicate reactors.

Table B-1 pH, working electrode potential and current information for each experiment (average from triplicates \pm standard deviation)

Experiment group		pH at the end of experiment	Working electrode potential peak (mV vs. SHE)	Maximum current after NB addition (mA)
Voltage effect	2V	N.A.*	-203 \pm 76	0.94 \pm 0.15
	3V	6.68 \pm 0.06	-333 \pm 33	1.49 \pm 0.07
	3.5V	7.11 \pm 0.18	-388 \pm 43	2.18 \pm 0.10
	4V	6.79 \pm 0.07	N.A. *	N.A. *
	4.5V	6.70 \pm 0.22	-412 \pm 55	2.79 \pm 0.13
	5V	6.90 \pm 0.13	N.A. *	N.A. *
concentration effect	5 μ M	6.35 \pm 0.03	-707**	1.20 \pm 0.15
	10 μ M	6.59 \pm 0.31	-599 \pm 12	1.24 \pm 0.04
	40 μ M	6.18 \pm 0.20	-409 \pm 10	1.27 \pm 0.06
	100 μ M	6.68 \pm 0.06	-333 \pm 33	1.49 \pm 0.07
NOM effect	w/ PW	6.80 \pm 0.74	-378 \pm 38	2.22 \pm 0.13
	w/ HA 0.44 mg C/L	6.22 \pm 0.35	-377 \pm 19	1.98 \pm 0.11
	w/ HA 4.4 mg C/L	7.05 \pm 0.40	-428 \pm 20	2.25 \pm 0.13
	w/ HA 14.4 mg C/L	6.20 \pm 0.25	-369**	1.54 \pm 0.07
	w/ HA 44 mg C/L	6.42 \pm 0.10	-421**	2.33 \pm 0.16
	w/ HA 88 mg C/L	6.60 \pm 0.28	-355 \pm 47	2.61 \pm 0.06
	w/ HA 220 mg C/L	6.95 \pm 0.37	-404**	2.31 \pm 0.11
	w/ HA 330 mg C/L	6.82 \pm 0.27	-431**	2.58 \pm 0.13

*: data not available.

** : standard deviation not available.

Appendix C. Supplementary materials for Chapter 5

Table C-1 Anacostia River sediment porewater characteristics

Chemical species	Value (average)
pH	7.56
Conductivity (mS cm ⁻¹)	1.27
ORP (mV, SHE)	-159.3
Fe ²⁺ (M)	5.62 E-4
Mn _(aq) (M)	4.75 E-5
Cd _(aq) (M)	Not detected
Zn _(aq) (M)	4.95 E-8
Ca _(aq) (M)	3.37 E-3
Mg _(aq) (M)	1.49 E-3
K _(aq) (M)	2.66 E-4
Na _(aq) (M)	2.16 E-3
S ²⁻ (M)	Not detected
Cl ⁻ (M)	3.15 E-3
SO ₄ ²⁻ (M)	7.27 E-6
HCO ₃ ⁻ (M)	8.0 E-3
DOC (mg/L)	17.0

Table C-2 Anacostia River sediment solid characteristics

Chemical species	Value (average ± standard deviation)
Water Content (%)	55.3 ± 0.4
Acid-volatile sulfides (AVS) (μmol g ⁻¹)	54.0 ± 4.3
Total Fe (mg g ⁻¹)	53.42 ± 6.65
Total Mn (mg g ⁻¹)	0.24 ± 0.022
Total Zn (mg g ⁻¹)	0.70 ± 0.087
Total Al (mg g ⁻¹)	12.33 ± 3.98
H.H*.extractable Fe (mg g ⁻¹)	21.8 ± 0.75
H.H. extractable Mn (mg g ⁻¹)	0.23 ± 0.056
H.H. extractable Zn (mg g ⁻¹)	0.65 ± 0.07
Simultaneously extracted metals (SEM) Zn (μmol g ⁻¹)	8.48 ± 0.76

Oxalate extractable Fe ²⁺ (mg g ⁻¹)	3.05 ± 0.07
Oxalate extractable Fe ³⁺ (mg g ⁻¹)	20.85 ± 1.22
*H.H.: Hydroxylamine Hydrochloride	

Table C-3 Composition of mineral mix

Chemical	Concentration (g/L)
NaCl	0.1
Na ₂ MoO ₄ ·2H ₂ O	0.025
NiCl ₂ ·6H ₂ O	0.024
Na ₂ WO ₄ ·2H ₂ O	0.025

Table C-4 Composition of vitamin mix

Chemical	Concentration (mg/L)
Biotin	2
Pantothenic Acid	5
B-12	0.1
p-aminobenzoic acid	5
Thioctic acid	5
Nicotinic acid	5
Thiamine	5
Riboflavin	5
Pyridoxine HCl	10
Folic acid	2

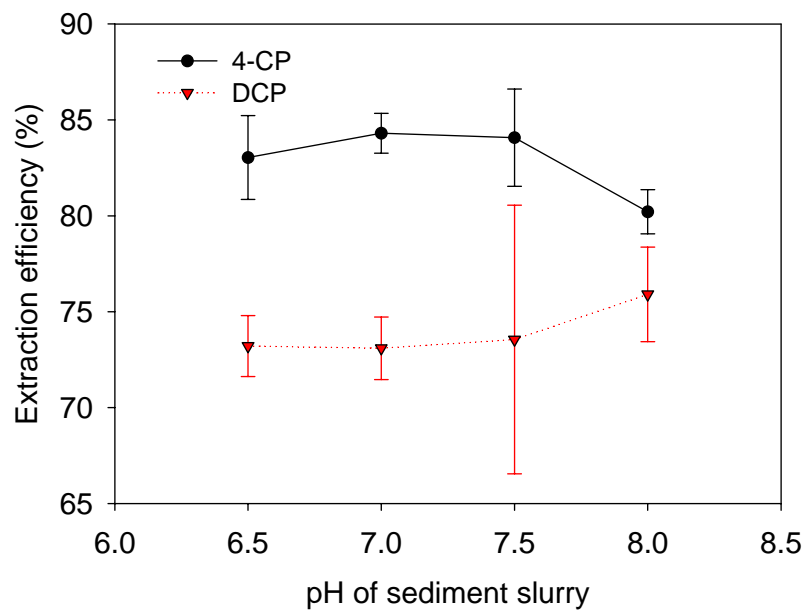


Figure C-1 effect of sediment slurry pH on extraction efficiency of DCP and 4-CP

Results from the average of triplicate extraction from sediment slurry spiked with 80 μ M DCP and 4-CP, and error bars represent standard deviation.

Appendix D. Supplementary materials for Chapter 6

Calculation of theoretical minimal energy consumption for selective bromide electrolysis:

$$\text{Energy consumption of selective bromide electrolysis} = \frac{\int_0^{t_{\text{total}}} V_{\text{cell}} I dt}{m_{\text{Br}^-}} \text{ (J/g)}$$

Where V_{cell} is the cell voltage (V); I is the cell current (A); t_{total} is the total reaction time (s); m_{Br^-} is the mass of bromide removed (g).

To calculate the theoretical minimal energy consumption, assume there is no overpotential during electrolysis, thus

$$V_{\text{cell}} = U_{\text{anode}} - U_{\text{cathode}} = U_{\text{Br}_2/\text{Br}^-} - U_{\text{H}^+/\text{H}_2} = 1.087\text{V} - 0\text{V} = 1.087\text{V}$$

Where U is the standard equilibrium potential for each electrode (V).

According to Faraday's Law of electrolysis:

$$\int_0^{t_{\text{total}}} I dt = Q = \frac{nFm_{\text{Br}^-}}{MW_{\text{Br}^-}}$$

Where Q is the total electric charge passed through (C); n (=1) is the number of electrons to remove one bromide ion; F the Faradic constant (96485 C/mol); MW_{Br^-} is the molecular weight of bromide (80 g/mol).

$$\begin{aligned} \text{Thus Energy consumption} &= \frac{\int_0^{t_{\text{total}}} V_{\text{cell}} Idt}{m_{\text{Br}^-}} = \frac{nFV_{\text{cell}}}{MW_{\text{Br}^-}} = \frac{1 \times 96485 \text{ C/mol} \times 1.087 \text{ V}}{80 \text{ g/mol}} \\ &= 1311 \text{ J/g} \doteq 1.3 \text{ kJ/g} \end{aligned}$$

Calculation of theoretical minimal energy consumption for reverse osmosis:

$$\text{Energy consumption of reverse osmosis} = \frac{PV_{\text{brine}}}{m_{\text{Br}^-}} \text{ (J/g)}$$

Where P is the applied pressure (Pa); V_{brine} is the volume of brine treated (m^3); m_{Br^-} is the mass of bromide removed (g).

To calculate the theoretical minimal energy consumption, assume the applied pressure (P) equals the osmosis pressure of the brine (π). Also assume the TDS of the brine equals to the median value (150 g/L) as shown in Table 1-2, and the brine can be approximate as NaCl solution. Thus

$$P = \pi = \sum C_{\text{TDS}} RT \doteq (C_{\text{Na}^+} + C_{\text{Cl}^-}) RT = 2C_{\text{NaCl}} RT \text{ (Pa)}$$

Where C_{TDS} , C_{Na^+} , C_{Cl^-} and C_{NaCl} are the molar concentration of TDS, Na^+ , Cl^- , and NaCl, respectively (mol/L); R is the idea gas constant (8.31 J/K·mol); T is the absolute temperature (assume 298°K, or 25°C).

Also assume the bromide concentration in the brine (c_{Br^-}) equals to the median value (1.2 g/L) as shown in Table 1-2. Note c_{Br^-} is the mass concentration, while C_{TDS} , C_{Na^+} , C_{Cl^-} and C_{NaCl} are molar concentrations.

$$\begin{aligned} \text{Then Energy consumption} &= \frac{PV_{brine}}{m_{Br^-}} = \frac{2C_{NaCl}RTV_{brine}}{c_{Br^-}V_{brine}} = \frac{2C_{NaCl}}{c_{Br^-}}RT \\ &= \frac{150\text{ g/L}}{58.5\text{ g/mol}} \times 2 \\ &= \frac{150\text{ g/L}}{1.2\text{ g/L}} \times 8.31\text{ J/K}\cdot\text{mol} \times 298\text{ K} = 10583\text{ J/g} \doteq 11\text{ kJ/g} \end{aligned}$$

Calculation of theoretical minimal energy consumption for capacitive deionization:

$$\text{Energy consumption of capacitive deionization} = \frac{\int_0^{t_{total}} V_{cell} Idt}{m_{Br^-}} \text{ (J/g)}$$

Where V_{cell} is the cell voltage (V); I is the cell current (A); t_{total} is the total reaction time (s); m_{Br^-} is the mass of bromide removed (g).

The cell voltage need to be insufficient to induced bromine or hydrogen production. Thus to calculate the theoretical minimal energy consumption, assume $V_{cell}=1\text{V}$. Here although there is no electrolysis taking place, the Faraday's Law of electrolysis is still valid for charged species transport:

$$\int_0^{t_{\text{total}}} Idt = Q = \frac{nFm_{\text{TDS}}}{MW_{\text{TDS}}}$$

Where Q is the total electric charge passed through (C); n is the number of electrons when transporting each mole of TDS; F the Faradic constant (96485 C/mol); m_{TDS} is the mass of TDS removed; MW_{TDS} is the average molecular weight of TDS. Again assume TDS and bromide concentration in the brine equals to the median value (150 g/L and 1.2 g/L, respectively) as shown in Table 1-2, and the brine can be approximate as NaCl solution (so $MW_{\text{TDS}}=58.5\text{g/L}$ and $n=2$).

$$\begin{aligned} \text{Thus Energy consumption} &= \frac{\int_0^{t_{\text{total}}} V_{\text{cell}} Idt}{m_{\text{Br}^-}} = \frac{nFV_{\text{cell}}m_{\text{TDS}}}{MW_{\text{TDS}}m_{\text{Br}^-}} = \frac{2 \times 96485 \text{ C/mol} \times 1\text{V} \times 150 \text{ g/L}}{58.5 \text{ g/mol} \times 1.2 \text{ g/L}} \\ &= 412329 \text{ J/g} \doteq 412 \text{ kJ/g} \end{aligned}$$

Calculation of theoretical minimal energy consumption for thermal distillation:

$$\text{Energy consumption of thermal distillation} = \frac{(c_p \Delta T + \Delta H_{\text{vap}})m_{\text{brine}}}{m_{\text{Br}^-}} \text{ (J/g)}$$

Where c_p specific heat capacity of brine (J/g·K); ΔT is the temperature change between untreated brine and boiling brine (K); ΔH_{vap} is the enthalpy of vaporization of brine (J/g); m_{brine} is the mass of brine treated (g); m_{Br^-} is the mass of bromide removed (g).

$$\frac{m_{brine}}{m_{Br^-}} = \frac{\rho_{brine} V_{brine}}{m_{Br^-}} = \frac{\rho_{brine}}{c_{Br^-}}$$

Where ρ_{brine} is the density of brine (g/L); V_{brine} is the volume brine treated (m³); c_{Br^-} is the mass concentration of bromide in the brine (assume is 1.2g /L)

Assume the thermal properties of brine are the same as water. Thus

$$c_p = 4.1813\text{J/g} \cdot \text{K}$$

$$\Delta H_{vap} = 2257\text{J/g}$$

$$\rho_{brine} = 1000\text{g} / \text{L}$$

Also assume $\Delta T = 100^\circ\text{C} - 25^\circ\text{C} = 75^\circ\text{C} = 75^\circ\text{K}$. Although in practice, thermal evaporation does not necessary need to bring brine temperature to boiling point, the energy consumption for increase brine temperature is one magnitude less that energy consumption for evaporation, thus the difference in temperature becomes less important.

$$\begin{aligned} \text{Then Energy consumption} &= \frac{(c_p \Delta T + \Delta H_{vap}) m_{brine}}{m_{Br^-}} = \frac{(c_p \Delta T + \Delta H_{vap}) \rho_{brine}}{c_{Br^-}} \\ &= \frac{(4.1813\text{J/g} \cdot \text{K} \times 75\text{K} + 2257\text{J/g}) \times 1000\text{g} / \text{L}}{1.2\text{g} / \text{L}} = 2142165\text{J} / \text{g} \doteq 2142\text{kJ} / \text{g} \end{aligned}$$